Deep Inelastic Scattering and The Bag Model

Anthony Ian Signal B.Sc. (Hons.).

A thesis submitted for the degree of
Doctor of Philosophy
at the University of Adelaide
(Department of Physics and Mathematical Physics).

August 1988

Abstract

This thesis is mainly concerned with the problem of calculating the twist two matrix elements contributing to deep inelastic scattering structure functions, using the quark wavefunctions of the bag models of hadron structure. To this end we review deep inelastic scattering, making extensive use of the operator product expansion, quantum chromodynamics based phenomenology, and also the theory of bag models. Along the way we will also examine the so-called EMC effect and the effects of non-perturbative QCD processes on the structure functions. Finally we present a novel method of calculating structure functions in the bag model and we examine the properties of the calculated structure functions.

Statement

This thesis contains no material which has been accepted for the award of any other degree or diploma in any University and that, to the best of my knowledge and belief, the thesis contains no material previously published or written by another person, except where due reference is made in the text of the thesis.

I consent to the thesis being made available for photocopying and loan if applicable, provided due acknowledgement is given.

Anthony I. Signal.

Acknowledgements

A large debt of gratitude is owed to my supervisor Professor Tony Thomas for his guidance, help and encouragement at every stage of my Ph.D. studies. Without his questioning and enthusiasm this thesis would never have seen the light of day.

I would also like to thank all the members of the Theoretical Nuclear and Particle Physics group at Adelaide and also our many visitors over the past three years. In particular Gerald Dunne, Andreas Schreiber and Dr. Micheal Weyrauch for the many helpful discussions we have had. Also thanks to Dr. Tony Williams, Dr. Paul Bickerstaff and Dr. Rod Crewther for their useful comments and criticisms. Special thanks to Lindy Sebestyan for her invaluable help in preparing many of the diagrams and graphs in this thesis.

Thanks also go to Judy Lang for drawing some of the graphs.

To all the postgraduate students in the Department of Physics; thanks for making my three years in Adelaide so enjoyable.

The author acknowledges the support of a Commonwealth Postgraduate Research Scholarship.

Finally I would like to thank my parents for their support, and, as always, Helen for her love and support.

P.S. I don't have to thank my typist, as I did all the tyuping and prooff- reading myself.

Contents

List of Figures

List of Tables

Chapter 1

Introduction

K'uei — Opposites

Heaven and earth are separate and apart, but the work they do unites them ... they are related through their actions. The outcome of such separation is great indeed!

The I Ching or *Book of Changes*

Ever since its discovery in the 1930s, there has been a great deal of effort by physicists to understand the strong interaction. Surely one of the most useful advances in this field has been the quark model, first introduced in the early 1960s by Gell-Mann, Ne'eman and Zweig [GN 64]. The quark model proposed that the three 'flavours' of quark u, d and s formed the fundamental representation of the group $SU(3)$. Then all of the low mass hadrons were found to fall into low dimensional representations of $SU(3)$, the mesons being quark-antiquark pairings while the baryons required three quarks.

Despite the discovery of the Ω^-as predicted by SU(3) symmetry for some time it was not clear whether quarks were real particles or a mathematical artifice. One problem was that free quarks had never been observed, so they had to be bound very

tightly inside the hadrons. Another major problem was states like the Δ^{++} which would have to consist of three u quarks in the same spin and spatial state. Since the quarks should be fermions, this state would violate Fermi statistics. To overcome this difficulty it was proposed that quarks came in three different 'colours'. Although this explanation was rather *ad hoc*, it became a great strength of the model when it was realized that a gauge theory of colour interactions (quantum chromodynamics or QCD) could be constructed, the symmetry group again being $SU(3)$. It was postulated that only 'colourless' states can exist in nature, so free quarks, which would carry a colour charge, cannot be observed. However hadrons, being colour singlet states, are allowed. It was (and still is) hoped that QCD would be a complete theory of strong interactions.

In the late 1960s a series of experiments at SLAC in the U.S. provided another puzzle. Just as large momentum transfers in scattering experiments between alpha particles and gold atoms had led Rutherford to propose a point-like atomic nucleus, large momentum transfers observed when scattering high energy electrons from protons and neutrons led to the conclusion that point-like objects existed inside hadrons. These results were explained by the parton model proposed by Feynman [Fey 69] and others, however in this model partons were free particles, so how could the free partons observed be reconciled with the quark model of tightly bound quarks? The answer came when Gross and Wilczek [GW 73] and Politzer [Pol 73] discovered that non-Abelian gauge theories ie. QCD had the property of 'asymptotic freedom', that is, at high momentum transfers, or short distances, the interactions

became weaker. Thus in high momentum transfer, or 'deep inelastic' experiments, quarks would appear to be free particles, as was observed. In the following chapter we will examine deep inelastic scattering (DIS) and the quark parton model (QPM) using the powerful tool, the operator product expansion.

At around the same time a great deal of evidence was found which supported the quark model and its sophisticated offspring QCD. The $SU(2) \times U(1)$ gauge theory of electro-weak interactions was developed, which seemed to require three colours of quark and also predicted a new flavour of quark, c. The spectacular discovery of the J/Ψ (a $c\bar{c}$ state) in 1974 seems to have demonstrated beyond reasonable doubt the reality of quarks as particles.

In the early 1970s 't Hooft and others [tHo 71,AL 73] showed that gauge theories like QCD were probably renormalizable, and moreover how calculations in non-Abelian gauge theories could be made. Adler [Adler 69] used current algebra methods to calculate the decay rate for $\pi \rightarrow 2\gamma$, getting an answer which was in good agreement with experiment when three colours were included, but was wrong by a factor of nine when colour was excluded. The strongest piece of experimental evidence for colour is found in e^+e^- annihilation, where the ratio of cross sections

$$R = \frac{\sigma(e^+e^- \rightarrow \text{hadrons})}{\sigma(e^+e^- \rightarrow \mu^+\mu^-)} \propto \sum_{\text{quarks}} e_q^2 \tag{1.1}$$

is found to agree well with the predictions of QCD, but is out by a factor of three over a very large range of energies if colour is left out.

Now that the quark model and QCD are well established, one could be forgiven for thinking that the problems of the strong interaction are solved. This could not be

further from the truth! The science of calculating hadronic properties from the QCD Lagrangian, using a discrete spacetime lattice, is barely in its infancy, yet requires huge amounts of computer power. It appears that realistic solutions involving light quarks like u, d and s may be many years away. For this reason phenomenological quark models have become popular in recent times. These models are constructed, with the properties of QCD in mind, in order to reproduce the properties of hadrons. They can then be used to make calculations of hadronic scattering or other processes. In Chapter Five of this thesis I will provide an introduction to the class of bag models, in particular the successful MIT and cloudy bag (CBM) models.

The plethora of phenomenological models that have sprung up has led to some cynicism, as there does not appear to be any experimental evidence that allows us to unambiguously choose one model above all others. While this is probably true at low energies (with the possible exception of charge symmetry breaking) because of the low resolution of the probes, deep inelastic scattering may yet be able to help us. Firstly there are some indirect tests we can apply. From measurements of the sea distributions $\bar{u}$, $\bar{d}$ and $\bar{s}$ in DIS we can infer properties of the pion and kaon meson clouds about the nucleon and also the size of the quark confinement radius. These tests are discussed in Chapter Four, particularly in conjunction with the CBM.

We would also like to use DIS to test the valence quark distributions of models. Unfortunately these calculations are very difficult. The final two chapters of this thesis will review this problem and propose a novel method of calculating the quark distributions in the two dimensional MIT bag model. Many properties of these dis-

tributions will be studied, including their behavior in a nuclear environment. This last point is of some importance because of the EMC effect discovered at CERN in the early 1980s [Aub+ 83]. The EMC group found that the quark distributions in a nucleon change with the atomic number of its nucleus, contrary to naive expectations. Since then an industry has grown in explaining the effect, as we will see in Chapter Three. It has become obvious however that no unambiguous conclusions can be drawn from analysis of the EMC effect data until the problem of relating the quark models to the quark distributions observed is solved. Hopefully the methods and results presented in this thesis mark some progress towards this solution.

We note that the conventions used in this thesis will, as much as possible, be those of Bjorken and Drell [BD 64 65].

Chapter 2

Operator Product Expansion and Deep Inelastic Scattering

2.1 Deep Inelastic Scattering Formalism

We want to examine the process $lA \longrightarrow l'X$, where l is a lepton, A is a nucleus (the nucleon being a special case), and X is the final hadronic state which is unobserved. As most experiments are of the type unpolarized beam on unpolarized target, we shall ignore polarization effects, though they can be handled in a similar fashion. For the time being we shall examine only the electromagnetic interaction between lepton and nucleus, but the extension to the weak interaction is fairly straightforward.

To lowest order in α, the process is described by one photon exchange, for which the invariant amplitude $\mathcal{M}$ is given by [BD 64 65]:

$$\mathcal{M} \propto \bar{u}(k')\gamma^{\mu}u(k)\frac{1}{q^2}\langle X|J_{\mu}(0)|p\rangle \tag{2.1}$$

where $J_{\mu}(0)$ is the hadronic electromagnetic current operator. When X is not observed the differential cross-section $d\sigma$ is given by:

$$d\sigma \propto \sum_{X}(2\pi)^4\,\delta^4(p+q-p_X)|\mathcal{M}|^2, \tag{2.2}$$

which can be written as a product of leptonic and hadronic tensors

$$d\sigma \propto l^{\mu\nu} W_{\mu\nu} \tag{2.3}$$

where

$$\begin{aligned} l^{\mu\nu} &= \frac{1}{2}\mathrm{Tr}\ \not{k}'\gamma^\mu\ \not{k}\gamma^\nu \\ &= 2(k'^\mu k^\nu + k'^\nu k^\mu - g^{\mu\nu} k.k') \text{ (ignoring the lepton mass)} \end{aligned} \tag{2.4}$$

and

$$W_{\mu\nu} = \frac{1}{4\pi}\sum_X (2\pi)^4\, \delta^4(p+q-p_X)\langle p|J_\mu^\dagger(0)|X\rangle\langle X|J_\nu(0)|p\rangle. \tag{2.5}$$

where the states are normalized

$$\langle p|p'\rangle = 2p^0(2\pi)^3\delta^3(\vec{p}-\vec{p}') \tag{2.6}$$

If we note that

$$(2\pi)^4\delta^4(p+q-p_X) = \int d^4\xi\ e^{i(p+q-p_X).\xi} \tag{2.7}$$

and that we can translate $J_\mu^\dagger(0)$ to spacetime point ξ, we can use completeness ($\sum_X |X\rangle\langle X| = 1$) to write $W_{\mu\nu}$ in the form:

$$W_{\mu\nu} = \frac{1}{4\pi}\int d^4\xi\ e^{iq.\xi}\langle p|J_\mu^\dagger(\xi)J_\nu(0)|p\rangle_c \tag{2.8}$$

where the subscript c on the matrix element denotes 'connected'. We can represent $W_{\mu\nu}$ graphically, as in Fig. 2.1, with the intermediate state being the sum over *all* hadronic states.

From Fig. 2.1 it would appear that there is some connection between $W_{\mu\nu}$ and forward, virtual Compton scattering. This is indeed the case. The product of currents in eqn. (2.8) can be replaced by a commutator:

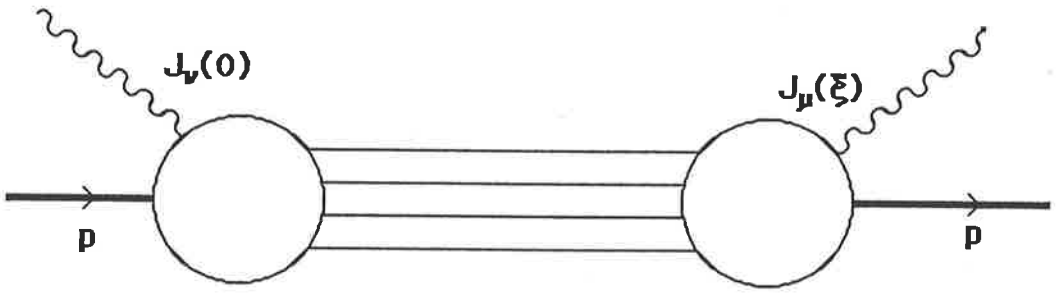

Fig 2.1 $\omega_{\mu\nu}$, which measures a current-current correlation function in the target state.

$$W_{\mu\nu} = \frac{1}{4\pi} \int d^4\xi \; e^{iq.\xi} \langle p|[J_\mu^\dagger(\xi), J_\nu(0)]|p\rangle_c \tag{2.9}$$

because the term that has been subtracted vanishes for $q^0 > 0$ (it violates energy-momentum conservation). The amplitude for forward, virtual Compton scattering is [IZ 80]:

$$T_{\mu\nu} = i \int d^4\xi \; e^{iq.\xi} \langle p|T(J_\mu^\dagger(\xi) J_\nu(0))|p\rangle_c \tag{2.10}$$

from which it can be seen that $W_{\mu\nu}$ is the imaginary part of $T_{\mu\nu}$ (when q^0 is taken to have an arbitrarily small positive imaginary part):

$$W_{\mu\nu} = \frac{1}{2\pi} Im T_{\mu\nu}. \tag{2.11}$$

This is often referred to as the 'optical theorem'.

It is important to note the subscript 'c' in the expressions for $W_{\mu\nu}$ and $T_{\mu\nu}$. Connected matrix elements include only processes which cannot take place in the vacuum ie. they exclude vacuum transitions of the form $\langle 0|J_\mu^\dagger(\xi) J_\nu(0)|0\rangle\langle p|p\rangle$, so that the current interacts with the target nucleus.

We can decompose $W_{\mu\nu}$ and $T_{\mu\nu}$ using current conservation ($q^\mu W_{\mu\nu} = 0$), into a pair of Lorentz invariant structure functions $W_{1,2}(T_{1,2})$:

$$\begin{aligned} W_{\mu\nu} &= -(g_{\mu\nu} - \frac{q_\mu q_\nu}{q^2}) W_1(\nu, q^2) \\ &\quad + \frac{1}{M_A^2}(p_\mu - \frac{p.q}{q^2} q_\mu)(p_\nu - \frac{p.q}{q^2} q_\nu) W_2(\nu, q^2). \end{aligned} \tag{2.12}$$

The structure functions $W_{1,2}(T_{1,2})$ are functions of the Lorentz invariants q^2 and $p.q = M_A \nu$ ($q^2 = -4EE' \sin^2 \frac{\theta}{2}$, $\nu = E - E'$ in the rest frame of the nucleus) where M_A is the mass of the nucleus. Note that in the case of the weak interaction ie.

(anti)neutrino scattering, which does not conserve parity, an extra term is allowed in the decomposition [LP 82]: $-\frac{i}{2M_A^2}\varepsilon^{\mu\nu\sigma\rho}p_\sigma q_\rho W_3$. W_1 and W_2 are measured experimentally by comparing cross sections at fixed q^2 and ν, but different values of E, E' and θ:

$$\frac{d^2\sigma}{dE'd\Omega} = \frac{4\alpha^2 E'^2 \cos^2\theta/2}{q^4}\left[W_2(\nu,q^2) + 2W_1(\nu,q^2)\tan^2\frac{\theta}{2}\right]. \tag{2.13}$$

Since q^2 is space-like, we define $Q^2 \equiv -q^2$ ($Q^2 > 0$), then the squared mass of the final hadronic state is:

$$M_X = (p+q)^2 = M_A^2 + 2M_A\nu - Q^2 \geq M_A^2. \tag{2.14}$$

Thus the dimensionless 'scaling' variable $x_A \equiv Q^2/2M_A\nu$ must lie in the range $0 \leq x_A \leq 1$. The term 'deep inelastic' refers to the kinetic domain where Q^2, ν and M_X are large compared with typical hadron masses and excitation energies. Often a uniform scaling variable is used: $x = x_N = Q^2/2M\nu$ ($M \equiv M_N$ the nucleon mass) $0 \leq x \leq A$ to compare the structure functions of different targets.

It was suggested by Bjorken [Bjor 66 69] that in the limit $Q^2 \to \infty$ at fixed x_A (called the Bjorken limit), the structure functions would become functions of x_A alone:

$$\begin{aligned}
\lim_{Bj} W_1(\nu,q^2) &= F_1(x_A) \\
\lim_{Bj} \frac{\nu}{M_A} W_2(\nu,q^2) &= F_2(x_A) \\
\lim_{Bj} \frac{\nu}{M_A} W_3(\nu,q^2) &= F_3(x_A)
\end{aligned} \tag{2.15}$$

which was subsequently verified by experiment [Pan 68]. This phenomenon is called 'scaling'.

It is important to note that for deep inelastic scattering in two spacetime dimensions the only changes needed to the expressions in this section are to replace superscript '4' by superscript '2' in eqns. (2.2) and (2.5–2.10).

2.2 Light-Cone Behaviour

It is important to understand the distance scales in deep inelastic scattering (DIS). To this end we shall work in the rest frame of the target nucleus and make extensive use of light-cone coordinates. If we choose the incident virtual photon's direction to be along the negative z-axis, then the photon's four momentum is:

$$q = (\nu, 0, 0, -\nu\sqrt{1 + Q^2/\nu^2}). \tag{2.16}$$

In the Bjorken limit $Q^2 \to \infty$, $x_A = Q^2/2M_A\nu$ fixed, we have $Q^2/\nu^2 \to 0$ and

$$q \to (\nu, 0, 0, -\nu - M_A x_A) \tag{2.17}$$

so that in light-cone coordinates ($q^{\pm} \equiv (q^0 \pm q^3)/\sqrt{2}$) we have:

$$q^- \to \infty \qquad\qquad q^+ \to -M_A x_A/\sqrt{2} = -x_A p^+. \tag{2.18}$$

Note that $M_A x_A = Q^2/2\nu$, so the limiting value of q^+ is independent of the mass of the nucleus.

Now we want to examine the spacetime separation ξ. Since q and ξ appear as conjugate variables in the definition of $W_{\mu\nu}$, eqn.(2.9), we require $q.\xi = q^+\xi^- + q^-\xi^+$ to be finite. Thus $q^- \to \infty$ forces $\xi^+ \to 0$, but ξ^- does not vanish. The commutator in eqn. (2.9) is causal because the hadronic currents must be local, hence

$$\xi^2 = 2\xi^+\xi^- - \vec{\xi_\perp}^{\,2} \geq 0. \tag{2.19}$$

But $\xi^+ \to 0$ in the Bjorken limit, thus $\vec{\xi_\perp}$ must also vanish. This leaves ξ^- the only non-vanishing component of ξ^λ in the Bjorken limit, and we have the important result that $\xi^2 \to 0$ in the Bjorken limit. This means that to examine the current commutator $[J_\mu^\dagger(\xi), J_\nu(0)]$ we must look at its behaviour on the light-cone, as DIS will be dominated by this light-cone behaviour. This will require us to use the operator product expansion (OPE).

We can gain some more insight into the separation ξ using the results of Fourier transform theory [Light 58]. Firstly we examine the relation between q^- and ξ^+. If we let

$$\tilde{f}(q^-) = \int d\xi^+ e^{iq^-\xi^+} f(\xi^+) \tag{2.20}$$

then if $f(\xi^+)$ is everywhere differentiable any number of times and well-behaved as $|\xi^+| \to \infty$, then $\tilde{f}(q^-)$ vanishes faster than any power of q^- as $q^- \to \infty$. However in the case of DIS there is a singularity in the integrand defining $W_{\mu\nu}$: the current commutator vanishes when $\xi^2 < 0$. This corresponds to $f(\xi^+)$ in eqn. (2.20) having a singularity at $\xi^+ = 0$. Now the behavior of $\tilde{f}(q^-)$ in the limit $q^- \to \infty$ is dominated by the behavior of $f(\xi^+)$ near the singularity. Using integration by parts we have, as $q^- \to \infty$

$$\tilde{f}(q^-) \sim \left(\frac{1}{q^-}\right) f(0) - \left(\frac{1}{q^-}\right)^2 f'(0) + \ldots \tag{2.21}$$

Thus in the limit $q^- \to \infty$, $W_{\mu\nu}$ will be dominated by $\xi^+ \approx 0$.

The relation between q^+ and ξ^- is more subtle. In the Bjorken limit we have $\xi^+ \to 0$, $\vec{\xi_\perp} \to 0$, so $W_{\mu\nu}$ is given by a Fourier transform in $q^+ = -Mx/\sqrt{2}$,

$\tilde{f}(q^+)$, of a smooth function of ξ^-, $f(\xi^-)$. However the Fourier transform is found experimentally to diverge [LP 82], at worst like x^{-1}, as $x \to 0$. Inverting the Fourier transform and integrating by parts we have

$$f(\xi^-) \sim \frac{1}{M\xi^-/\sqrt{2}} \tilde{f}(x=0) + \ldots \tag{2.22}$$

from which we deduce that $|\xi^-| < \sqrt{2}/Mx$. Thus for small x the current correlation may well extend over large distances, $|\xi^3| < 1/Mx$, but is always on the light-cone.

2.3 The Operator Product Expansion

There is an immediate problem in considering the products of currents at light-cone separations. In general the product $A(\xi)B(0)$ of two local field operators A and B is singular for both $\xi \approx 0$ and $\xi^2 \approx 0$. The root of the problem lies in the fact that operators in local quantum field theories should be regarded as distributions, and the product of such distributions is not well defined at the same spacetime point. Thus the operator product expansion (OPE) has been developed to manage the singularities of operator products.

The idea behind the OPE is that the product of two local field operators A and B may be expanded in terms of a complete set of linearly independent local fields $O_n(\xi)$, which are regular in the relevant limit ($\xi_\lambda \to 0$ or $\xi^2 \to 0$), with c-number coefficients $C_n(\xi)$ which may be singular in the limit:

$$\lim_{\substack{\xi^2 \to 0 \\ (\xi_\lambda \to 0)}} A(\xi)B(0) = \sum_{n=1}^{\infty} \sum_{\{\beta\}} C^{(n)}_{\{\beta\}}(\xi^2)\xi_{\lambda_1} \ldots \xi_{\lambda_n} O^{(n),\lambda_1 \ldots \lambda_n}_{\{\beta\}}(0) \tag{2.23}$$

where it is customary and convenient to extract the factors of ξ_λ in the coefficients. $\{\beta\}$ are all the labels that might occur in the expansion eg. Lorentz, internal sym-

metry etc. The operators are traceless, symmetric and of rank n in their Lorentz structure ie. they are of spin n. The main difference between the OPE in the limits $\xi_\lambda \to 0$ and $\xi^2 \to 0$ is that only a finite number of the c-number coefficients $C^{(n)}_{\{\beta\}}(\xi)$ are singular or non-vanishing in the $\xi_\lambda \to 0$ limit, whereas all the $C^n_{\{\beta\}}(\xi^2)$ may be singular or non-vanishing in the $\xi^2 \to 0$ limit.

The short-distance ($\xi_\lambda \to 0$) OPE was introduced by Wilson [Wil 69]and further developed by him and Zimmerman [WZ 72]. Wilson also proposed that the expansion eqn. (2.23) could be used to find the singularity behavior of the coefficient functions. Frishman, and Brandt and Preparata [Fri 71,BP 71] showed that the light-cone ($\xi^2 \to 0$) OPE exists by making use of the short-distance OPE. A simple example of the short-distance OPE is the time-ordered product of two massless scalar fields.

$$T(\phi(\xi)\phi(0)) = \Delta(\xi)I + :\phi(\xi)\phi(0): \tag{2.24}$$

where

$$\begin{aligned} \Delta(\xi) &= \frac{i}{(2\pi)^4}\int d^4k \frac{e^{-ik.\xi}}{k^2 + i\epsilon} \\ &= \frac{1}{(2\pi)^2}\frac{1}{\xi^2 - i\epsilon}. \end{aligned} \tag{2.25}$$

The time-ordered product is expanded as the sum of regular local operators I and $:\phi(\xi)\phi(0):$ with the singularity only occurring in the c-number coefficients $\Delta(\xi)$.

2.3.1 Scale Invariance

A local operator $O(\xi)$ is scale invariant if there exists a unitary operator $U(s)$ such that

$$U^\dagger(s)O(\xi)U(s) = s^{d_0}O(s\xi) \tag{2.26}$$

where d_0 is called the dimension of O, in mass units. Applying scale invariance eqn.(2.26) to both sides of the light-cone OPE eqn.(2.23) we obtain

$$s^{d_A+d_B}A(s\xi)B(0) = \sum_n C^{(n)}(\xi^2)s(\xi_{\lambda_1}\dots\xi_{\lambda_n})s^{d_n}O^{(n),\lambda_1\dots\lambda_n}(0) \tag{2.27}$$

where d_n is the dimension of $O^{(n)}$ and we have dropped the labels $\{\beta\}$. However if we put $\xi \to s\xi$ in eqn.(2.23) we have

$$A(s\xi)B(0) = \sum_n C^{(n)}(s^2\xi^2)s(\xi_{\lambda_1}\dots\xi_{\lambda_n})O^{(n),s(\lambda_1\dots\lambda_n)}(0). \tag{2.28}$$

Now the operators $O^{(n)}$ are linearly independent, so rearranging we get an expression for the c-number coefficients $C^{(n)}$:

$$C^{(n)}(s^2\xi^2) = s^{d_n-n-d_A-d_B}C^{(n)}(\xi^2) \tag{2.29}$$

from which it follows that $C_{(n)}$ is singular as $\xi^2 \to 0$ only if

$$d_n - n \leq d_A + d_B. \tag{2.30}$$

The important quantity $d_n - n$ (dimension - spin) of an operator is called its 'twist'.

The 'dynamical' dimension d_0 of an operator O, defined as in eqn. (2.26), will coincide with the canonical mass dimension of O, as obtained from the Lagrangian, for free field theories. This is easily seen in a free fermion theory where the canonical dimensions of $\bar{\psi}(\xi)$ and $\psi(\xi)$ are both $\frac{3}{2}$ (in four spacetime dimensions). Now the invariance of the action under scale transformations such as eqn. (2.26) implies that

$$\begin{aligned}\int d^4\xi\bar{\psi}(\xi)\partial_{\mu(\xi)}\psi(\xi) &= \int d^4\xi s^{2d_\psi}\bar{\psi}(s\xi)\partial_{\mu(\xi)}\psi(s\xi) \\ &= \int d^4\zeta s^{-4}\bar{\psi}(\zeta)s\partial_{\mu(\zeta)}\psi(\zeta) \quad \text{where } \zeta = s\xi\end{aligned} \tag{2.31}$$

so that $2d_\psi = 4 - 1$ ie. $d_\psi = \frac{3}{2}$.

Now when we renormalize our field theory we expect that scale invariance would be broken, because we have introduced an arbitrary renormalization scale (usually an arbitrary mass scale making the coupling dimensionless). However we can still use scale invariance to look at the behavior of the c-number coefficients $C^{(n)}$, but in general the operator dimensions become non-canonical. The renormalization group is important here, because it allows scale invariance to be realized, and predicts the 'anomalous' dimensions of the renormalized field operators.

2.3.2 Twist Two

From eqns.(2.29) and (2.30) we have that contributions to the OPE of the product $A(\xi)B(0)$ in the limit $\xi^2 \to 0$ come from operators O^n with twist $\leq d_A + d_B$, and it is expected that the leading light-cone singularity comes from the coefficient corresponding to the operator of lowest twist (τ_{min})

$$C(\xi^2) \overset{\xi^2 \to 0}{\sim} (\xi^2)^{(\tau_{min} - d_A - d_B)/2}. \tag{2.32}$$

It is easy to see that twists are additive, that elementary fields have twist 1, and hence that the minimum twist of an operator involving j elementary fields is j [Dunne 86,WZ 72,Ynd 83]. From this it follows that for an operator of given twist τ there are at most τ elementary fields involved, and since the number of elementary fields is limited then the number of types of operators of twist τ must also be limited.

In the case of DIS we are concerned with products of the current operators $J(\xi)$. Now from our fundamental theory, QCD, we expect that the current operators will

be of the form $\bar{\psi}\psi$ where ψ is a quark field. Thus the product of current operators has dimension 6 (in 4 spacetime dimensions). However we expect that higher twist ($\tau > 2$) terms in the OPE will be suppressed at least by $O(1/Q^2)$ compared to twist 2 because of the extra propagators involved. We may think of twist 2 operators as corresponding to diagrams where there is no interaction between the 'struck' quark and the 'spectators'. Some examples of twist 2 and twist 4 operators are shown in Fig. 2.2. We can see that all the twist 4 diagrams are suppressed by $O(1/Q^2)$ or $O(1/Q^4)$ relative to the twist 2 diagram Fig. 2.2a. We will see that Fig. 2.2a will correspond to the naive quark-parton model.

In QCD we have two types of operators: singlet and non-singlet. Singlet operators are invariant under a change in flavour labels ie. $u \leftrightarrow d$ whereas non-singlet operators are changed under such changes in flavour labels. Obviously gluon operators are singlet operators. Thus there are three classes of operator to consider:

1. non-singlet quark operators:

$$O_{NS}^{\lambda_1 \cdots \lambda_n} = i^{n-1} \mathcal{S} \bar{q} \tau^a \gamma^{\lambda_1} D^{\lambda_2} \cdots D^{\lambda_n} (1 \pm \gamma_5) q \tag{2.33}$$

2. singlet quark operators:

$$O_{S}^{\lambda_1 \cdots \lambda_n} = i^{n-1} \mathcal{S} \bar{q} \gamma^{\lambda_1} D^{\lambda_2} \cdots D^{\lambda_n} (1 \pm \gamma_5) q \tag{2.34}$$

3. singlet gluon operators:

$$O_{G}^{\lambda_1 \cdots \lambda_n} = i^{n-2} \mathcal{S} \mathrm{Tr} F^{a \lambda_1} D^{\lambda_2} \cdots D^{\lambda_{n-1}} F_a^{\lambda_n} \tag{2.35}$$

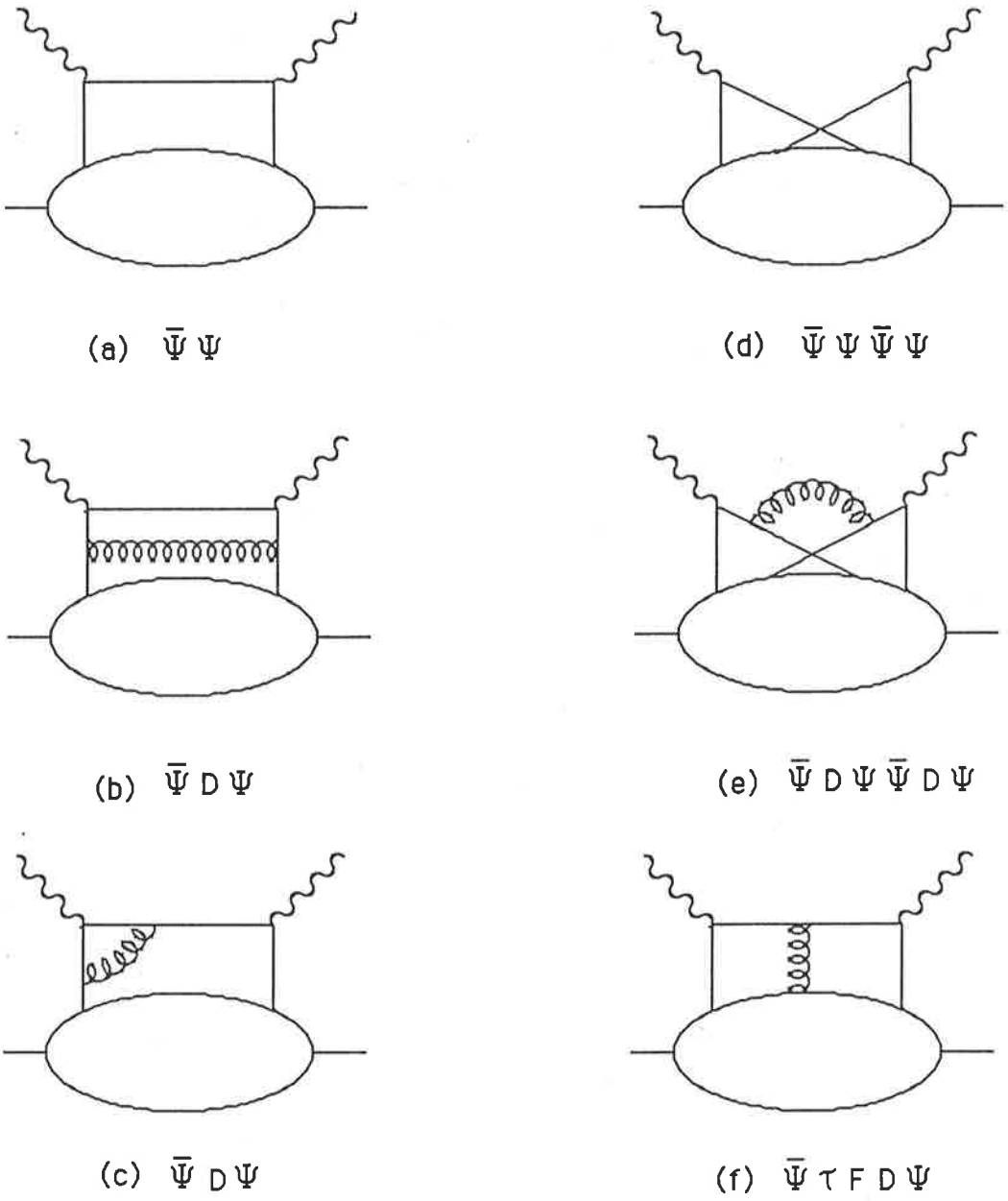

Fig 2.2 Some contributions to the Operator Product Expansion of $T_{\mu\nu}$. Figures (a), (b), and (c) are twist 2 operators, figures (d) and (e) are twist 4 and figure (f) is twist 6.

where $\mathcal{S}$ symmetrizes over the Lorentz indices, and the subtraction of all trace terms is understood. D_λ is the usual covariant derivative $D_\lambda = \partial_\lambda - igA_\lambda$, and $F_{\mu\nu}$ is the gauge field strength tensor $F_{\mu\nu} = \partial_\mu A_\nu - \partial_\nu A_\nu + g[A_\mu, A_\nu]$. The γ_5 matrices are only used when considering weak currents ie. (anti)neutrino scattering, or when polarization is important. It can be seen that 'non-singlet' and 'singlet' refer to the presence and absence, respectively, of the flavour generators τ^a.

2.3.3 Expansion of Structure Functions

To apply the light-cone OPE to the forward, virtual Compton amplitude $T_{\mu\nu}$ we first decompose $T_{\mu\nu}$ similarly to eqn. (2.12)

$$\begin{aligned} T_{\mu\nu} &= (g_{\mu\nu} - \frac{q_\mu q_\nu}{q^2})T_L(x,q^2) \\ &\quad +(\frac{p_\mu q_\nu + p_\nu q_\mu}{M\nu} + \cdots)T_2(x,q^2). \end{aligned} \tag{2.36}$$

At this stage we will only consider the non-singlet contribution to T_2. Now expanding $T(J_\mu J_\nu)$ and taking the Fourier transform, we have

$$T_{2_{NS}} = \sum_n \int d^4\xi \; e^{iq\cdot\xi} C_{NS}^{(n)}(\xi^2)\xi_{\lambda_1}\ldots\xi_{\lambda_n}\langle p|O_{NS}^{(n)\lambda_1\ldots\lambda_n}(0)|p\rangle_c. \tag{2.37}$$

The matrix element in eqn.(2.37) is a problem as we have no information about the states $|p\rangle$. However the matrix element does have a fairly simple general form because $O^{\lambda_1\ldots\lambda_n}$ is traceless and symmetric

$$\langle p|O_{NS}^{(n)\lambda_1\ldots\lambda_n}(0)|p\rangle = A_{NS}^{(n)}(p^{\lambda_1}\cdots p^{\lambda_n}) + \text{trace terms}. \tag{2.38}$$

The $A_{NS}^{(n)}$ are called reduced matrix elements. The integral in eqn.(2.37) is now the Fourier transform of $C_{NS}^{(n)}(\xi^2)\xi_{\lambda_1}\ldots\xi_{\lambda_n}$ which must be proportional to $q_{\lambda_1}\ldots q_{\lambda_n}$:

$$\int d^4\xi\, e^{iq.\xi} C_{NS}^{(n)}(\xi^2)\xi_{\lambda_1}\cdots\xi_{\lambda_n} = (-1)^n \frac{q_{\lambda_1}\cdots q_{\lambda_n}}{(q^2)^n}\tilde{C}_{NS}^{(n)}(q^2). \tag{2.39}$$

Now contracting the q_{λ_i} with the terms in eqn.(2.38) will give $(q.p)^n = (M\nu)^n$ from the non-trace terms, plus terms $O(\frac{M^2}{q^2})$ from the trace terms, which we neglect. The error in neglecting these terms is of order $n\frac{M^2}{q^2}$. In the limit $q^2 \to -\infty$ we have the leading behavior:

$$T_{2_{NS}} \approx 4\sum_n \left(\frac{1}{x}\right)^n \tilde{C}_{NS}^{(n)}(q^2) A_{NS}^{(n)}, \quad x = -\frac{q^2}{2p.q} \tag{2.40}$$

where factors of 2^{-n} are absorbed in $\tilde{C}_{NS}^{(n)}(q^2)$. This looks like a Taylor expansion in $(1/x)$, but we must remember that it is the first term in an asymptotic expansion in $(1/q^2)$ as $q^2 \to -\infty$.

The form of eqn.(2.40) is quite remarkable because the x and q^2 dependence are separated from the matrix element dependence, which is solely in the $A^{(n)}$. This behavior follows directly from the form of the OPE, in which the singular light-cone behavior appears only in the c-number coefficients, while the operators remain regular. The form of eqn.(2.40) is quite general; the same procedure works for the singlet operators and for the other structure functions in the decomposition of $T_{\mu\nu}$ [Dunne 86,Ynd 83,Buras 80,Pet 79].

2.4 Dispersion Relations

Eqn.(2.40) defines $T_{\mu\nu}$ as a function of complex x which is analytic as $|x| \to \infty$ and has a cut $-1 \leq x \leq 1$. Unfortunately the physical region corresponds to $0 \leq x \leq 1$ so we need to use dispersion relations to find out about the physical structure functions.

For simplicity we drop the Lorentz indices from $T_{\mu\nu}$ and consider the analytic function $T(\nu, q^2)$ at fixed q^2. First we note that $T(\nu, q^2)$ is crossing symmetric ie. $T(\nu, q^2) = T(-\nu, q^2)$, which implies that only even values of n contribute to eqn.(2.40). Furthermore $T(\nu, q^2)$ has cuts along the real axis from $\mp q^2/2M$ to $\pm\infty$. The right-hand cut corresponds to physical Compton scattering, and the left-hand cut corresponds to the 'crossed' process $p \to \gamma + X$. The discontinuity across the right-hand cut is:

$$\mathrm{disc}T(\nu, q^2) = 2i\mathrm{Im}T(\nu, q^2) = 4\pi i W(\nu, q^2). \tag{2.41}$$

Using Cauchy's theorem on the contour in Fig. 2.3 we obtain

$$T(\nu, q^2) = 4\int_{-q^2/2M}^{\infty} d\nu' \frac{\nu'}{\nu'^2 - \nu^2} W(\nu', q^2) \tag{2.42}$$

where ν' is real, and the physical Compton amplitude is obtained by letting ν approach the positive real axis from above, $\nu \to \nu_R + i\epsilon$. The integral may not converge if $W(\nu', q^2)$ falls too slowly in the limit $\nu' \to \infty$. In that case we make a subtraction between two different values of ν

$$T(\nu, q^2) = T(0, q^2) + 4\nu\int_{-q^2/2M}^{\infty} d\nu' \frac{\nu'}{\nu(\nu'^2 - \nu^2)} W(\nu', q^2). \tag{2.43}$$

If necessary we can make further subtractions, and the process works if $W(\nu', q^2)$ is polynomial bounded as $\nu' \to \infty$, which we assume. Changing to more convenient variables $\omega \equiv 1/x = -2M\nu/q^2$ we have

$$T(\omega, q^2) = P_{m-1}(\omega, q^2) + 4\omega^{m+1}\int_1^{\infty} d\omega' \frac{\omega'}{\omega'^m(\omega'^2 - \omega^2)} W(\omega', q^2) \tag{2.44}$$

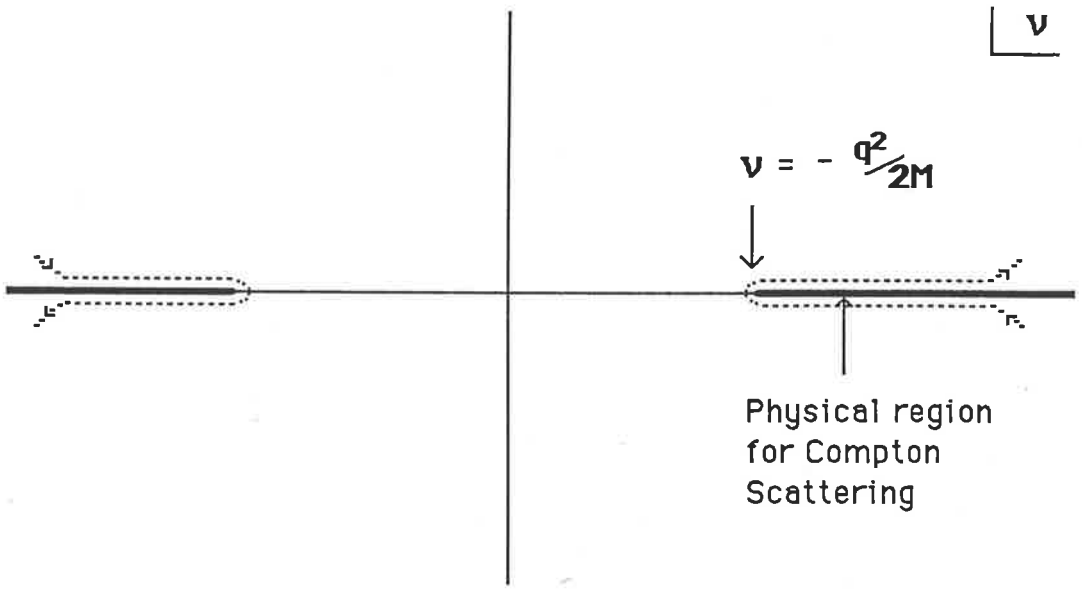

Fig 2.3 The complex ν plane. The contour shown is used to derive dispersion relations.

where P_{m-1} is a polynomial of degree $m-1$. Now using the fact that $(1-\omega^2)^{-1} = \sum_n \omega^{2n}$ we have

$$\begin{aligned} T(\omega, q^2) &= P_{m-1}(\omega, q^2) + 4 \sum_{\substack{n=m+1 \\ n\ even}}^{\infty} \omega^n \int_1^{\infty} \frac{d\omega'}{\omega'^{n+1}} W(\omega', q^2) \\ &= P_{m-1}\left(\frac{1}{x}, q^2\right) + 4 \sum_n^{\infty} \left(\frac{1}{x}\right)^n \int_0^1 dx x^{n-1} W(x, q^2). \end{aligned} \tag{2.45}$$

Comparing eqn.(2.45) with eqn.(2.40) gives

$$\tilde{C}^{(n)}(q^2) A^{(n)} = \int_0^1 dx x^{n-1} W(x, q^2) \tag{2.46}$$

where n is even. Thus the behavior of the c-number coefficients in the light-cone OPE is related to the moments of the physical structure functions for DIS. At this point we could go on to discuss the q^2 dependence of the $\tilde{C}^{(n)}(q^2)$, and of the structure functions, that is introduced because of renormalization of the theory. However we shall postpone this and look next at the quark-parton model.

2.5 The Quark-Parton Model

The Quark-Parton Model (QPM) was first introduced in the late 1960's by Bjorken and Feynmann [Bjor 66 69,BjP 71,Fey 69]. We may regard it as a free field approximation to the full QCD field theory. The currents J are treated as in a free field theory, but not the states. Thus we ignore final state interactions and vertex corrections (to the currents). The currents couple only to quarks or antiquarks. The structure function $W_{\mu\nu}$ is obtained by putting the intermediate state on-shell, with the struck quark or antiquark and the remnants of the target appearing as separate, physical intermediate states as shown in Fig. 2.4. As we have already noted in Sec-

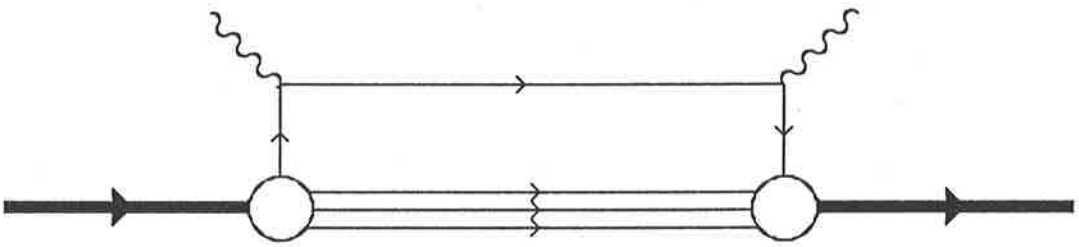

Fig 2.4 The Quark-Parton model. The struck quark and the target remains are both on-shell.

tion 2.3.2, terms with twist greater than 2 in the light-cone OPE are expected to be suppressed at least by $O(1/Q^2)$, so they are ignored in the QPM. In fact when QCD is renormalized we find that terms which vanish like a power of Q^2 in the QPM may only vanish like a power of $\log Q^2$ in the full theory. It is also important to keep in mind the fact that quantities which scale in the QPM, ie. become functions of Bjorken x alone, will be modulated by powers of $\log Q^2$ when QCD interactions are included.

Of course the QPM cannot be correct: in the intermediate state the quarks cannot be free, but must be confined by non-perturbative QCD processes. The major assumption made is that these non-perturbative processes do not affect the dominant terms at large Q^2, and this assumption is justified by the idea of 'asymptotic freedom' in QCD.

2.5.1 Derivation of the Quark-Parton Model

In a free quark theory the currents are [Jaffe 86]

$$J_\mu(\xi) = \bar{\psi}(\xi)\mathcal{Q}\gamma_\mu\psi(\xi) \tag{2.47}$$

where $\mathcal{Q}$ is the quark charge matrix ($\mathcal{Q} = \mathrm{diag}(2/3, -1/3, -1/3\ldots)$). The current commutator in the definition of $W_{\mu\nu}$, eqn. (2.9), reduces to

$$\begin{aligned}[J_\mu^\dagger(\xi), J_\nu(0)] \;=\; & \bar{\psi}(\xi)\gamma_\mu\{\psi(\xi), \bar{\psi}(0)\}\mathcal{Q}^2\gamma_\nu\psi(0) \\ & - \bar{\psi}(0)\gamma_\nu\{\psi(0), \bar{\psi}(\xi)\}\mathcal{Q}^2\gamma_\mu\psi(\xi)\end{aligned} \tag{2.48}$$

with [IZ 80]

$$\{\psi(\xi), \bar{\psi}(0)\} = \frac{1}{2\pi}\gamma_\rho \frac{\partial}{\partial \xi_\rho}[\varepsilon(\xi^0)\delta(\xi^2) + O(m^2/Q^2)\ldots]. \tag{2.49}$$

We ignore the terms in the quark masses as they generate only $O(m^2/Q^2)$ corrections in the Bjorken limit. To simplify eqn. (2.48) we use the Dirac matrix identity [IZ 80]:

$$\begin{aligned} \frac{1}{2}(\gamma_\mu\gamma_\rho\gamma_\nu + \gamma_\nu\gamma_\rho\gamma_\mu) &= (g_{\mu\rho}g_{\nu\sigma} + g_{\mu\sigma}g_{\nu\rho} - g_{\mu\nu}g_{\rho\sigma})\gamma^\sigma \\ &\equiv S_{\mu\rho\nu\sigma}\gamma^\sigma, \end{aligned} \tag{2.50}$$

then substituting eqns. (2.48–2.50) into the definition of $W_{\mu\nu}$ we have

$$\begin{aligned} \lim_{Bj} W_{\mu\nu} &= \frac{1}{8\pi^2} S_{\mu\rho\nu\sigma} \int d^4\xi \, e^{iq\cdot\xi}[\frac{\partial}{\partial \xi_\rho}\varepsilon(\xi^0)\delta(\xi^2)] \\ &\quad \times \langle p|\bar{\psi}(\xi)\gamma^\sigma \mathcal{Q}^2\psi(0) - \bar{\psi}(0)\gamma^\sigma \mathcal{Q}^2\psi(\xi)|p\rangle_c, \end{aligned} \tag{2.51}$$

where the $\lim_{Bj}$ reminds us that our QPM assumptions are only valid as $Q^2 \to \infty$ with fixed $x = Q^2/2M\nu$. Integrating by parts, we can drop the term in which $\partial/\partial\xi_\rho$ acts on the matrix element, as this will generate factors p^ρ or ξ^ρ, both of which are negligible with respect to q^ρ in the Bjorken limit (the F.T. of ξ^ρ is q^ρ/q^2). Introducing light-cone coordinates and working in the target rest frame, we then have

$$\begin{aligned} \lim_{Bj} W_{\mu\nu} &= \lim_{q^-\to\infty} \frac{-i}{8\pi^2} S_{\mu\rho\nu\sigma} q^\rho \int d\xi^+ d\xi^- d^2\vec{\xi}_\perp \, e^{iq^+\xi^- + iq^-\xi^+} \\ &\quad \times \varepsilon(\xi^+ + \xi^-)\delta(2\xi^+\xi^- - \vec{\xi}_\perp^2) \\ &\quad \times \langle p|\bar{\psi}(\xi)\gamma^\sigma \mathcal{Q}^2\psi(0) - \bar{\psi}(0)\gamma^\sigma \mathcal{Q}^2\psi(\xi)|p\rangle_c. \end{aligned} \tag{2.52}$$

If we look at the form of $S_{\mu\rho\nu\sigma}$, we see that the coefficient of $g_{\mu\nu}$ in $W_{\mu\nu}$ will equal half the trace of $W_{\mu\nu}$. From our decomposition of $W_{\mu\nu}$ in eqn. (2.12) this leads to

$$W_1 = \frac{1}{2}\left[3W_1 - \left(1 + \frac{\nu}{2M_A x_A}\right) W_2\right]$$

or, using the structure functions defined in eqn. (2.15) and noting that $1 \ll \nu/M_A$,

$$F_2(x_A) = 2x_A F_1(x_A) \tag{2.53}$$

which is known as the Callen-Gross relation, and follows from the quark spin being 1/2 (see [Close 79] or [LP 82] for details).

We can use the δ-function in eqn. (2.52) to do the integral over $\vec{\xi}_\perp^2$ using $\int d^2\vec{\xi}_\perp \delta(\vec{\xi}_\perp^2 - 2\xi^+\xi^-) = \pi$, and introducing the structure function $F_2(x_A)$ we have

$$\begin{aligned} F_2(x_A) &= 2x_A \lim_{q^-\to\infty} \frac{-iq^-}{8\pi} \int d\xi^+ d\xi^-\, e^{iq^+\xi^- + iq^-\xi^+} \\ &\quad \times[\theta(\xi^+)\theta(\xi^-) - \theta(-\xi^+)\theta(-\xi^-)] \\ &\quad \times\langle p|\bar{\psi}(\xi)\gamma^+\mathcal{Q}^2\psi(0) - \bar{\psi}(0)\gamma^+\mathcal{Q}^2\psi(\xi)|p\rangle_c|_{\vec{\xi}_\perp^2 = 2\xi^+\xi^-} \end{aligned} \tag{2.54}$$

where the indices ρ and σ must be $-$ and $+$ respectively as $g^{++} = g^{--} = 0$. Integrating by parts over ξ^+ and keeping only the leading term at large q^-:

$$\begin{aligned} F_2(x_A) &= \frac{x_A}{4\pi} \int d\xi^-\, e^{iq^+\xi^-} \langle p|\bar{\psi}(\xi^-)\gamma^+\mathcal{Q}^2\psi(0) \\ &\qquad -\bar{\psi}(0)\gamma^+\mathcal{Q}^2\psi(\xi^-)|p\rangle_c|_{\xi^+ = \vec{\xi}_\perp = 0} \end{aligned} \tag{2.55}$$

$$\begin{aligned} &= \frac{\sqrt{2}x_A}{4\pi} \int d\xi^-\, e^{iq^+\xi^-} \langle p|\psi_+^\dagger(\xi^-)\mathcal{Q}^2\psi_+(0) \\ &\qquad +\psi_+(\xi^-)\mathcal{Q}^2\psi_+^\dagger(0)|p\rangle_c|_{\xi^+ = \vec{\xi}_\perp = 0} \end{aligned} \tag{2.56}$$

where we have used the projection operator

$$\psi_\pm \equiv P^\pm\psi\ ,\ P^\pm = \frac{1}{2}\gamma^\mp\gamma^\pm = \frac{1}{2}(I \pm \alpha^3). \tag{2.57}$$

To interchange the quark fields in the second term of eqn. (2.56) we have used the fact that the singularity in the product of the fields is in fact not connected, so it can't contribute to the *connected* matrix element ie.

$$\langle p|\bar{\psi}(0)\psi(\xi)|p\rangle_c = -\langle p|\psi(\xi)\bar{\psi}(0)|p\rangle_c \tag{2.58}$$

Eqn. (2.56) is very important, and we shall make much use of it. We note first that $F_2(x_A)$ measures light-cone quark correlation functions: the first term measures the amplitude to remove a quark from the target nucleus and replace it at a point ξ on the light-cone, and the second measures the amplitude to remove and replace an antiquark.

To get to the more familiar form of the QPM we introduce a complete set of states $\sum_n |n\rangle\langle n| = 1$, which we insert between the quark fields. Translating the ξ^- dependence out of the quark fields and integrating over ξ^- gives

$$\begin{aligned} F_2^A(x_A) &= x_A \sum_a e_a^2 \sum_n \frac{1}{\sqrt{2}} \delta(p^+ + q^+ - p_n^+)\{|\langle n|\psi_{a+}(0)|p\rangle|^2 \\ &\qquad + |\langle n|\psi_{a+}^\dagger(0)|p\rangle|^2\} \qquad (2.59) \\ &= x_A \sum_a e_a^2 (f_{a/A}(x_A) + f_{\bar{a}/A}(x_A)) \qquad (2.60) \end{aligned}$$

where we have summed explicitly over quark flavours a, e_a being the charge of a quark of flavour a, and the superscript A on F_2 is to remind us of the target dependence of F_2. Remembering that $q^+ = -x_A p^+$ in the nucleus rest frame, the distributions $f(x_A)$ are written as

$$\begin{aligned} f_{a/A}(x_A) &= \frac{1}{\sqrt{2}} \sum_n \delta(p^+ - x_A p^+ - p_n^+)|\langle n|\psi_{a+}|p\rangle|^2 \\ f_{\bar{a}/A}(x_A) &= \frac{1}{\sqrt{2}} \sum_n \delta(p^+ - x_A p^+ - p_n^+)|\langle n|\psi_{a+}^\dagger|p\rangle|^2. \end{aligned} \tag{2.61}$$

So $f_{a/A}(x_A)$ is the probability per unit x_A to remove from the target a quark of flavour a with plus component of momentum $x_A p^+$, leaving behind a physical state $|n\rangle$ with plus component of momentum $p_n^+ = (1 - x_A)p^+$. Similarly $f_{\bar{a}/A}(x_A)$ is the probability to remove an antiquark of flavour a, plus component of momentum $x_A p^+$, leaving a physical state with $p_n^+ = (1 - x_A)p^+$. Note that in our target rest frame formulation of the QPM, p^+ appears where P_∞ appears in the 'infinite momentum frame' formulation.

We can also note that the distribution function $f(x_A)$ is related to the forward virtual quark-target scattering amplitude $\mathcal{A}_{\mu\nu}(p,k)$ in the $A^+ = 0$ gauge [Jaffe 83],

$$\mathcal{A}_{\mu\nu}(p,k) = \int d^4\xi \; e^{-ik.\xi} \langle p|T(\bar{\psi}_\mu(\xi)\psi_\nu(0))|p\rangle_c. \tag{2.62}$$

To obtain $f(x_A)$ we take the trace of $\mathcal{A}_{\mu\nu}(p,k)$ with γ^+ and integrating over k at fixed $k^+ = x_A p^+$:

$$f(x_A) = \int \frac{d^4k}{(2\pi)^4} \delta(k^+ - x_A p^+) \frac{1}{p^+} \mathrm{Tr}[\gamma^+ \mathcal{A}_{\mu\nu}(p,k)]. \tag{2.63}$$

The distribution functions $f(x_A)$ have several important properties. Firstly, the state $|n\rangle$ in eqn. (2.61) is physical so $p_n^+ > 0$, thus $f(x_A)$ must vanish for $x_A \geq 1$. Secondly, on $0 < x_A < 1$ the $f(x_A)$ are manifestly positive. For $x_A < 0$ consider

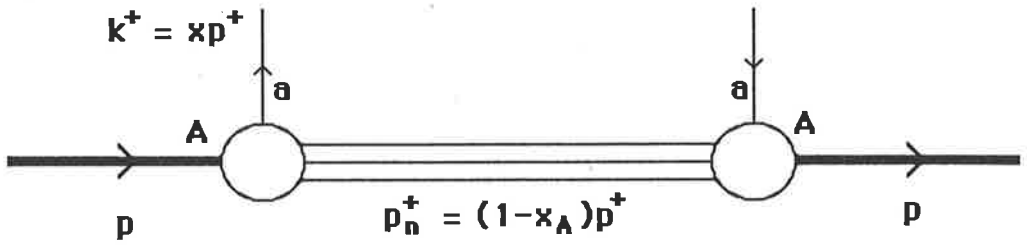

Fig 2.5a The quark distribution function $f_{a/A}(x_A)$

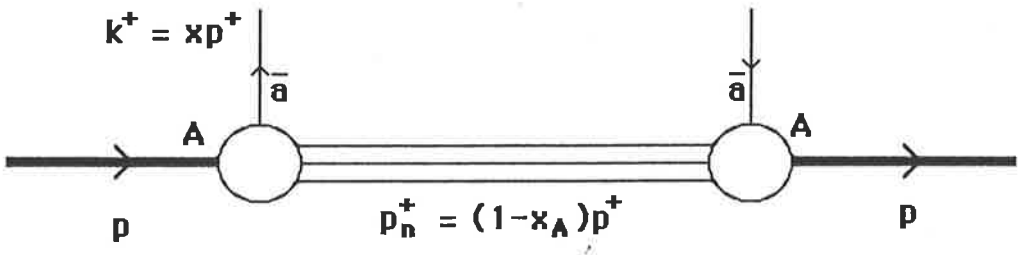

Fig 2.5b The anti-quark distribution function $f_{\bar{a}/A}(x_A)$

eqn. (2.56)

$$\begin{aligned} f_{a/A}(x_A) &= \frac{\sqrt{2}}{4\pi}\int d\xi^- \, e^{iq^+\xi^-}\langle p|\psi^\dagger_{a+}(\xi)\psi_{a+}(0)|p\rangle_c|_{\xi^+=\vec{\xi}_\perp=0} \\ &= -\frac{\sqrt{2}}{4\pi}\int d\xi^- \, e^{iq^+\xi^-}\langle p|\psi_{a+}(0)\psi^\dagger_{a+}(\xi)|p\rangle_c|_{\xi^+=\vec{\xi}_\perp=0} \\ &\qquad\qquad\qquad\qquad\qquad\qquad\qquad\qquad\qquad\qquad\qquad\qquad \text{(using eqn.(2.58))} \\ &= -\frac{\sqrt{2}}{4\pi}\int d\xi^- \, e^{-iq^+\xi^-}\langle p|\psi_{a+}(\xi)\psi^\dagger_{a+}(0)|p\rangle_c|_{\xi^+=\vec{\xi}_\perp=0} \\ &\qquad\qquad\qquad\qquad\qquad\qquad\qquad\qquad\qquad\qquad\qquad\qquad (\xi^- \to -\xi^- \text{and translating}) \\ &= -f_{\bar{a}/A}(-x_A). \end{aligned} \tag{2.64}$$

So for negative x_A the quark distribution function is determined by the antiquark distribution for positive x_A, and vice versa. This means that x_A is restricted to $-1 \leq x_A \leq 1$, and that measurements in the physical region $0 < x_A \leq 1$ determine the distribution functions everywhere. We shall discuss this point later.

We can integrate $f_{a/A}(x_A)$ over all x_A. Using eqn. (2.56) and $x_A = -\sqrt{2}q^+/M_A$ we have

$$\begin{aligned} \int_{-\infty}^{\infty} dx_A \, f_{a/A}(x_A) &= \frac{1}{2\pi M_A}\int dq^+ d\xi^- \, e^{iq^+\xi^-} \\ &\qquad\qquad \times\langle p|\psi^\dagger_{a+}(\xi)\psi_{a+}(0)|p\rangle_c|_{\xi^+=\vec{\xi}_\perp=0} \\ &= \frac{1}{M_A}\langle p|\psi^\dagger_{a+}(0)\psi_{a+}(0)|p\rangle_c. \end{aligned} \tag{2.65}$$

Now $\psi^\dagger_{a+}\psi_{a+} = \frac{1}{\sqrt{2}}j_{a+}$ is a conserved current, and its expectation value is the number of quarks of flavour a minus the number of antiquarks of flavour a. Combining this with the relation given in eqn. (2.64) and the physical limits on x_A gives

$$\int_0^1 dx_A \, (f_{a/A}(x_A) - f_{\bar{a}/A}(x_A)) = N_{a/A} - N_{\bar{a}/A} \tag{2.66}$$

so we may interpret $f_{a/A}(x_A)$ ($f_{\bar{a}/A}(x_A)$) as the probability per unit x_A to find a quark (antiquark) of flavour a with $k^+ = x_A p^+$ in the nucleus A:

$$f_{a/A}(x_A) = dP_{a/A}/dx_A. \tag{2.67}$$

This interpretation is the real power of the QPM. A host of sum rules may be derived immediately from this result. Probably the most important here is the 'momentum sum rule':

$$\int_0^1 dx_A \, x_A(f_{a/A}(x_A) - f_{\bar{a}/A}(x_A)) = (k^+_{a/A} + k^+_{\bar{a}/A})/p^+ \tag{2.68}$$

where $k^+_{a/A}/p^+$ is the fraction of the p^+ of the nucleus carried by quarks of flavour a. If hadrons contained only quarks and antiquarks, the sum over flavours of eqn.(2.68) would be 1. Experimentally, it is typically $\sim 50\%$ [LP 82], indicating that a substantial proportion of the four momentum of the nucleus is carried by glue.

2.5.2 The Operator Product Expansion and the Quark-Parton Model

We have an expression eqn. (2.40) for the structure function T_2 in terms of the reduced matrix elements $A^{(n)}$

$$\frac{p.q}{M^2} T_2(x) = 4x \sum_{n \, even} \left(\frac{1}{x}\right)^n \tilde{C}^{(n)} A^{(n)} \tag{2.69}$$

where we have dropped the dependence on q^2 in accordance with the assumptions of the QPM. Now if we set all the Lorentz indices to + in eqn. (2.38), which defines the reduced matrix elements, we have

$$A^{(n)} = \left(\frac{1}{p^+}\right)^n \langle p|O^{+\cdots+}|p\rangle_c. \tag{2.70}$$

The trace terms have vanished as $g^{++} = 0$. The matrix elements is simply given by all two particle irreducible insertions of the vertex $\psi\gamma^+(k^+)^{n-1}\psi$ (in the $A^+ = 0$ gauge, where $D_\mu \to d_\mu$) in the virtual forward quark scattering amplitude $\mathcal{A}_{\mu\nu}(p,k)$, eqn. (2.62) (see Fig. 2.6). Thus

$$A^{(n)} = \left(\frac{1}{p^+}\right)^n \int \frac{d^4k}{(2\pi)^4} (k^+)^{n-1} \mathrm{Tr}[\gamma^+ \mathcal{A}_{\mu\nu}(p,k)]. \tag{2.71}$$

Comparing with eqn. (2.63) for the quark distribution function we have

$$A^{(n)} = \int_{-1}^{1} dx\, x^{n-1} f(x). \tag{2.72}$$

This gives the reduced matrix elements in terms of the moments of the quark distribution functions. Comparing with eqn. (2.46) shows that in the QPM the $\tilde{C}^{(n)}$ are all unity. This is not unexpected. The OPE expansion eqn. (2.40) separated the Q^2 dependence from the matrix element dependence, so in the QPM model,where we assume that there is no Q^2 dependence as $Q^2 \to \infty$, it is no surprise that the $C^{(n)}$ are trivial [Pet 79].

Now substituting eqn. (2.72) into the expansion eqn. (2.69) with $C^{(n)} = 1$, and interchanging the sum and the integral we have:

$$\begin{aligned} \frac{p.q}{M^2} T_2(x) &= 4 \int_{-1}^{1} dx' \sum_{n\ even} \left(\frac{x'}{x}\right)^n f(x) \\ &= 2x \int_{-1}^{1} dx'\, f(x) \left(\frac{1}{x - x'} - \frac{1}{x + x'}\right). \end{aligned} \tag{2.73}$$

To get to the physical region we analytically continue T_2, substituting $x \to x - i\epsilon$ with x real and $0 < x \leq 1$

$$\frac{p.q}{M^2} T_2(x) = 4\pi i x [f(x) - f(-x)]. \tag{2.74}$$

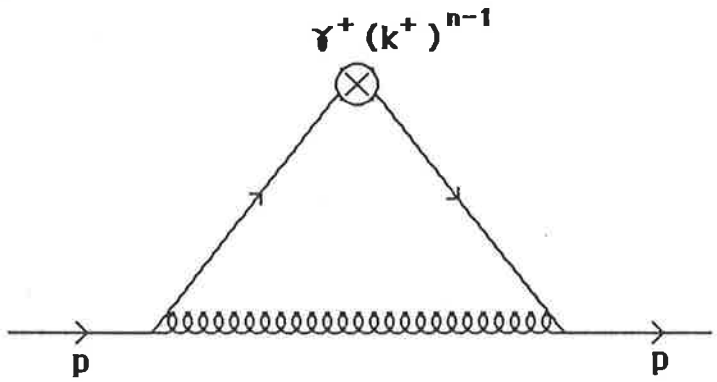

Fig 2.6 Contributions to $A^{(n)}$ equation (2.70)

Finally we take the imaginary part of T_2 to obtain the structure function F_2,

$$F_2(x) = x[f(x) - f(-x)] \qquad 0 < x \leq 1 \tag{2.75}$$

which, when we use the relation between the quark and antiquark distribution functions eqn. (2.64), is the same as obtained earlier.

It is important to note that the QPM emerges by choice. In the expression eqn. (2.61)

$$f(x) = \frac{1}{\sqrt{2}} \sum_n \delta(p^+ - xp^+ - p_n^+) |\langle n|\psi_+|p\rangle|^2 \tag{2.76}$$

the matrix element is not connected. This means that the partially connected terms shown in Figs. 2.7b–d can contribute to $f(x)$ for $x < 0$. Similarly for

$$f(x) = -\frac{1}{\sqrt{2}} \sum_n \delta(p^+ + xp^+ - p_n^+) |\langle n|\psi_+^\dagger|p\rangle|^2 \tag{2.77}$$

the partially connected terms shown in Figs. 2.8b–d can contribute for $x > 0$. The QPM follows from *choosing* Fig. 2.7a for $x > 0$ and Fig. 2.8a for $x < 0$ [Jaffe 83].

Making this choice means that we are ignoring diagrams which include strong interaction vertices, and we are keeping only the diagrams in which the struck quark or antiquark appears to be free, that is, unaffected by strong interactions. This now means that we can approximate the current and quark operators by free operators, which gives the QPM.

2.6 Renormalization and Q^2 Dependence

In an interacting field theory, as opposed to a free theory such as the QPM, the measured structure functions F_1 and F_2, and hence the quark distribution functions

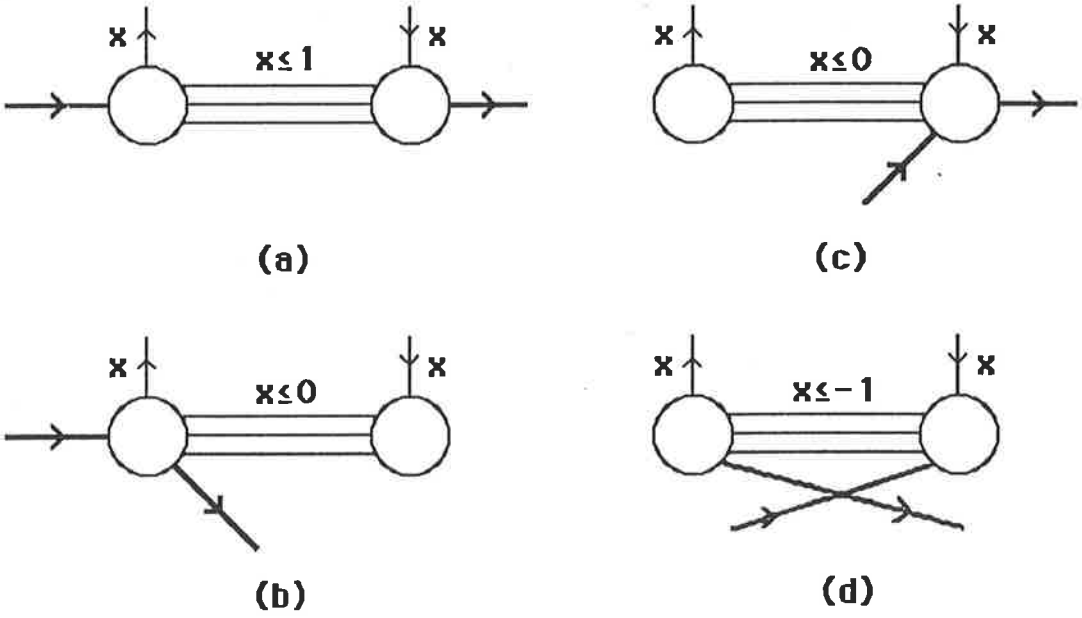

Fig 2.7 Connected and semi-connected contributions to f(x) given by equation (2.74)

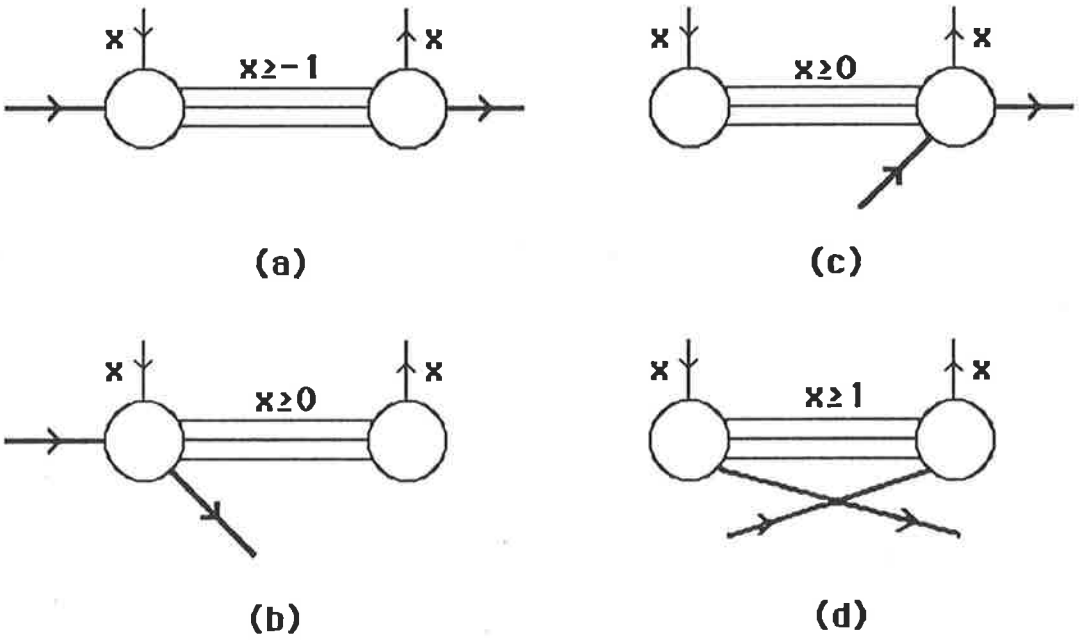

Fig 2.8 Connected and semi-connected contributions to f(x) given by equation (2.75)

f_a, must depend on Q^2 as well as x. We do not yet know how to rigorously predict $F_2(x, Q^2)$ at fixed Q^2 for a hadronic target, as it must depend strongly on the non-perturbative processes which confine the quarks. However perturbative QCD will enable us to predict the Q^2 dependence of $F_2(x, Q^2)$, so that given $F_2(x, Q_0^2)$, where Q_0^2 is reasonably large, we can predict $F_2(x, Q^2)$ for all Q^2 greater than $\sim 1\text{GeV}^2$.

Intuitively we can see that by increasing Q^2, the virtual photon (or W or Z boson) can probe the structure of the hadronic target at smaller distances. This means that we can resolve a quark into a quark plus a gluon, or quark plus quark-antiquark pair. This approach was adopted by Altarelli and Parisi [AP 77], and a similar approach using Weizsäcker-Williams kinetics has been explored by Jaffe [Jaffe 86]. However with the power of the OPE at our disposal, we shall adopt a more formal approach.

To renormalize our field theory (QCD), we must introduce an arbitrary mass scale μ^2, but this will destroy the exact scale invariance we have previously exploited in section 2.3. However the very arbitrariness of our renormalization scale leads to the renormalization group equations, which play the rôle of dimensional analysis of the operators. By introducing the concept of 'anomalous' dimensions of the operators and using the renormalization group equations, we can restore scale invariance, and find the Q^2 dependence of the coefficient functions in the OPE.

Using eqn. (2.46) let us define the moments of the structure function F_2:

$$M_2^{(n)}(Q^2) \equiv \int_0^1 dx\, x^{n-2} F_2(x, Q^2) \tag{2.78}$$

$$= C_2^{(n)}(q^2/\mu^2, g)\langle p|O^{(n)}(\mu^2)|p\rangle_c \tag{2.79}$$

where we have made explicit the dependence of the operators on the renormalization

scale μ^2, and the coefficient functions are calculated as a perturbation series in the coupling g. We are justified in the use of a perturbation series because at large Q^2 the coupling g becomes small—asymptotic freedom. We shall firstly consider non-singlet operators. These operators are multiplicatively renormalizable ie. $O^{(n)}_{NS(renorm)} = Z(\mu)O^{(n)}_{NS(unrenorm)}$. Now the moments are physically measurable, so they must be independent of the renormalization scale μ ie.

$$\mu\frac{\partial}{\partial\mu}M^{(n)}_{2_{NS}}(Q^2) = 0 \tag{2.80}$$

or

$$\langle p|O^{(n)}_{NS}|p\rangle\mu\frac{\partial}{\partial\mu}C^{(n)}_{2_{NS}} + C^{(n)}_{2_{NS}}\mu\frac{\partial}{\partial\mu}\langle p|O^{(n)}_{NS}|p\rangle = 0. \tag{2.81}$$

We now define the anomalous dimensions of $O^{(n)}_{NS}$, denoted $\gamma^{(n)}_{NS}$

$$\mu\frac{\partial}{\partial\mu}O^{(n)}_{NS(renorm)} \equiv \gamma^{(n)}_{NS}O^{(n)}_{NS(renorm)} \tag{2.82}$$

and the 'Callen-Symanzik' function $\beta(g) \equiv \mu(\partial g/\partial\mu)$. Substituting these into eqn. (2.81) gives us the renormalization group equation for the coefficient functions:

$$\left(\mu\frac{\partial}{\partial\mu} + \beta(g)\frac{\partial}{\partial g} + \gamma^{(n)}_{NS}(g)\right)C^{(n)}_{2_{NS}}(q^2/\mu^2, g) = 0. \tag{2.83}$$

But $\mu(\partial/\partial\mu) = -2q^2(\partial/\partial q^2)$, so solving eqn.(2.83) gives:

$$C^{(n)}_{2_{NS}}(q^2/\mu^2, g) = C^{(n)}_{2_{NS}}(q^2 = \mu^2, g(q^2))\exp\left[\int_{g(\mu^2)}^{g(q^2)} dg'\,\frac{\gamma^{(n)}_{NS}(g')}{\beta(g')}\right]. \tag{2.84}$$

This solution is exact, but to make use of it we require perturbation expansions of $\beta(g)$, $\gamma^{(n)}_{NS}(g)$ and $C^{(n)}_{2_{NS}}(q^2 = \mu^2, g)$. These are available, and to leading order yield

[Buras 80]:

$$\beta(g) = -\beta_0 \frac{g^3}{16\pi^2} + O(g^5) \tag{2.85}$$

$$\gamma_{NS}^{(n)}(g) = \gamma_{NS}^{(n)(0)} \frac{g^2}{16\pi^2} + O(g^4) \tag{2.86}$$

$$C_{2_{NS}}^{(n)}(1,g) = C_{2_{NS}}^{(n)}(1,0)\{1 + C_{2_{NS}}^{(n)(1)}(1,0)\frac{g^2}{16\pi^2} + O(g^4)\} \tag{2.87}$$

$$g(Q^2) = \frac{16\pi^2}{\beta_0 \log(Q^2/\Lambda^2)} \tag{2.88}$$

where

$$\beta_0 = \frac{1}{3}(33 - 2n_f) \qquad (n_f = \text{number of flavours}) \tag{2.89}$$

$$\gamma_{NS}^{(n)(0)} = \frac{8}{3}\left[1 - \frac{2}{n(n+1)} + 4\sum_{j=2}^{n}\frac{1}{j}\right] \tag{2.90}$$

$$\Lambda^2 = \mu^2 \exp[-16\pi^2/\beta_0 g(\mu^2)] \tag{2.91}$$

and $C_{2_{NS}}^{(n)}(1,0)$ is the free field value and is a constant.

Combining these leading order expansions, we have the leading order behavior of the coefficient function

$$C_{2_{NS}}^{(n)}(q^2/\mu^2, g) = C_{2_{NS}}^{(n)}(1,0)\left[\frac{g(\mu^2)}{g(Q^2)}\right]^{-d_{NS}^{(n)}} \tag{2.92}$$

where

$$d_{NS}^{(n)} \equiv \frac{\gamma_{NS}^{(n)(0)}}{2\beta_0}. \tag{2.93}$$

We can now derive an expression for the Q^2 dependence of the moments $M_{2_{NS}}^{(n)}$, remembering that the matrix elements in eqn. (2.79) have no Q^2 dependence

$$M_{2_{NS}}^{(n)}(Q^2) = M_{2_{NS}}^{(n)}(Q_0^2)\left[\frac{\ln(Q^2/\Lambda^2)}{\ln(Q_0^2/\Lambda^2)}\right]^{-d_{NS}^{(n)}}. \tag{2.94}$$

Comparing this with eqn.(2.72), we see that QCD predicts logarithmic scaling violations in comparison to the naive expectations of the QPM.

For the singlet operators we have the complication that the fermion (quark) and gluon operators mix under renormalization ie.

$$[O_{S(renorm)}] = \begin{bmatrix} O_F \\ O_G \end{bmatrix}_{(renorm)} = \begin{bmatrix} Z_{FF} & Z_{FG} \\ Z_{GF} & Z_{GG} \end{bmatrix} \begin{bmatrix} O_F \\ O_G \end{bmatrix}_{(unrenorm)} . \tag{2.95}$$

However the same principles apply as in the non-singlet case, but with more complicated manipulations and notations. We again obtain a logarithmic dependence of the moments on Q^2:

$$[M_S^{(n)}(Q^2)] = [M_S^{(n)}(Q_0^2)] \left[\frac{\ln(Q^2/\Lambda^2)}{\ln(Q_0^2/\Lambda^2)}\right]^{D^{(n)}} \tag{2.96}$$

$$D^{(n)} = \frac{16}{33-2n_f} \begin{bmatrix} \frac{33-2n_f}{16} d_{NS}^{(n)} & \frac{3n_f}{8} \frac{n^2+n+2}{n(n+1)(n+2)} \\ \frac{n^2+n+2}{2n(n^2-1)} & \frac{33-2n_f}{16} \frac{9}{4} [\frac{1}{n(n-1)} + \frac{1}{(n+1)(n+2)} - \sum_{j=2}^{n} \frac{1}{j}] \end{bmatrix} . \tag{2.97}$$

Scaling violations have been seen experimentally (see Fig. 2.9), and have been shown to be consistent with leading order QCD fits. We do not yet have complete predictive power of the structure functions because of the dependence on the QCD scale parameter Λ. Most fits to the data use a value of Λ in the range 100–500 MeV, with more recent data and fits favoring a value at the lower end of this range.

As mentioned earlier, leading order QCD evolution works fairly well for Q^2 greater than $\sim$1 GeV^2. The reason we cannot go to momentum transfers less than this is that $O(1/Q^2)$ effects, of which there are many,come into play. The OPE (eqn. (2.40)) we have been using applies only to twist 2 operators, and we have also ignored terms of $O(M^2/Q^2)$ which will obviously be important at low Q^2. There

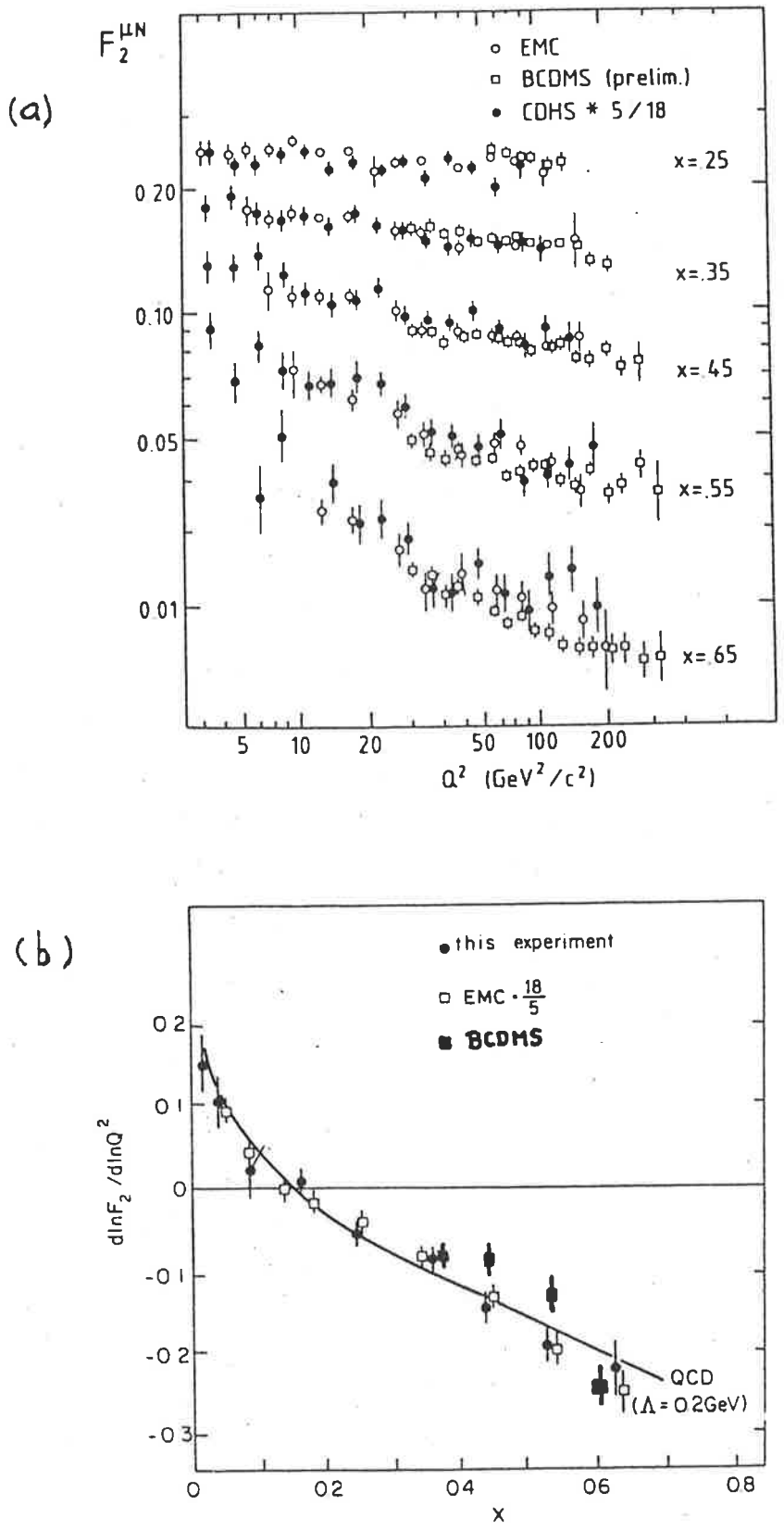

Fig 2.9 Scaling violations seen in measurements of F_2 [Eis 82].
(a) F_2 as a function of Q^2 for various fixed values of x.
(b) The rate of change of ln F_2 with respect to ln Q^2 , as a function of x. The solid curve is a leading order QCD fit with Λ = 200 MeV.

have been numerous calculations of higher twist effects and of mass effects to which the interested reader may refer [EFP 82 83,SV 81,JS 82,Jaffe 83].

2.7 Sum Rules

As we have noted in Section 2.5, the QPM interpretation of the quark distribution functions $f(x)$ as a probability function to find a quark with plus component of momentum $k^+ = xp^+$ in the target nucleus, leads us to sum rules for the distribution functions. We would like to carry this successful interpretation over to our more sophisticated QCD-based model.

The three different types of operator in the light-cone OPE (eqns. (2.31)–(2.33)) can be interpreted as contributions from 'valence' and 'sea' quarks and from gluons. The non-singlet operators represent flavour-changing interactions (ie. electro-weak) because of the presence of the flavour generators τ^a. Quarks interacting this way will carry the (flavour) quantum numbers of the target and are called 'valence' quarks. The singlet operators represent non-flavour changing interactions (ie. strong), the quark operators representing the strong interactions of all quarks and antiquarks, while the gluon operators represent the gluon interactions in the QCD theory.

Take the first moment of F_2:

$$\begin{aligned} M_2^{(1)A} &= \int_0^1 dx \, \frac{1}{x} F_2^A(x, Q^2) \\ &= \sum_a e_a^2 \int_0^1 dx \, (f_{a/A}(x_A) + f_{\bar{a}/A}(x_A)) \text{ in the QPM} \\ &= \sum_a e_a^2 (N_{a/A} + N_{\bar{a}/A}). \end{aligned} \tag{2.98}$$

Now for the non-singlet contribution to this moment, the anomalous dimension $\gamma_{NS}^{(1)}$

vanishes (this is an example of the general result that the anomalous dimensions of a conserved operator vanish), so that the number of valence quarks (antiquarks) is independent of Q^2. So we do have a basis for carrying over the QPM interpretation of the quark structure functions to our generalized model. This interpretation allows the number of sea quarks and gluons to vary with Q^2 (as the singlet anomalous dimension matrix $D^{(1)}$ does not vanish), but we have a good intuitive understanding of the mechanisms responsible for this variation: gluon bremmstrahlung and pair creation (see Fig. 2.10).

Let us now examine the distribution functions for the proton and neutron, and for the isospin averaged nucleon. By isospin symmetry we have

$$\begin{aligned}
u_p(x,Q^2) &\equiv f_{u/p}(x,Q^2) = f_{d/n}(x,Q^2), \\
d_p(x,Q^2) &\equiv f_{d/p}(x,Q^2) = f_{u/n}(x,Q^2), \\
\bar{u}_p(x,Q^2) &\equiv f_{\bar{u}/p}(x,Q^2) = f_{\bar{d}/n}(x,Q^2) \\
\bar{d}_p(x,Q^2) &\equiv f_{\bar{d}/p}(x,Q^2) = f_{\bar{u}/n}(x,Q^2) \\
s_p(x,Q^2) &\equiv f_{s/p}(x,Q^2) = f_{s/n}(x,Q^2) \simeq f_{\bar{s}/p}(x,Q^2) = f_{\bar{s}/n}(x,Q^2)
\end{aligned} \tag{2.99}$$

and for the nucleon we have

$$\begin{aligned}
f_{u/N}(x,Q^2) = f_{d/N}(x,Q^2) &= f_V(x,Q^2) + f_S(x,Q^2) \\
f_{\bar{u}/N}(x,Q^2) = f_{\bar{d}/N}(x,Q^2) &= f_S(x,Q^2).
\end{aligned} \tag{2.100}$$

For the heavier quarks we typically assume

$$\begin{aligned}
f_{s/N}(x,Q^2) &= f_{\bar{s}/N}(x,Q^2) \lesssim f_S(x,Q^2) \\
f_{c/N}(x,Q^2) &= f_{\bar{c}/N}(x,Q^2) \approx 0.
\end{aligned} \tag{2.101}$$

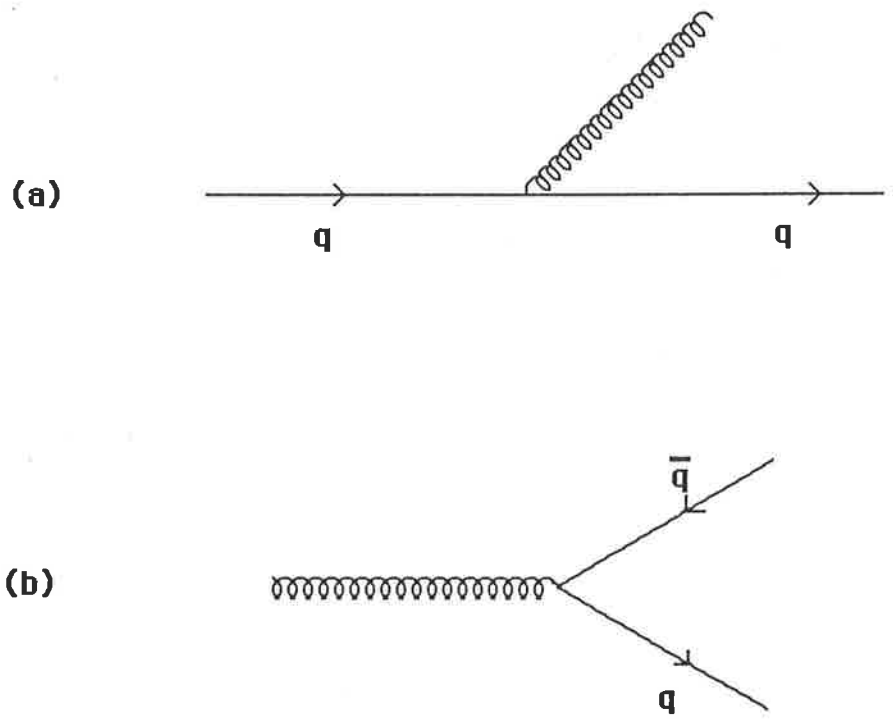

Fig 2.10 Gluon bremmstrahlung and pair creation which are responsible for the dependence of the structure functions on Q^2

We can express the measured structure functions in terms of the quark distribution functions and the quark charges

$$\begin{aligned}
F_2^{ep}(x,Q^2) &= \frac{x}{9}[4(u_p(x,Q^2)+\bar{u}_p(x,Q^2)) \\
&\quad +d_p(x,Q^2)+\bar{d}_p(x,Q^2)+s_p(x,Q^2)+\bar{s}_p(x,Q^2)] \\
F_2^{en}(x,Q^2) &= \frac{x}{9}[4(d_p(x,Q^2)+\bar{d}_p(x,Q^2)) \\
&\quad +u_p(x,Q^2)+\bar{u}_p(x,Q^2)+s_p(x,Q^2)+\bar{s}_p(x,Q^2)] \\
F_2^{\nu p}(x,Q^2) &= F_2^{\bar{\nu}n}(x,Q^2) = x[d_p(x,Q^2)+\bar{u}_p(x,Q^2)+s_p(x,Q^2)] \\
F_2^{\nu n}(x,Q^2) &= F_2^{\bar{\nu}p}(x,Q^2) = x[u_p(x,Q^2)+\bar{d}_p(x,Q^2)+\bar{s}_p(x,Q^2)] \\
xF_3^{\nu p}(x,Q^2) &= xF_3^{\bar{\nu}n}(x,Q^2) = x[d_p(x,Q^2)-\bar{u}_p(x,Q^2)] \\
xF_3^{\nu n}(x,Q^2) &= xF_3^{\bar{\nu}p}(x,Q^2) = x[u_p(x,Q^2)-\bar{d}_p(x,Q^2)]
\end{aligned} \tag{2.102}$$

where for weak interactions we have ignored the Cabbibo angle ($\sin\theta_C \simeq 0.05$) and the heavier quarks. Thus we can derive sum rules which are approximately verified by experiment [LP 82]:—

Baryon number

$$\int_0^1 dx\,[f_{u/p}+f_{d/p}+f_{s/p}-f_{\bar{u}/p}-f_{\bar{d}/p}-f_{\bar{s}/p}] = 3, \tag{2.103}$$

the Adler sum rule

$$\int_0^1 dx\,\frac{1}{x}[F_2^{\bar{\nu}p}-F_2^{\nu p}] = \int_0^1 dx\,\frac{1}{x}[F_2^{\bar{\nu}n}-F_2^{\nu n}] = 1, \tag{2.104}$$

and the Gross - Llewellyn-Smith sum rule

$$\int_0^1 dx\,[F_3^{\nu p}+F_3^{\nu n}] = 3. \tag{2.105}$$

A particularly interesting relation is the Nachtmann inequality:

$$\frac{1}{4} \leq \frac{F_2^{en}(x)}{F_2^{ep}(x)} \leq 4. \tag{2.106}$$

The experimental data shows that for large x the ratio is close to $\frac{1}{4}$ which suggests that at large x the momentum of the proton is being carried mainly by u quarks ie. $f_{u/p} \gg f_{d/p}$ as $x \to 1$. For small x the ratio is close to unity which suggests that the valence quarks are of lesser importance, and the symmetric sea dominates. In fact as $x \to 0$ we find experimentally that $f_V(x) \to \frac{1}{\sqrt{x}}$ and $f_S(x) \to \frac{1}{x}$.

Finally we have a relation between the electromagnetic and weak structure functions for the nucleon:

$$F_2^{eN}(x, Q^2) \simeq \frac{5}{18} F_2^{\nu N}(x, Q^2) \tag{2.107}$$

where we have ignored the strange quarks. This relation is well verified in scattering from deuterium, where only a small nuclear effect is expected. With the aid of this relation we can compare $\frac{18}{5} F_2^{eN}$ and $x F_3^{\nu N}$ (see Fig. 2.11). For $x > 0.3$ they are approximately equal, implying that valence quarks dominate in this region.

It is possible to summarize the known momentum distributions within the nucleon, at $Q^2 \approx 5\text{GeV}^2$ [Eis 82].

$$\sum_a \int_0^1 dx \, [f_a(x) + f_{\bar{a}}(x)] \approx 46\% \tag{2.108}$$

$$\sum_a \int_0^1 dx \, [f_a(x) - f_{\bar{a}}(x)] \approx 36\% \tag{2.109}$$

$$\frac{1}{2} \int_0^1 dx \, [f_{\bar{u}}(x) + f_{\bar{d}}(x)] \approx 2\% \tag{2.110}$$

$$\int_0^1 dx \, f_{\bar{s}}(x) \approx 1\%. \tag{2.111}$$

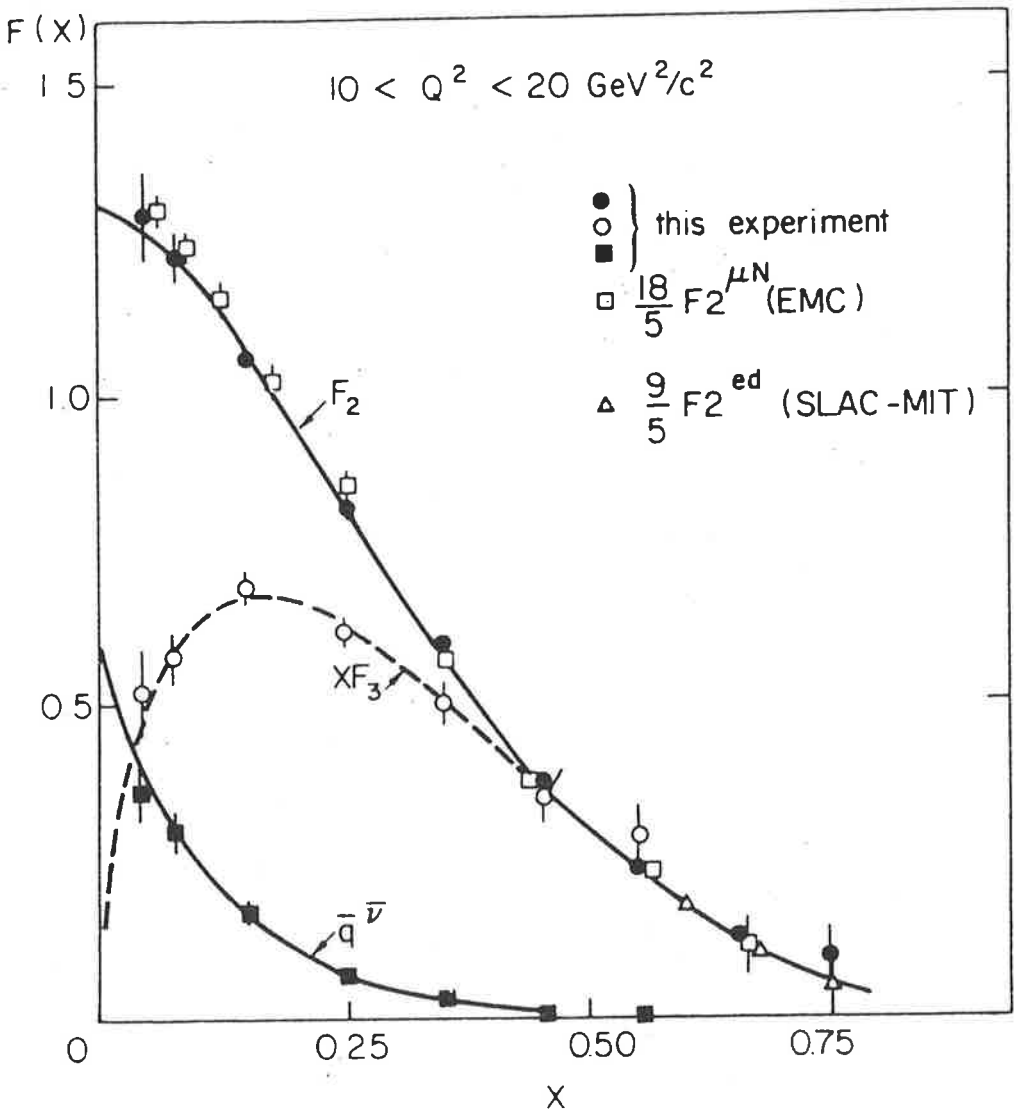

Fig 2.11 $F_2(x)$ from charged and uncharged lepton experiments. Also shown are $F_3(x)$ and $\bar{q}(x)$ from uncharged lepton scattering. [Eis 82]

Thus we have that valence quarks carry slightly more than a third of the nucleon's momentum, with a little more than a half carried by the gluons and about 10% carried by the sea. The sea breaks SU(3) flavour symmetry, with about four times as many non-strange as strange quarks. This is probably because of the higher mass of the strange quark.

Chapter 3

The E.M.C. Effect

3.1 Introduction

Prior to 1982 it was generally thought that the structure functions of different nuclei were more or less the same up to any Fermi motion corrections. That is, the nucleons in a nucleus were believed to contribute incoherently to the scattering cross-section. However the first experimental test of this assumption, by the European Muon Collaboration [Aub+ 83] (EMC), showed it to be quite wrong. The EMC group compared the structure functions $\frac{1}{A}F_2^A(x)$ for deuterium and iron ($x = Q^2/2M_N\nu$), and found that for $x < 0.3$ the structure function of iron was enhanced relative to deuterium, and for $0.3 < x < 0.7$ it was depleted. As the deuterium nucleus has a low density, its nucleons are almost free, and so the EMC effect is interpreted as a marked change in the structure functions of nucleons in nuclei which is brought about by the nuclear environment. Given the wide range of Q^2 at which the data in the various experiments have been taken ($3 < Q^2 < 200\text{GeV}^2$), and the absence of almost any Q^2 dependence (within experimental errors), the EMC effect is almost certainly not a higher twist effect.

The EMC effect has caused much excitement among nuclear and particle physicists. The reason for the excitement is that analysis of the EMC effect may provide answers to many questions about the properties of nuclear matter and nuclear forces, and to what degree QCD degrees of freedom are involved in the nucleus. Many people believe that the EMC effect stems from quark and gluonic degrees of freedom in the nucleus, and several explanations and models of the effect have been proposed along these lines.

We may summarize the experimental information which has been gathered over the past few years from charged lepton experiments [Aub+ 83,Arn+ 84,Bari+ 85], [Aub+ 87]. At very low x ($x < 0.05$) there is a depletion of the structure function of the nucleus relative to the free nucleon structure function. This depletion is highly A dependent and is probably due to 'shadowing'. In the range $0.05 < x < 0.3$ the structure function of the nucleus is enhanced, with the maximum enhancement being $\sim 10\%$ at $x \approx 0.1$, and the magnitude of the enhancement increasing with A. For $0.3 < x < 0.8$ the structure function of the nucleus is again depleted, the maximum effect being at $x \approx 0.65$ and increasing like $\log A$. Finally at higher x the structure function of the nucleus is enhanced, at least in part because of the Fermi motion of the nucleons.This information is summarized in Fig. 3.1.

From the above information we can make a simple parton model analysis. Firstly, because the 'sea' quark distribution is negligible for $x > 0.35$, the depletion in the region $0.3 < x < 0.8$ means that the valence quark distributions in nuclei are shifted to lower x. Secondly, the enhancement in the region $0.05 < x < 0.3$ corresponds to a

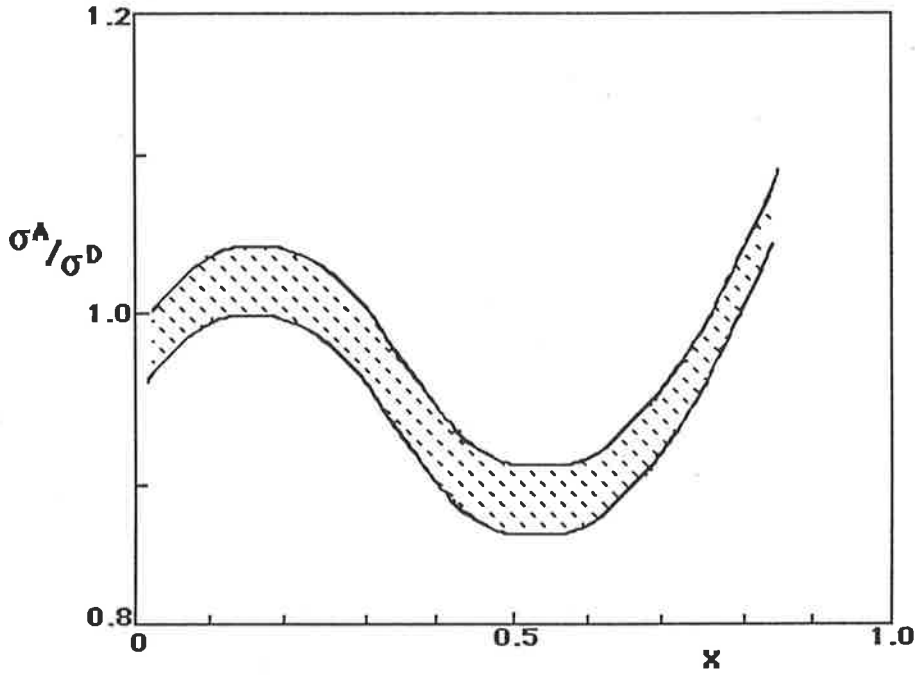

Fig 3.1 The EMC Effect. Experimental data for most nuclei lies within the hatched area.

small increase in the number of sea quark pairs. Thus there is an overall shift in the quark distributions to lower x. QCD tells us that changing the quark distributions will affect the gluon distribution. This appears to be confirmed by J/Ψ production. The EMC group found that the cross-section per nucleon for J/Ψ production was much larger for iron than deuterium [Aub+ 85], which implies an enhanced gluon distribution. Unfortunately the statistics were too low to make any conclusion about the x and A dependence of this enhancement.

In Section 2.2 we saw that $|\xi^3| < 1/Mx$ in the lab frame, where ξ^3 is the spatial separation of the quark fields in the correlation function defining $W_{\mu\nu}$. Thus a shift of the quark distributions to lower x implies longer range quark correlations in the ground state of the nucleus. This is the starting point for most explanations of the EMC effect, that the effect measures an increased quark light-cone correlation length in nuclei as compared with free nucleons. One reason for this increased correlation length arises quite naturally if we regard quark/nuclear matter to be at zero temperature, but having a phase transition at some critical density ρ_c. For densities below ρ_c, quarks are confined in nucleons, but above ρ_c we have a more or less degenerate quark gas. Support for this picture comes from QCD where it is known that the theory becomes asymptotically free at large chemical potential [Ynd 83], which is equivalent to high density. If we take the free nucleon to be the zero density limit of quark matter, then as we combine nucleons in a nucleus the mean density will increase, as the surface to volume ratio decreases. This increase in density will lead to an increase in quark correlation lengths as a prelude to a

deconfining phase transition, where the correlation lengths will be very large.

3.2 Rescaling

Rescaling models explain the EMC effect by using QCD evolution to change the momentum transfer scale of the parton distributions in a nucleus. These models stem from the observation by Close, Roberts and Ross [CRR 83] that, in the range $0.2 < x < 0.7$, the structure functions of a nucleus A at a scale Q^2 is similar to that of a nucleon at a higher scale $\xi_{NA}Q^2$:

$$\bar{F}_2^A(x, Q^2) = F_2^N(x, \xi_{NA}Q^2) \qquad (\bar{F}_2^A = \frac{1}{A}F_2^A). \tag{3.1}$$

The authors called this effect 'dynamical rescaling'.

Eqn.(3.1) by itself does not constitute a model, it is merely a phenomenological observation. A model must be able to predict the rescaling parameter ξ_{NA}, using a method that has a sound physical basis. If dynamical rescaling holds, then there are immediate implications from QCD. Consider the moments of the structure function per nucleon

$$M_2^{(n)A}(Q_A^2) = \int_0^A dx\, x^{n-2} \bar{F}_2^A(x, Q_A^2). \tag{3.2}$$

Then dynamical rescaling implies

$$M_2^{(n)A}(Q_A^2) = M_2^{(n)A}(\xi_{NA}Q_A^2) \tag{3.3}$$

which can be trivially satisfied if ξ_{NA} is n-dependent. However the observation that ξ_{NA} is independent of x in the range $0.2 < x < 0.7$ means that ξ_{NA} is more or less independent of n for n in the range 1 to 4.

If we consider the non-singlet moments of the structure functions for a nucleus A and a nucleon N, we have, from eqn. (2.94):

$$M_{NS}^{(n)A}(Q^2) = \left[\frac{\alpha_c(Q^2)}{\alpha_c(Q_0^2)}\right]^{d_{NS}^{(n)}} M_{NS}^{(n)A}(Q_0^2) \tag{3.4}$$

where

$$\alpha_c(Q^2) = \frac{4\pi}{\beta_0 \log(Q^2/\Lambda^2)} \tag{3.5}$$

is the QCD running coupling constant. For a nucleon at the two scales $\xi_{NA}(Q_0^2)$ and $\xi_{NA}(Q^2)$ we have the relation between the moments:

$$M_{NS}^{(n)N}(\xi_{NA}(Q^2)Q^2) = \left[\frac{\alpha_c(\xi_{NA}(Q^2)Q^2)}{\alpha_c(\xi_{NA}(Q_0^2)Q_0^2)}\right]^{d_{NS}^{(n)}} M_{NS}^{(n)N}(\xi_{NA}(Q_0^2)Q_0^2). \tag{3.6}$$

Now we use eqn.(3.3) to eliminate the moments

$$\frac{\alpha_c(Q^2)}{\alpha_c(Q_0^2)} = \frac{\alpha_c(\xi_{NA}(Q^2)Q^2)}{\alpha_c(\xi_{NA}(Q_0^2)Q_0^2)}. \tag{3.7}$$

To lowest order in α_c,

$$\alpha_c^{-1}(\xi Q^2) = \frac{\beta_0}{4\pi}\log\xi + \alpha_c^{-1}(Q^2), \tag{3.8}$$

which gives an expression for $\xi_{NA}(Q^2)$ to lowest order:

$$\xi_{NA}(Q^2) = \left(\xi_{NA}(Q_0^2)\right)^{\alpha_c(Q_0^2)/\alpha_c(Q^2)}. \tag{3.9}$$

The extension to next order is given by Close, Roberts, Ross and Jaffe [CJRR 85]. For $Q^2 > Q_0^2$ we have $\alpha_c(Q_0^2)/\alpha_c(Q^2) > 1$ and

$$1 < \xi_{NA}(Q_0^2) < \xi_{NA}(Q^2). \tag{3.10}$$

This implies that a small change in the scale at low Q_0^2 can be magnified into a large change at large Q^2.

The use of leading order QCD and leading twist means that this analysis of dynamical rescaling is valid only over a limited range of x, usually estimated to be $0.2 < x < 0.7$. Also we have only analysed non-singlet moments, whereas the experimental results are mostly for $F_2(x)$ (because of the predominant use of charged lepton probes), which is dominated by non-singlet (ie. valence) distributions only for $x > 0.3$. To test these non-singlet predictions in the low x region requires data on $xF_3(x)$ from (anti)neutrino scattering experiments. However there is very little of this data available at present.

A particular point to note is that dynamical rescaling models should predict where the EMC ratio passes through unity in the region of $x = 0.3$. This is because $(d/d(\log Q^2))F_2(x, Q^2)$ has a zero [BK 79] near $x = 0.2$. The various models generally predict that the EMC ratio is unity somewhere between $x = 0.2$ and $x = 0.3$. Thus if an experiment could find precisely where the EMC ratio is unity it would help us to choose between the various models.

It is quite natural to interpret dynamical rescaling as originating in the dynamics at low Q^2, the regime appropriate to confinement. Then some small change in the scale at low Q^2 will lead to the large rescaling effect seen at high Q^2. We need to be careful here. In the confinement regime higher order QCD and higher twists become very important, and the effects on these operators of a change in scale are poorly understood. Typically, higher order corrections to eqn.(3.8) contain factors of $\log n$,

which makes perturbation theory worse for large n. This is the reason rescaling fails at large x, as the large n moments probe the large x region.

At this stage we will confine our attention to two of the successful dynamical rescaling models: rescaling based on a change of length scales in nuclei, which is the model of Close, Roberts, Ross and Jaffe (CRRJ) [CJRR 85,JCRR 85], and rescaling based on a change of mass scales in nuclei, which is the 'Off Shell' model of Dunne and Thomas (DT) [DT 85,DT 86,Dunne 86].

3.2.1 The CRRJ Model

From Sections 2.7 and 2.8, we can postulate that there exists a mass scale μ_N^2 at which, approximately, the nucleon consists only of valence quarks (ie. there is no gluon bremmstrahlung or pair production). CRRJ estimate this scale to be $\mu_N^2 \approx 0.7\text{GeV}^2$. The CRRJ hypothesis is that a nucleon in a nucleus has a shifted mass scale μ_A^2

$$\mu_A^2 = \frac{\mu_N^2}{\xi_{NA}(\mu_N^2)}, \tag{3.11}$$

and that these mass scales μ_A^2 and μ_N^2 are related to some characteristic length scales λ_A and λ_N:

$$\frac{\mu_N^2}{\mu_A^2} = \left(\frac{\lambda_A}{\lambda_N}\right)^2 = \xi_{NA}(\mu_N^2). \tag{3.12}$$

Now, from the data we require $\xi_{NFe}(Q^2 = 20\text{GeV}^2) \simeq 2.0$, and using eqn.(3.9) we find $\xi_{NFe}(Q^2 = \mu_N^2) \simeq 1.3$ or $(\lambda_{Fe}/\lambda_N) \simeq 1.15$. Thus an increase of $\sim 15\%$ in the length scale of the twist-two matrix elements for iron can explain the EMC effect.

This model is rather natural from the point of view of the MIT bag model [Cho+ 74]. For massless quarks the only dimensionful parameter is B, the bag constant. When the confinement radius of the bag, λ, changes, the momentum carried by a quark, p, also changes, such that the dimensionless quantity $p\lambda$ is always constant. The intrinsic scale μ^2 is then proportional to p^2, and there is no other scale in the problem. This heuristically explains why the rescaling is n independent.

There is some concern about these dimensional arguments. The bag model scales exactly, whereas we must have scaling violations in any QCD based theory. These scaling violations are a direct consequence of renormalization which entails different ideas of dimensionality (see Section 2.3), thus the naive dimensional argument we have used above to connect the bag model to QCD must be used with some caution. Without a satisfactory QCD theory of confinement we cannot get much closer to a full understanding of this rescaling model.

To model the A dependence of the EMC effect, CRRJ derived the ratio (λ_A/λ_N) from a simple model of partial deconfinement. When two nucleons in a nucleus overlap it was assumed that their quarks were free to propagate over the combined volume of the two overlapping nucleons. Then from a given two-nucleon correlation function, and from nuclear density functions, it was possible to calculate the overlapping volume per nucleon and hence the ratio (λ_A/λ_N). This procedure is discussed in detail in the papers by CRRJ.

The important parameters in this model are discussed below:-

1. The choice of correlation function, $f(r)$. CRRJ used three correlation functions: a) no correlation ($f(r) = 1$); b) Fermi gas correlation; c) Reid soft core correlation. The last two give similar values of (λ_A/λ_N), the first gives slightly larger values. The effect of neglecting 3 (or more) nucleon overlap is small, especially in the case of the soft core correlation.

2. The rms radius of the nucleon, a_{rms}. CRRJ used $a_{rms} = 0.9$ fm, which is a bit larger than some recent determinations. However they based this value on the measured rms charge radius of the proton, which includes effects from the pionic cloud of the proton, and is not a reliable estimate of the confinement radius. Taking this effect into account would lower (λ_A/λ_N).

3. The scale, μ_A^2. This scale is determined by examining the ratio of moments

$$\left[\frac{M^{(n)A}(Q^2)}{M^{(n)A}(\mu_A^2)}\right]^{-1/d_{NS}^{(n)}} = 1 + Y \log\left(\frac{Q^2}{\mu_A^2}\right) \tag{3.13}$$

where, to leading order, Y is independent of n and given by

$$Y = 1/\log(\mu_A^2/\Lambda^2). \tag{3.14}$$

Plotting the lefthand side of eqn.(3.13) against $\log(Q^2)$, we get unity when $Q^2 = \mu_A^2$. CRRJ do this for $n = 4, 5, 6$ and average to obtain $\mu_{Fe}^2 = 0.50 \pm 0.11\text{GeV}^2$, which corresponds to $\mu_N^2 = 0.66 \pm 0.14\text{GeV}^2$. We note that this method depends on the free nucleon moments which have been evaluated by Jaffe and Ross [JR 80] in an approximation to the MIT bag model. This

calculation by Jaffe and Ross will be re-examined later in this thesis using a different method of calculating the nucleon moments from the bag model.

4. The QCD scale parameter, Λ. CRRJ use $\Lambda = 250$ MeV and point out that variations in Λ do not greatly affect the values of $\xi_{NA}(Q^2)$ obtained from (λ_A/λ_N). However the procedure for finding μ_A^2 is not independent of the the value of Λ, because the combination of Λ and μ_A^2 has to give the correct slope. There is a great deal of uncertainty both in using perturbative QCD and in determining the bag model moments, probably too much for us to apply a consistency relation between Λ and μ_A^2.

The CRRJ model has been very successful in its agreement with experimental data for most A, particularly in the range $0.2 < x < 0.7$. For $x > 0.7$ a naive Fermi smearing has been attempted [BBM 86], but this leads to an over-correction. This is a problem but can probably be rectified. The medium x depletion of the structure functions of nuclei is well reproduced, with the depletion becoming slightly more pronounced as Q^2 increases. There is a small enhancement at low x, which actually diminishes as Q^2 increases. This is because the sea quark distributions are becoming more important but they only evolve logarithmically, so that although $\xi_{NA}(Q^2)$ is increasing the ratio of distributions does not.

3.2.2 The 'Off Shell' Model

The 'off shell' model of Dunne and Thomas (DT) uses a different physical basis to explain the EMC effect via rescaling. As might be guessed from the name, the off

shell model rescales the QCD moments on the squared four momentum of the off mass shell nucleons in a nucleus. The off shell model also includes a modification of the usual Fermi averaging procedure to take into account off mass shell effects. This Fermi averaging procedure is similar to that of Akulinichev, Shlomo, Kulagin and Vagradov [Aku+ 85a,85b].

The hypothesis of DT is that the mass scales μ_A^2 and μ_N^2 are the invariant masses respectively of an off shell nucleon in nucleus A, and a free nucleon. The rescaling parameter is then given by

$$\xi_{NA}(Q^2) = \left(\frac{\mu_N^2}{\mu_A^2}\right)^{\alpha_c(\mu_A^2)/\alpha_c(Q^2)} = \left(\frac{M_N^2}{k_A^2}\right)^{\alpha_c(k_A^2)/\alpha_c(Q^2)} \tag{3.15}$$

where k_A is the four momentum of the struck nucleon in nucleus A.

We can obtain the nuclear structure function by integrating the nucleon structure function times some momentum probability distribution $\rho(k^2)$ over the three momentum $\vec{k}_A$. However the nucleon structure function is evaluated not at x but at

$$\begin{aligned} x_F &= \frac{Q^2}{2p.q}\frac{p.q}{k_A.q} \\ &= x\frac{M_A}{k_0 + k_3} \qquad 0 < x_F < A \end{aligned} \tag{3.16}$$

Thus we obtain

$$F_2^A(x) = \int d^3k\, \rho(k^2) F_2^N\left(\frac{M_A x}{k_0 + k_3}\right) \tag{3.17}$$

where $\rho(k^2)$ is the momentum probability distribution which may be obtained from particular nuclear models. Defining

$$y \equiv \frac{k_0 + k_3}{M_A} \tag{3.18}$$

eqn.(3.17) becomes

$$F_2^A(x) = \int_x^A dy\ f(y) F_2^N\left(\frac{x}{y}\right). \tag{3.19}$$

The function $f(y)$ is given for off shell nucleons by

$$f(y) = 2\pi M_A \int_{(M_A^2 y^2 + M_N^2)/2M_A y}^{\infty} dz\ z\rho(z^2 + (M_N y - k_0)^2) \tag{3.20}$$

where

$$z = \frac{M_A^2 y^2 + M_N^2 + \vec{k}_\perp^2}{2M_A y}. \tag{3.21}$$

The form of eqn.(3.19) leads to the interpretation of $f(y)$ as the momentum fraction distribution of nucleons in the nucleus. The consistency conditions on $f(y)$ are:

$$\int dy\ f(y) = A \tag{3.22}$$

$$\int dy\ y f(y) = 1. \tag{3.23}$$

We may now combine the Fermi averaging with the rescaling (eqn.(3.15)), and summing explicitly over the nucleon states gives

$$F_2^A(x, Q^2) = \sum_i n_i \int_x^A dy\ f_i(y) F_2^N(\frac{x}{y}, \xi_{NA_i}(Q^2) Q^2) \tag{3.24}$$

where

$$f_i(y) = N_i \int dz\ z\rho_i(z^2 + (yM_N - M_i)^2) \tag{3.25}$$

$$n_i = \text{occupation number of state } i$$

$$M_i = \sqrt{k_i^2} = \text{mass of bound nucleon in state } i$$

and N_i is a normalization constant which imposes the conditions eqns. (3.22, 3.23) on $f_i(y)$.

DT use the harmonic oscillator shell model to find the momentum distributions $\rho_i(k^2)$ and hence the $f_i(y)$. They also use this model to find the masses M_i from the available data on separation energies [BJ 77,Neg 70,JM 73].

Many of the provisos and cautions about rescaling models outlined earlier still apply to the off shell model. Whilst the effects of rescaling are valid only in the range $0.2 < x < 0.7$, the inclusion of Fermi effects allows us to look at the EMC effect at even higher x. We note also that the rescaling effect is smaller in the off shell model than in the CRRJ model, firstly because the change in scale between a free nucleon and a bound nucleon in a nucleus is much smaller (5% vs. 25%), and also because the change in scale is made at a higher scale (0.9 GeV^2 vs. 0.5 GeV^2).

One important thing to note about the off shell model is DT's treatment of the deuteron. Not only is the struck nucleon in the deuteron off shell because of binding, but there is also a significant effect from the recoil of the spectator nucleon, which is on shell. This recoil effect is negligible in heavier nuclei, but DT claim that it is important for light nuclei. The average squared 3-momentum ($\langle \vec{k}^2 \rangle$) of a nucleon in deuterium is about 0.01 GeV^2. Dividing this by twice the nucleon mass gives the average kinetic energy, which is 5.3 MeV. This kinetic energy pushes the struck nucleon further away from the mass shell. Including the binding energy, the total effect for deuterium is 7.5 MeV.

The important parameters in the off shell model are:-

1. The QCD scale parameter, Λ. DT used $\Lambda = 300$ MeV, and as in the CRRJ model, variations in Λ of up to 100 MeV do not greatly affect the values of

$\xi_{NA}(Q^2)$. The fact that the off shell model rescales at higher Q^2 than the CRRJ model also weakens the Λ dependence.

2. The invariant masses of the bound nucleons, M_i, and the harmonic oscillator well depths $\hbar\omega$. These were fitted using published data for the separation energies in various nuclei. This data is mostly for protons, which are less tightly bound than neutrons. DT used the same binding energies for both neutrons and protons. Later work estimated that the neutrons were bound 5–10 MeV tighter than protons , but did not give significantly different results.

To find the normalization constants N_i, DT applied the first consistency condition eqn.(3.22). However checking these in the second condition, eqn(3.23) yields

$$\int_0^A dy\, y f_i(y) = \frac{M_i}{M_N} < 1. \tag{3.26}$$

Thus the nucleons do not carry all the momentum of the nucleus. As this results from binding effects, it is tempting to think that the 'missing' momentum is carried by pions and other hadrons in the nucleus. One might then make a link between a rescaling model and so-called 'convolution' models of the EMC effect [LlS 83,ET 83, BCW 84] which explicitly include pionic and other degrees of freedom in the nucleus. However these connections are somewhat speculative at this stage.

The off shell model agrees fairly well with the data in the range $0.2 < x < 0.85$, the upper limit being close to the upper limit of the data. It also reproduces the A dependence fairly well. It has very similar Q^2 dependence to that of the CRRJ model.

The off shell Fermi averaging is at least as important as the rescaling in the off shell model. This is very different to the results of Bodek and Ritchie [BR 81] who used an on shell treatment. Thus nuclear properties are manifesting themselves in DIS, contrary to our naive expectations in applying a rescaling model.

We do not observe increased quark correlation lengths in the off shell model. Dunne, Thomas and Bickerstaff [DT 86,Dunne 86,BT 87a] have criticized the interpretation of the EMC effect as an increase in quark correlation lengths, as this interpretation is based on an equal-time correlation function rather than a light-cone correlation function. Instead the softening of the valence quark distribution at medium x occurs because the scaling variable we have used is not the correct one. For a bound nucleon the correct scaling variable, ie. the momentum fraction carried by the struck quark, is approximately $x(M_N/M_i) > x$. This is easily seen by approximating $f(y)$ by a sharp distribution peaked about $y = M_i/M_N$, then we have

$$\bar{F}_2^A(x,Q^2) \simeq F_2^N(\frac{M_N}{M_i}x, Q^2). \tag{3.27}$$

Because F_2^N decreases rapidly at medium to large x, eqn.(3.27) gives rise to a depletion in $\bar{F}_2^A(x)$. Detailed discussion of the effects of 'x-rescaling' may be found in a paper by Bickerstaff and Miller [BM 86].

It appears that we may have come full circle here. From the beginning it has been hoped that the EMC effect would lead to the inclusion of quark degrees of freedom in the description of the nucleus. However a more detailed study of binding effects shows that most of the effect may not involve new physics at all. As is often the

case, more experimental information is needed to decide which of these two views is correct. There is hope that Drell-Yan experiments of proton-nucleus scattering [BBM 86] may provide the necessary information in the future.

3.3 Neutrino Experiments

There have been some experiments which have measured $F_2^A(x)$ for neutrinos or antineutrinos scattering on nuclei. In general the results for the ratios of the structure function of a heavy nucleus to that of deuterium are similar to those obtained from the scattering of charged leptons. However we can obtain new information as to whether the EMC effect is the same for neutrons and protons. With incident antineutrinos we have the two reactions

$$\bar{\nu}_\mu + n \rightarrow \mu^+ + X^-, \qquad \bar{\nu}_\mu + p \rightarrow \mu^+ + X^0, \tag{3.28}$$

so by summing the charges of the final hadronic state, we can distinguish between scattering from neutrons or protons. Two experiments have been performed to measure the cross-sections of neutrons and protons in a nucleus: one using deuterium at CERN [All+ 81] and a second using neon at Fermilab [Asr+ 85,86].

The two experiments measured the x-dependence of the differential cross- sections for neutrons and protons. Using the QPM we can write the differential cross-sections for the reactions (3.28) at high energies ($E \gg M$) as [LP 82]

$$\frac{d\sigma^{A^{\nu n,\nu p}}}{dx} = \frac{G^2 ME}{\pi}[\frac{2}{3}F_2^{A^{\nu n,\nu p}}(x) - \frac{1}{3}xF_3^{A^{\nu n,\nu p}}(x)], \tag{3.29}$$

where G is the weak coupling constant. Thus the ratio of neutron to proton cross-sections will be

$$R_A(x) = \frac{d\sigma^{A^{\nu n}}}{dx} \Big/ \frac{d\sigma^{A^{\nu p}}}{dx} \tag{3.30}$$

$$= \frac{2F_2^{A^{\nu n}}(x) - xF_3^{A^{\nu n}}(x)}{2F_2^{A^{\nu p}}(x) - xF_3^{A^{\nu p}}(x)} \tag{3.31}$$

$$= \frac{x[f_{d/A}(x) + 3f_{\bar{u}/A}(x) + 3f_{\bar{s}/A}(x)]}{x[f_{u/A}(x) + 3f_{\bar{d}/A}(x) + 3f_{\bar{s}/A}(x)]}. \tag{3.32}$$

If we concentrate on the region $x > 0.3$, then there will be very little enhancement of the sea, and F_2 and F_3 will be approximately the same, and the ratio

$$R'_A(x) \equiv \frac{F_2^{A^{\nu n}}(x)}{F_2^{A^{\nu p}}(x)} \tag{3.33}$$

will not differ appreciably from $R_A(x)$ in this region.

Asratyan *et. al.* [Asr+ 85,86] computed the ratio of their results from neon with the earlier results from deuterium,

$$\rho(x) = R_{Ne}(x)/R_D(x) \tag{3.34}$$

and found that $\rho(x)$ differed appreciably from unity, indicating that neutrons and protons are affected differently by the EMC effect.

To test whether the change in $R_A(x)$ is a manifestation of the EMC effect, we have computed $R'_A(x)$ using the two rescaling models detailed earlier. We are restricted to computing $R'_A(x)$ because the rescaling analysis is only applicable to non-singlet moments. We would hope that the off shell model might be able to reproduce the change in $R_A(x)$ because, using the harmonic oscillator shell model, we can input different separation energies for neutrons and protons. We have used the

parametrisation of Buras and Gaemers [BG 78] to obtain the parton distributions for a free nucleon, and we have kept their best fit value of the QCD scale parameter, $\Lambda = 0.3$ GeV.

Using the CRRJ model and the results of Close *et. al.*, the parameters we used are

1. $\lambda_{Ne}/\lambda_N = 1.104, \quad \lambda_D/\lambda_N = 1.015.$

2. $\mu^2_{Ne} = 0.55 \pm 0.12 \text{ GeV}^2, \quad \mu^2_D = 0.65 \pm 0.14 \text{ GeV}^2.$

Using eqns. (3.9) and (3.12) we can determine the rescaling parameters,

$$\xi_{N,Ne}(Q^2 = 20\text{GeV}^2) = 1.69, \; \xi_{ND}(Q^2 = 20\text{GeV}^2) = 1.08. \tag{3.35}$$

Now using the rescaling ansatz (eqn. (3.1)) we can determine the neutron and proton structure functions and hence $R'_A(x)$ and $\rho(x)$. These are shown in Figs. 3.2 and 3.4. We note that the neutron and proton were taken to have the same radius. Taking a slightly smaller value for the neutron radius would slightly decrease λ_A/λ_N for neutrons, and hence the rescaling effect would be slightly less for neutrons than protons. The effect on $R'_A(x)$ and $\rho(x)$ would only be a few percent.

To use the off shell model we need to find the invariant masses of the bound nucleons and the well depths. These are summarized in Table 3.1.

The energy split in deuterium comes from the neutron-proton mass difference. In neon the neutrons are more tightly bound than protons by 5 to 12 MeV. Using this data we calculated the structure functions and hence $R'_A(x)$ and $\rho(x)$. These are shown in Figs. 3.3 and 3.4.

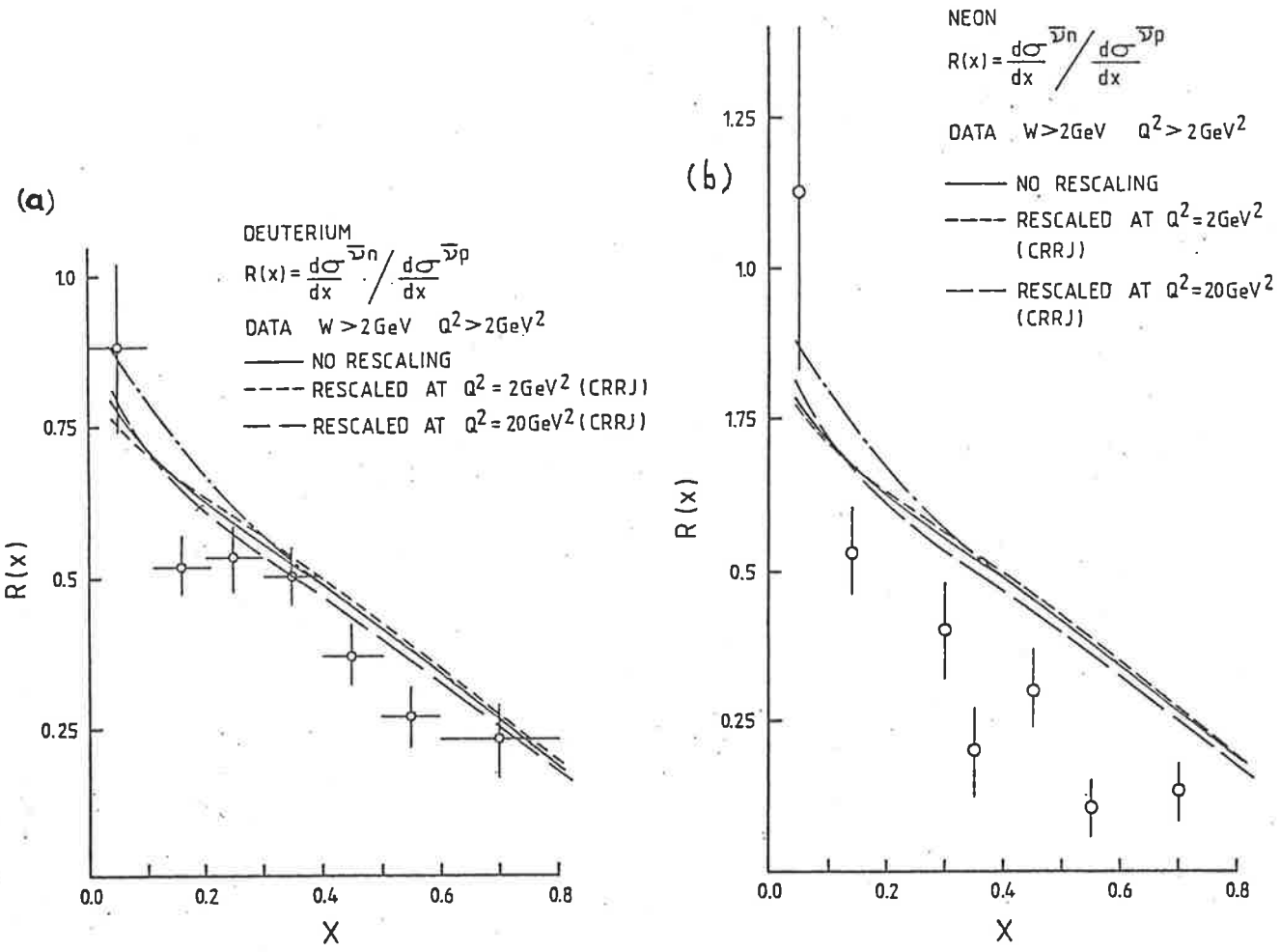

Fig 3.2 Ratio of neutron to proton cross sections R(x) for (a) deuterium and (b) neon. The data are for W > 2 GeV (where W is the final invariant mass). The curves are for the dynamical rescaling CRRJ model: solid curve, no rescaling short-dashed curve, rescaled at $Q^2 = 2GeV^2$; long-dashed curve, rescaled at $Q^2 = 20GeV^2$.

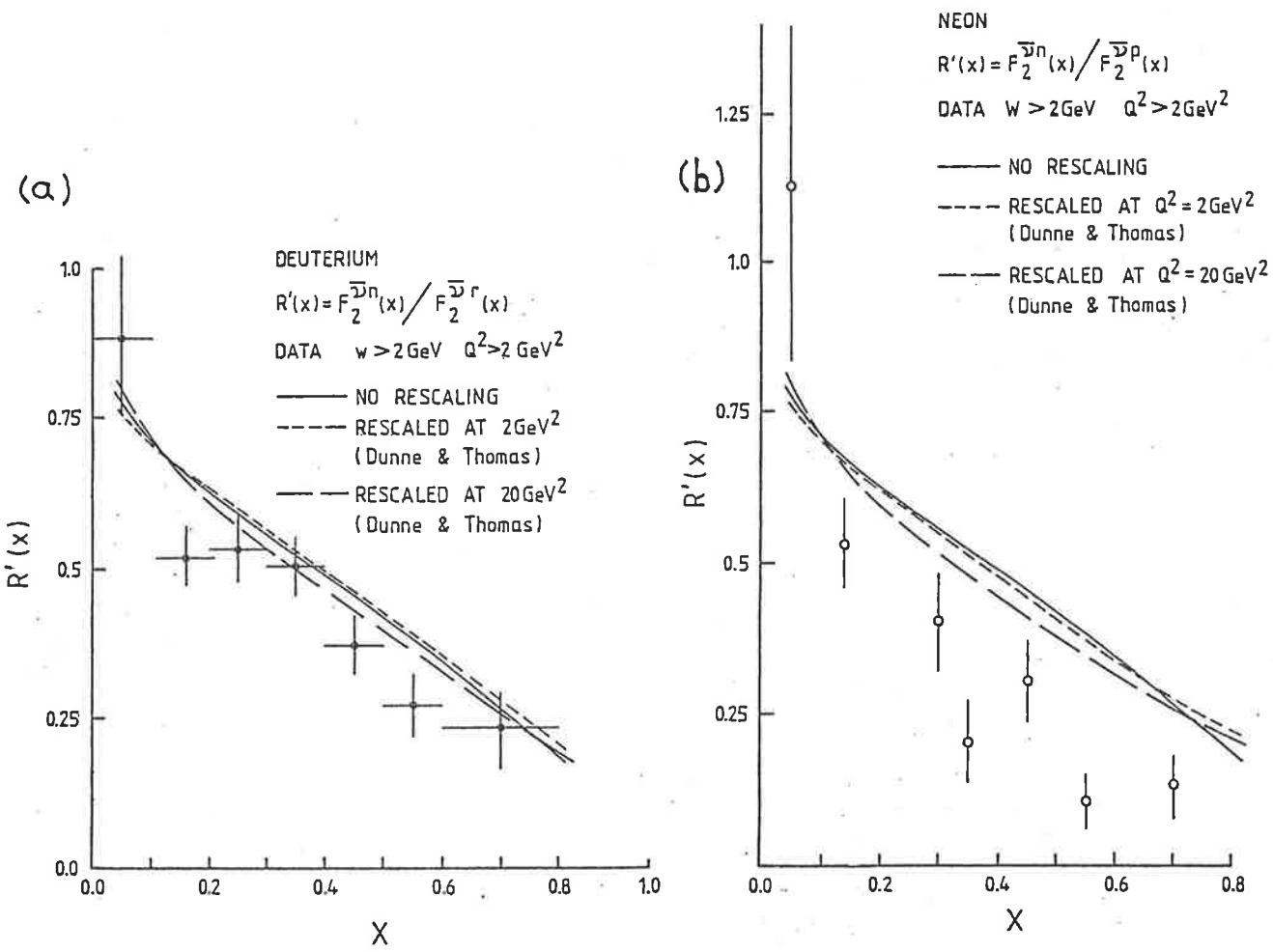

Fig 3.3 Ratio of neutron to proton structure functions R'(x) for (a) deuterium and (b) neon. The data are for $W > 2$ GeV and $Q^2 > 2$ GeV^2. The curves are for the off-mass-shell DT model: solid curve, no rescaling; short-dashed curve, rescaled at $Q^2 = 2$ GeV^2; long-dashed curve, rescaled at $Q^2 = 20$ GeV^2.

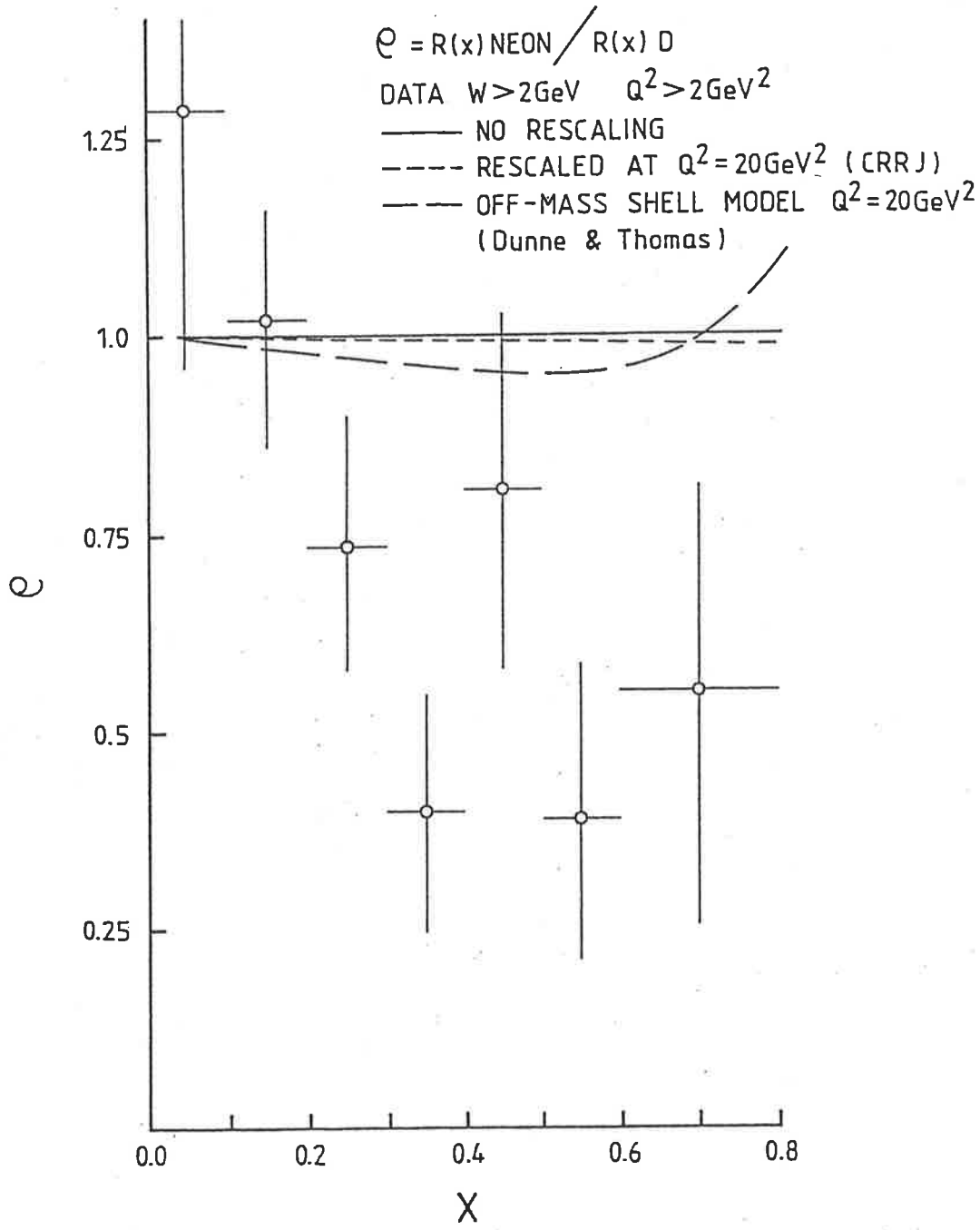

Fig 3.4 Comparison of experimental data and theoretical predictions for the ratio $\rho(x) = R'_{Ne}(x)/R'_D(x)$. The data are for $W > 2$ GeV and $Q^2 > 2$ GeV^2. Theoretical curves: solid curve, no rescaling; short-dashed curve, rescaled at $Q^2 = 20$ GeV^2 for the dynamical rescaling CRRJ model; long-dashed curve, rescaled at $Q^2 = 20$ GeV^2 for the off-mass-shell DT model.

	Protons	Neutrons
Deuterium		
M_0 (0s) 1p, 1n	930.7	932
$h\omega$	7	7
Neon		
M_0 (0s) 2p, 2n	897	889
M_1 (0p) 6p, 6n	912	905
M_2 (0p) 2p, 2n	927	922
$h\omega$	14	16

Table 3.1: Invariant Masses and Oscillator Strengths in MeV

For both models, there was little rescaling effect in deuterium, which is to be expected, and we obtained reasonable agreement with the experimental data. The CRRJ model also predicts a small effect in neon, presumably because the changes in each structure function more or less cancel. The off shell model gives a significant change in $R'_A(x)$ at medium x, but not enough to agree with the data. Finally, both models give very little change from unity in $\rho(x)$. The CRRJ model deviates by about 1%, and the off shell model by about 5% at most. The rise in $\rho(x)$ at large x in the off shell model comes from Fermi motion effects in neon.

Both models fail to give anything like the value $\rho \approx 0.5$ obtained experimentally. There is a good possibility of systematic error in comparing the two experiments done at different times and in different places. The lack of agreement between the data and the models' predictions for neon points in this direction. One source of error might be rescattering corrections in the nuclear medium, which can alter the charge of the observed final state, this would alter the $\bar{\nu}n$ and $\bar{\nu}p$ cross-sections. However if more experiments were done , with the systematic errors carefully controlled, which confirmed the data, then our ideas about nuclear corrections for DIS would need to

be re-examined [Rith 86].

Chapter 4

Non-Perturbative Contributions to Parton Distributions

We have seen in Chapter 2 that sea, or non-valence, quarks are of a great deal of importance in DIS. Perturbative QCD processes such as gluon bremmstrahlung and quark-antiquark pair production generate progressively more sea quarks as Q^2 increases. However, it has long been realized that some fraction of the sea may be generated by non-perturbative processes such as the pion cloud of the nucleon, which ensures chiral symmetry. This component was first calculated by Sullivan in 1972 [Sull 72]. More recent experimental data has made it possible to put limits on the size of this pionic contribution — and indirectly on the quark confinement radius [Tho 83a]. The program has been extended by Signal and Thomas [ST 87a] to kaonic contributions, which has led to a calculation of the non-perturbative part of the strange sea. We call the contributions which we shall examine non-perturbative, because the processes which give rise to them are relatively long range ($\sim$ 1 fm) compared to the distance scales at which perturbative QCD is applicable ($\sim$ 0.1 fm), and so the non-perturbative properties of QCD, such as confinement and the

dressing of the nucleon by meson clouds are of the most importance.

Naively one might not expect that the dressing of the nucleon by mesons, which is a long range phenomenon compared to the distance scales of DIS, would have much to do with DIS. However the internal short-distance structure of the mesons, which is described by their own structure functions (F_2^π and F_2^K), can be probed by the virtual photon (or W or Z boson) which leads to a contribution to the nucleon structure function.

4.1 The Pion Field of the Nucleon

The pion field of the nucleon arises because of considerations of chiral symmetry. The Lagrangian density for a free nucleon

$$\mathcal{L}(x) = i\bar{\psi}\ \partial\!\!\!/\psi - M_N\bar{\psi}\psi \tag{4.1}$$

is not invariant under chiral transformations

$$\psi \rightarrow \psi - i(\vec{\tau}\cdot\vec{\epsilon}/2)\gamma^5\psi, \tag{4.2}$$

though it is well known that $SU(2)_L \times SU(2)_R$ chiral symmetry is a good hadron symmetry. The problem is the mass term in the Lagrangian, which is 'chirally odd'.

In order to restore chiral invariance, the so-called 'σ-model' of Gell-Mann and Levy [GL 60,IZ 80] introduces new fields $(\sigma, \vec{\pi})$, an isoscalar-scalar field and an isovector-pseudoscalar field. The most general renormalizable Lagrangian density involving nucleon, σ- and $\vec{\pi}$- fields which is consistent with chiral symmetry is

$$\mathcal{L}(x) = i\bar{\psi}\ \partial\!\!\!/\psi + g\bar{\psi}(\sigma + i\vec{\tau}\cdot\vec{\pi}\gamma^5)\psi + \frac{1}{2}(\partial_\mu\sigma)^2 + \frac{1}{2}(\partial_\mu\vec{\pi})^2 - \frac{1}{4}\lambda^2[(\sigma^2+\vec{\pi}^2) - \nu^2]^2, \tag{4.3}$$

where the second term replaces the nucleon mass term. The final term is the potential energy $V(\sigma, \vec{\pi})$, which is of most interest when $\lambda^2 > 0$ and $\nu^2 > 0$. Then the potential has the famous 'Mexican hat' shape, and leads, via a natural transformation, to a Lagrangian where the chiral symmetry is hidden.

Now Goldstone's theorem which tells us that when a continuous symmetry of the Lagrangian is hidden, a massless excitation of the system (Goldstone boson) appears. We identify this with the pion. To introduce a mass for the pion, we 'tip' the Mexican hat ($\mathcal{L} \rightarrow \mathcal{L} + c\sigma$), which gives a preferred direction in $(\sigma, \vec{\pi})$ space. Thus the pion cloud arises as a consequence of the need to have a Lagrangian density which is invariant under $SU(2)_L \times SU(2)_R$ transformations.

The mechanism by which the pion cloud contributes to the nucleon structure function is shown in Fig. 4.1. The amplitude for this contribution is written as

$$A^{\mu} = g_{HN\pi} \frac{\bar{u}_H i\gamma_5 u_N}{k^2 - M_{\pi}^2} (X|j^{\mu}|\Pi(k)) \tag{4.4}$$

where k is the four-momentum of the pion, X is the debris of the struck pion, $\bar{u}$ and u are Dirac spinors, and $g_{HN\pi}$ ($H = N$ or Δ) the appropriate coupling constant. Now if we square this amplitude, then sum over final states and average over initial spins, we have

$$2M_N \frac{dW_{\mu\nu}^N}{dk^2 dx'} = \frac{x}{x'^2} \frac{g_{HN\pi}^2}{4\pi} \frac{\mathrm{Tr}[(\not{p}_N + M_N)\gamma_5(\not{p}_H + M_H)\gamma_5]}{(k^2 - M_{\pi}^2)} \frac{1}{\pi} \mathrm{Im} C_{\mu\nu}^{\pi} \tag{4.5}$$

where

$$\mathrm{Im} C_{\mu\nu}^{\pi} = \sum_X \delta^{(4)}(q + k + p_X) \langle \Pi(k)|j_{\mu}(0)|X\rangle\langle X|j_{\nu}(0)|\Pi(k)\rangle \tag{4.6}$$

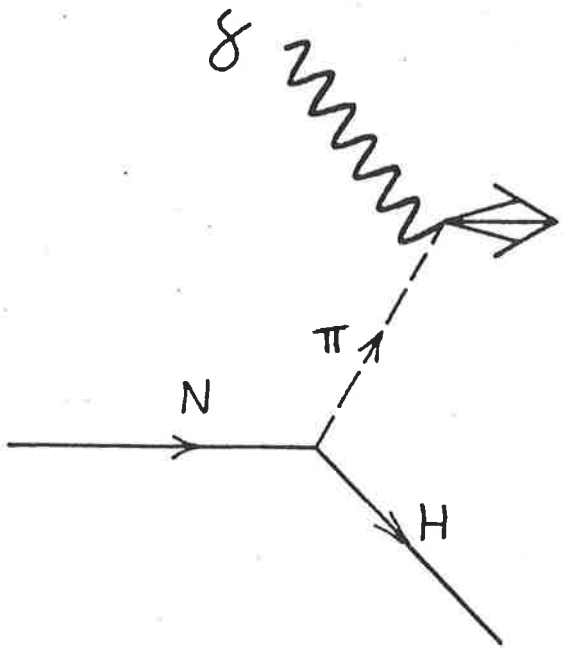

Fig 4.1 The contribution of the pion to the structure function of the nucleon.

and x (x') is the Bjorken scaling variable appropriate to the lepton-nucleon (lepton-pion) collision.

The spin trace can be easily evaluated:

$$\begin{aligned} \mathrm{Tr}[(\not{p}_N + M_N)\gamma_5(\not{p}_H + M_H)\gamma_5] &= -2p_N.p_H + 2M_N M_H \qquad (4.7) \\ &= -t - (M_H - M_N)^2 \qquad (4.8) \end{aligned}$$

where, as usual

$$t = -k^2 = -(p_N - p_H)^2 \geq 0. \qquad (4.9)$$

The expression in eqn.(4.6) we recognize as the structure function of the struck pion, which is off mass shell. We shall neglect any dependence of $\mathrm{Im}C^{\pi}_{\mu\nu}$ on the invariant mass of the pion, as the effect of any off shell behavior is probably smaller than the errors in the experimental determination of the structure function of the pion. We may now write the contribution of Fig. 4.1 to the nucleon structure function as:

$$\delta F_2^N(x,Q^2) = \int_x^1 dy\, f_\pi(y) F_2^\pi(\frac{x}{y},Q^2) \qquad (4.10)$$

where $y = x/x'$ is the fraction of the plus component of momentum of the nucleon that that is carried by the pion,

$$\begin{aligned} f_\pi(y) &= \sum_{H=N,\Delta} y\frac{3g^2_{HN\pi}}{16\pi^2}\int_{t_{min}}^{\infty} dt\, \frac{t+(M_H-M_N)^2}{(t-M_\pi^2)^2}|F(t)|^2 \\ &\simeq 3y\frac{g^2_{\pi NN}}{16\pi^2}\int_{t_{min}}^{\infty} dt\, \frac{t}{(t-M_\pi^2)^2}|F(t)|^2. \qquad (4.11) \end{aligned}$$

t_{min} is the minimum value of $-k^2$,

$$t_{min} = \frac{y^2 M_N^2}{1-y}, \qquad (4.12)$$

and $F(t)$ is the high-momentum cut-off (or form factor) at the $HN\pi$ vertex. We use the value of the coupling constant $g^2_{\pi NN}/4\pi = 13.5$. For the form factor we take a simple analytic form, which is motivated by the cloudy bag model (CBM) [Tho 84]

$$F(t) = \exp[-\lambda(t + M_\pi)^2/M_\pi^2] \tag{4.13}$$

where R has the interpretation of a bag radius and $\lambda = 0.106 M_\pi^2 R^2$.

We have ignored the contribution from the process $N \rightarrow \Delta\pi$ because the larger mass of the resonance raises the lower limit of the integral and gives only a small contribution. The calculation by Sullivan shows that the process $N \rightarrow N\pi$ gives the dominant contribution to eqn. (4.10) in the region $x > 0.05$.

The function $f_\pi(y)$ may be interpreted as the probability of finding a kaon carrying fraction y of the plus component of the momentum of the nucleon. The integral of $f_\pi(y)$ over the interval $y = 0$ to 1 will give the average fraction of the plus component of momentum of the nucleon that is carried by the pion cloud. The essential features are that $f_\pi(y)$ peaks near $x = 0.25$, and that the value at the peak increases rapidly as R decreases, that is as the form factor becomes harder.

Now because the pion is composed primarily of non-strange quarks, the pion cloud contribution to the nucleon structure function contributes to the breaking of the SU(3) flavour symmetry of the sea. As we mentioned in Chapter 2, the SU(3) flavour symmetry is expected to be broken because of the large mass of the strange quark, so it would not be reasonable to attribute all of the non-strange excess to the pion cloud. However we can use data on SU(3) flavour breaking to impose a limit on pionic contributions to the nucleon structure function.

Integrating eqn. (4.10) over x we have

$$\int_0^1 dx\, \delta F_2^N(x) = \left[\int_0^1 dx'\, F_2^\pi(x')\right]\left[\int_0^1 dy\, f_\pi(y)\right]. \tag{4.14}$$

The second bracket on the right of eqn. (4.14) is the average fraction of momentum of the nucleon that is carried by the pions, which we denote $\langle y\rangle_\pi$. Now the excess of non-strange quarks in the sea will be given by $\bar{U}+\bar{D}-2\bar{S}$, so the excess contribution to the electro-magnetic structure function of the iso-scalar nucleon is

$$F_{2,\text{excess}}^N = \frac{5}{9}[\bar{U}+\bar{D}-2\bar{S}], \tag{4.15}$$

and so our bound on $\langle y\rangle_\pi$ is

$$\langle y\rangle_\pi \leq \frac{5}{9}[\bar{U}+\bar{D}-2\bar{S}]/\int_0^1 dx'\, F_2^\pi(x'). \tag{4.16}$$

The pion structure function has been determined experimentally by the NA3 group at CERN using the Drell-Yan process $\pi N \to X$, with the result [Bad+ 83]

$$\int_0^1 dx'\, F_2^\pi(x') = 0.015 \pm 0.004. \tag{4.17}$$

Getting a good estimate of the non-strange excess in the sea is somewhat complicated by the EMC effect. Almost all the data on sea distributions has come from (anti)neutrino scattering experiments on iron, where the sea is enhanced relative to the free nucleon. Because of the confusion surrounding the enhancement of the sea in the EMC effect (including whether the enhancement is SU(3) symmetric or not), we use the determination of Field and Feynmann [FF 77] for the non-strange excess in a free nucleon, $\frac{1}{2}[\bar{U}+\bar{D}-2\bar{S}] = 0.7\%$. Together with the pion structure function, this gives an upper bound on $\langle y\rangle_\pi$:

$$\langle y \rangle_\pi \leq 5 \pm 1.5\%. \tag{4.18}$$

The bound on $\langle y \rangle_\pi$ also implies a bound on the CBM bag radius. Because $\langle y \rangle_\pi$ decreases as the bag radius increases, we find a lower bound for the CBM bag radius of

$$R \geq 0.87 \pm 0.10\text{fm}. \tag{4.19}$$

In the context of the bag model, this bound implies that the bag radius is of the order of 1 fm rather than 0.5 fm or less, and that the pion cloud, necessary to restore chiral symmetry, is fairly sparse (see [Tho 83a,Tho 84] for more details).

We note that the pion cloud's contribution to DIS from nucleons (eqn. (4.10)) is the basis for the so-called 'convolution' models of the EMC effect [LlS 83,ET 83], [BCW 84]. In these models the momentum probability function in a nucleus $f_\pi^A(y)$ is given by $f_\pi(y)$ for free nucleons modified by a spin-isospin longitudinal response function per nucleon $R(\omega, |\vec{q}|)$, and the integral over t is replaced by integrating over the $(\omega, |\vec{q}|)$ plane:

$$f_\pi^A(y) = 3y \frac{g_{\pi NN}}{16\pi^2} \int_{M_N^2 y^2}^{\infty} d\vec{q}^2 \int_0^{|\vec{q}|-M_N y} d\omega \, \frac{\vec{q}^2}{(\vec{q}^2 + M_\pi^2)^2} |F(\vec{q}^2)|^2 R(\omega, |\vec{q}|). \tag{4.20}$$

The result is an excess distribution of pions contributing to DIS for a nucleon in a nucleus over that for a free nucleon. Because $f_\pi^A(y)$ still peaks near $y = 0.25$, this excess leads to the low-x enhancement seen in the EMC effect, and, because of momentum conservation considerations, also leads to the medium-x depletion of the valence distributions. We note that Berger *et. al.*, using light-cone coordinates, derive a different $f_\pi^A(y)$ which is much broader [BCW 84]. However there is an

inconsistency in their calculation as their $NN\pi$ interaction is written conserving 3-momentum rather than p^+.

4.2 Non-Perturbative Strange Sea

The kaon cloud of the nucleon arises out of similar considerations to those that gave us the pion cloud. In this case the symmetry required in the Lagrangian is $SU(3)_L \times SU(3)_R$. However now the symmetry is badly broken, because of the larger mass of the strange quark. This leads to the kaon having a much larger mass than the pion, and the kaon cloud being more sparse.

The mechanism by which non-perturbative contributions to the strange sea of the nucleon arise is shown in Fig. 4.2. For the final hyperon we include only the Λ and Σ. Any contributions from excited baryon resonances will be restricted to small x, as we have pointed out in the pionic case, where the assumption of incoherence eventually breaks down. By analogy with eqn. (4.10), we may write the contribution of Fig. 4.2a to the nucleon structure function as:

$$\delta F_2^N(x,Q^2) = \int_x^1 dy\, f_K(y) F_2^K(\frac{x}{y},Q^2) \tag{4.21}$$

where y is the fraction of the plus component of momentum of the nucleon that is carried by the kaon,

$$f_K(y) = \sum_{H=\Lambda,\Sigma} y f_H^I \frac{g_{HNK}^2}{16\pi^2} \int_{t_{min}}^{\infty} dt\, \frac{t+(M_H-M_N)^2}{(t-M_K^2)^2} |F(t)|^2, \tag{4.22}$$

t_{min} is the minimum value of $-k^2$,

$$t_{min} = y[M_H^2 - (1-y)M_N^2]/(1-y). \tag{4.23}$$

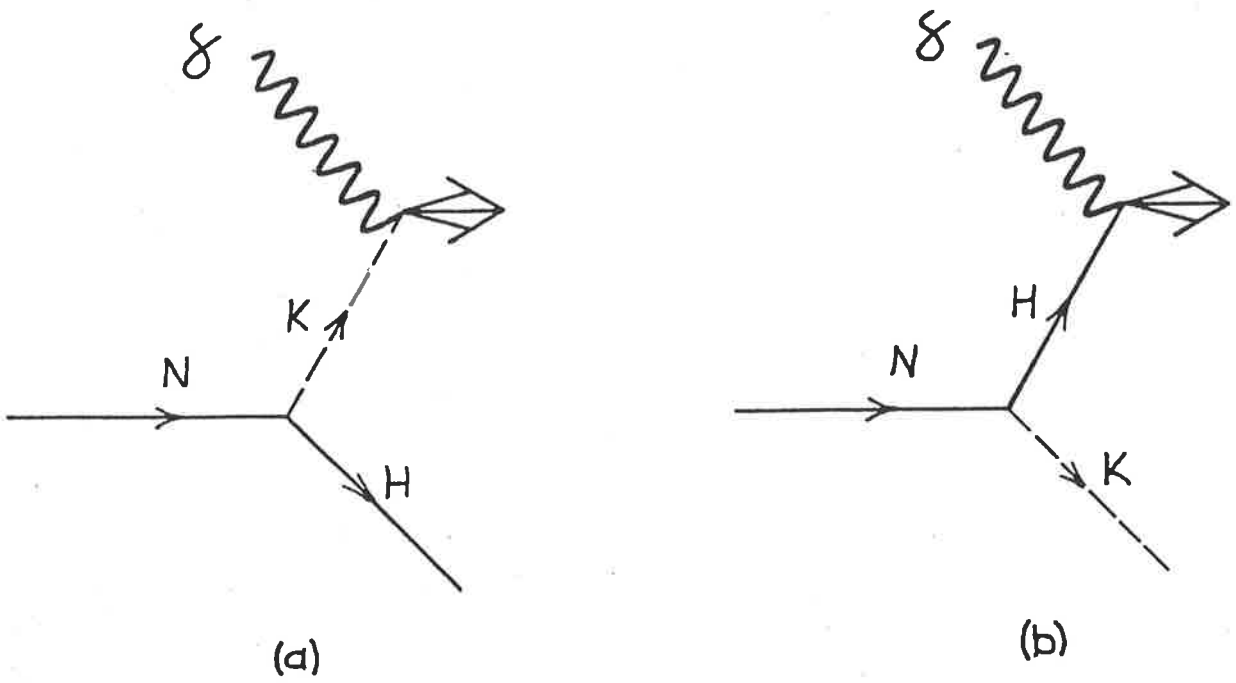

Fig 4.2 Non-perturbative contributions to the strange sea of the nucleon. (a) The incoming photon is absorbed by a virtual kaon. (b) The incoming photon is absorbed by a virtual hyperon.

For the coupling constants we use $g^2_{\Sigma NK}/4\pi = 3.7$ and $g^2_{\Lambda NK}/4\pi = 13.7$. The factor f^I_H is an isospin factor, which is 3 for $H = \Sigma$ and 1 for $H = \Lambda$. For the form factor we again use eqn. (4.13), with M_π replaced by M_K.

The function $f_K(y)$ has similar properties to $f_\pi(y)$ calculated in Section 4.1. Again it is interpreted as a probability function for finding a kaon carrying fraction y of the plus component of the momentum of the nucleon. The integral of $f_K(y)$ over the interval $y = 0$ to 1 will give the average fraction of the plus component of momentum of the nucleon that is carried by kaons. In Fig. 4.3 we show $f_K(y)$ for three values of R. The essential features are that $f(y)$ peaks near $x = 0.1$, and that the value at the peak increases rapidly as R decreases. Because of experimental uncertainties in the values of the coupling constants $g^2_{HNK}/4\pi$, there is an overall uncertainty of $\pm 14\%$ in $f(y)$, however this uncertainty does not affect the shape of $f(y)$. For $R = 0.85$ fm we find

$$\int_0^1 dy\, f(y) \simeq 0.5\% \tag{4.24}$$

so we may conclude that kaons only carry about 0.5% of the four-momentum of the nucleon, and that the contribution of kaon exchange processes, like Fig. 4.2a, to the electromagnetic structure function of the nucleon will be very small.

Our main interest in kaon exchange processes is in the non-perturbative strange sea that is generated. We adopt the usual notation

$$s_p(x) = f_{s/p}(x),\ \bar{s}_p(x) = f_{\bar{s}/p}(x) \tag{4.25}$$

and denote the non-perturbative parts of these distributions by $s^{NP}_p(x)$ and $\bar{s}^{NP}_p(x)$

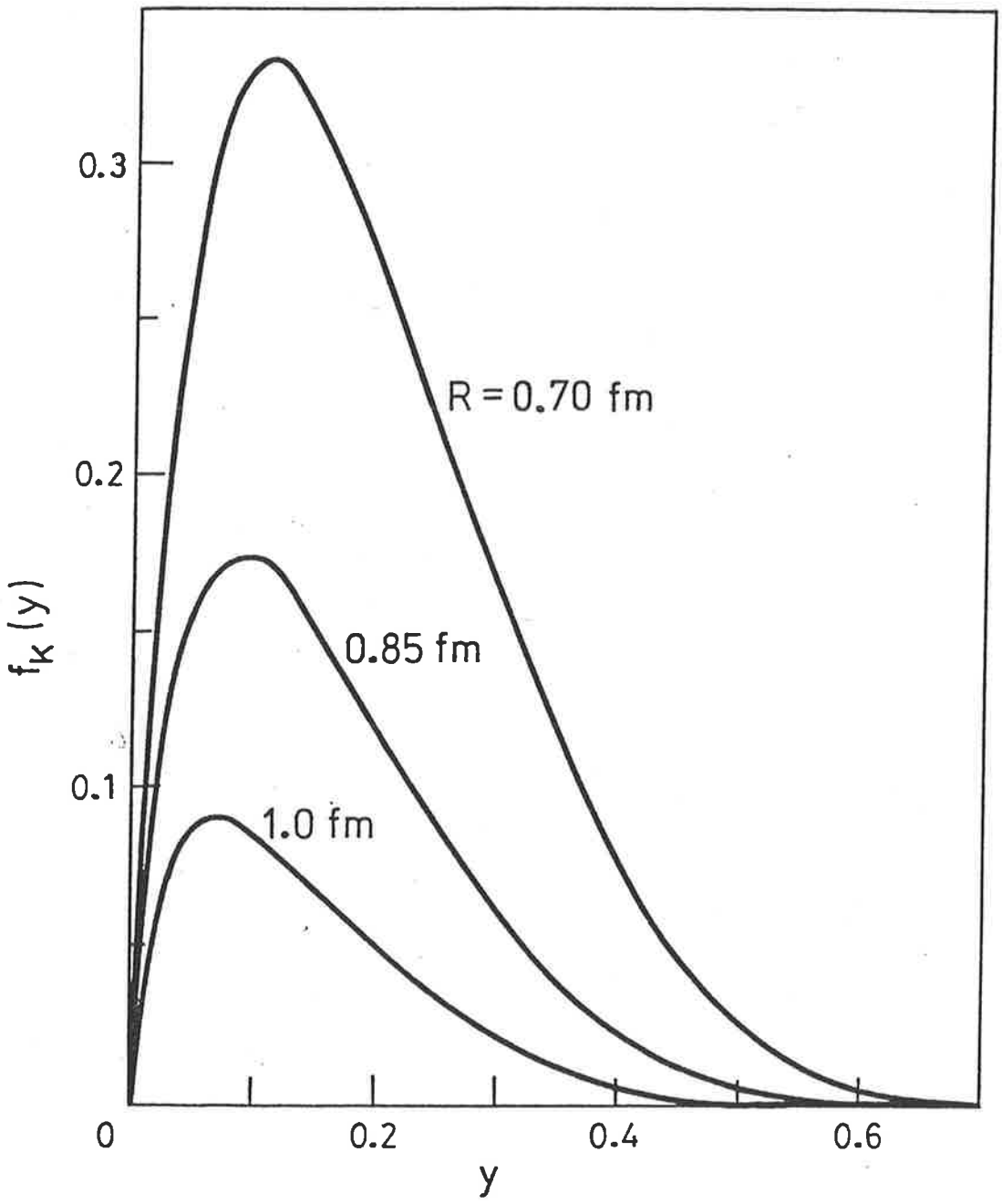

Fig 4.3 The probability $f_k(y)$ of finding a kaon carrying fraction y of the momentum of the nucleon for three values of the bag radius R.

respectively. The exchanged kaon contains one valence anti-strange quark, so from eqn. (4.21) we have

$$x\bar{s}_p^{NP}(x,Q^2) = \int_x^1 dy\, f_K(y) \left(\frac{x}{y}\right) \bar{s}_K \left(\frac{x}{y}, Q^2\right). \tag{4.26}$$

In order to find $\bar{s}_K$ we make use of the experimental observation that the pion and kaon structure functions are equal within experimental errors[Bad+ 80,Bad+ 83]. So we approximate $\bar{s}_K$ by the approximate valence distribution of the pion found experimentally:

$$z\bar{s}_K \simeq N_{\bar{s}} z^{1.0}(1-z)^{1.5}. \tag{4.27}$$

Small variations in the exponents do not change our results substantially. We show our results for the non-perturbative anti-strange sea, $x\bar{s}_p^{NP}(x)$, in Fig. 4.4.

It is less obvious how to calculate the non-perturbative strange sea, $xs_p^{NP}(x)$. The simplest approach, suggested by Berger, Coester and Wiringa [BCW 84] in the pionic case, is to evaluate Fig. 4.2b using the same $f_K(y)$ as above. The primary source of the non-perturbative strange sea of the nucleon is therefore the valence strange quarks in the recoiling hyperon. We estimate the valence distribution of the Λ and Σ to be similar to that of valence u-quarks in the nucleon:

$$s_H(z) \simeq N_s z^{-1/2}(1-z)^3. \tag{4.28}$$

Again, small variations in these exponents would change none of our conclusions. Our expression for s_p^{NP} is then:

$$xs_p^{NP}(x,Q^2) = \int_0^{1-x} dy\, f_K(y) \left(\frac{x}{1-y}\right) s_H \left(\frac{x}{1-y}, Q^2\right). \tag{4.29}$$

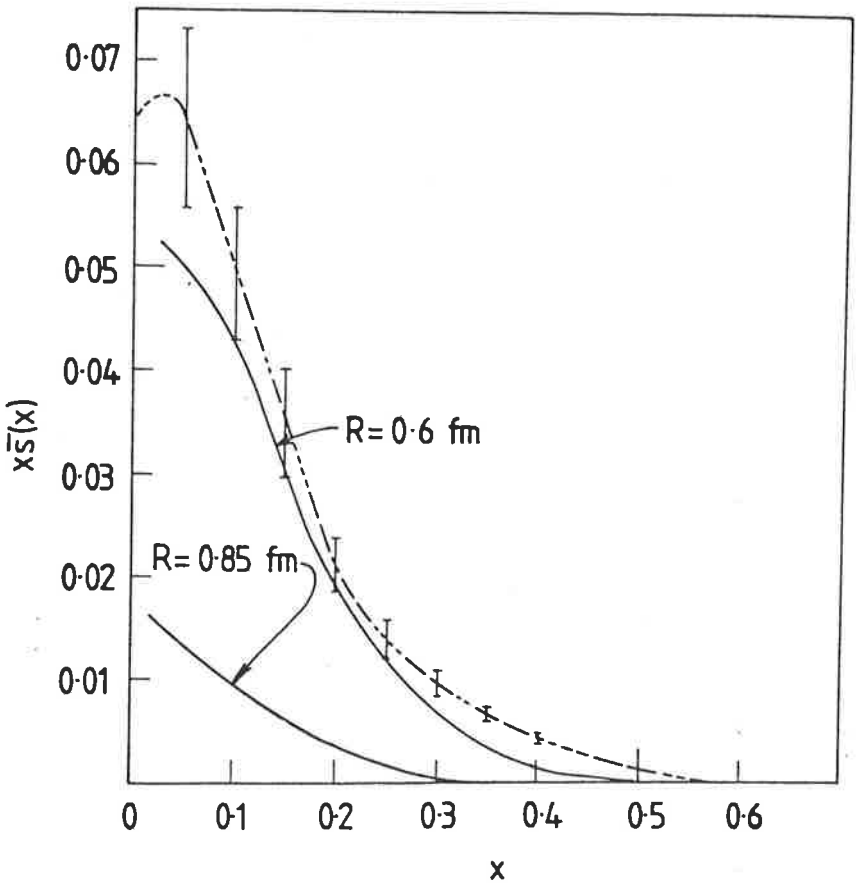

Fig 4.4 The non-perturbative contribution to $x\bar{s}(x)$ for two bag radii compared with the experimental determination of $x\bar{s}(x)$ (dot-dash line).

The immediate result of calculating s_p^{NP} and $\bar{s}_p^{NP}$ is that the two distributions have quite different shapes (see Fig. 4.5). Whereas $\bar{s}^{NP}$ has a similar shape to the usual parameterisations of sea-quark distributions, which die out beyond $x \sim 0.3$, s^{NP} is quite different. Because the origins of s^{NP} are in the valence distributions of the Λ or Σ hyperon, it extends to large values of x and also carries more momentum. If we denote the momentum fraction carried by strange and anti-strange quarks as S and $\bar{S}$ respectively, then for bag radius $R = 0.8$ fm we find $S^{NP} = 0.52\%$ and $\bar{S}^{NP} = 0.28\%$. With $R = 0.6$ and 1.0 fm, the results are $S^{NP} = 1.4\%$, $\bar{S}^{NP} = 1.0\%$ and $S^{NP} = 0.18\%$, $\bar{S}^{NP} = 0.08\%$ respectively. We may compare these fractions with the data of the CDHS group (at $Q^2 \approx 5$ GeV^2), which found [Abr+ 82,83]

$$(\bar{U} + \bar{D} + 2\bar{S}) = 7 \pm 0.5\%, \; \frac{2S}{(\bar{U} + \bar{D})} = 52 \pm 9\%. \tag{4.30}$$

If, as is usually assumed in phenomenology, we set $S = \bar{S}$ this implies $\bar{S} = 1.2 \pm 0.2\%$, which clearly restricts the allowed values of R, though this bound is not as good as that obtained from our earlier considerations of the pion cloud of the nucleon.

We can make further comparisons between our results and the CDHS data. Most of the relevant data have come from di-muon (μ^+, μ^-) coincidence measurements in (anti)neutrino scattering. The second muon comes from the decay of a charmed quark. According to the QPM and Cabbibo theory [LP 82], the cross-sections for di-muon events with an isoscalar target are

$$\begin{aligned} \frac{d\sigma^{\nu}}{dx} &\propto \sin^2\theta_C[xu(x) + xd(x)] + \cos^2\theta_C[2xs(x)], \\ \frac{d\sigma^{\bar{\nu}}}{dx} &\propto \sin^2\theta_C[x\bar{u}(x) + x\bar{d}(x)] + \cos^2\theta_C[2x\bar{s}(x)]. \end{aligned} \tag{4.31}$$

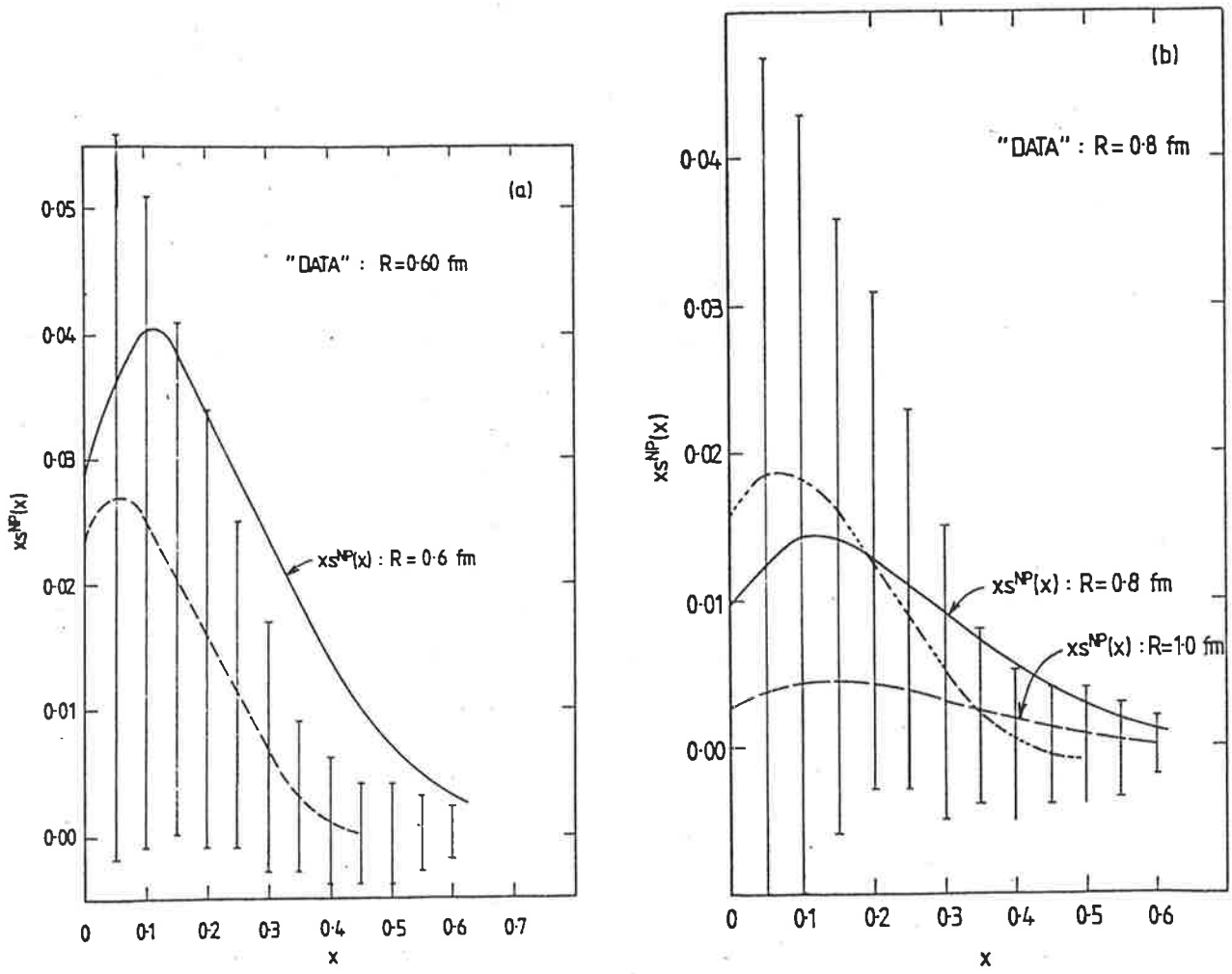

Fig 4.5 Comparison of $xs^{NP}(x)$ between this calculation and experiment. (a) For bag radius R = 0.6 fm the calculated non-perturbative contribution is larger than experiment allows. (b) For bag radii R ≤ 0.8 fm there is reasonable agreement between this calculation and experiment.

Since $\cos^2\theta_C \gg \sin^2\theta_C$ the antineutrino data gives a good determination of $x\bar{s}(x)$. This is compared with our calculation for the non-perturbative contribution in Fig. 4.4. Clearly the shapes agree well, and, for reasonable values of R, the non-perturbative contribution is less than the total distribution.

The situation for neutrino scattering is not as simple. The large valence contributions to $u(x)$ and $d(x)$ counteract the small value of $\sin^2\theta_C$, so that $s(x)$ extracted from the ν data has large errors. We have used the parameterisations of Buras and Gaemers [BG 78] between 5 and 10 GeV^2 to subtract $xu(x)$ and $xd(x)$ from the CDHS data leaving $xs(x)$. If we assume that the perturbative contributions to $s(x)$ and $\bar{s}(x)$ are equal then we have

$$xs^P(x) = x\bar{s}^P(x) = x\bar{s}(x) - x\bar{s}^{NP}(x), \tag{4.32}$$

and we can subtract $xs^P(x)$ from $xs(x)$ to extract the experimental non-perturbative distribution $xs^{NP}(x)$. This is compared with our calculations for $xs^{NP}(x)$ in Fig. 4.5. We can see that theory and experiment are in reasonable agreement in both shape and magnitude for $R \sim 0.8$ fm . However the large error bars make any definite conclusions impossible. The lack of support at large x ($x > 0.5$) rules out R less than about 0.8 fm, but little else can be said. Clearly an improvement in the experimental data would enable us to test the theory better. The errors are mainly statistical in origin, and should be improved by an increase in data.

Chapter 5

Bag Models

K'an — The Perilous Chasm

He is bound with thick cords and restrained by a thicket of thorns.

While QCD is generally regarded as the correct theory of strong interactions, as yet the QCD field equations have not been solved. In the absence of exact solutions we must turn to phenomenological models which incorporate the features expected from QCD. These features are:

1. confinement—quarks can only exist in colour singlet configurations,

2. asymptotic freedom—the coupling constant $\alpha_c(Q^2)$ decreases with Q^2,

3. chiral symmetry— the u and d quarks are very light.

One of the earliest models to be developed was the non-relativistic quark model (NRQM) [DGG 75,Isgur 80]. In this model the quark masses are of order 300 MeV, and the quarks must be considered to be dressed by higher order processes. Confinement is obtained through a phenomenological potential. The NRQM does not incorporate asymptotic freedom, nor does chiral symmetry appear naturally. The

success of the NRQM is that perturbation theory works fairly well, the hyperfine $q-q$ interaction arising from one gluon exchange being obtained as an expansion in powers of v/c.

Bag models are more ambitious phenomenological models which attempt to incorporate all three of the above features. Confinement and asymptotic freedom are incorporated by letting massless quarks move freely inside, but only inside, a cavity. While it might appear that having massless quarks would also lead to chiral symmetry being conserved, this is not the case. Interactions between the quarks and the bag wall badly break chiral symmetry, and in order to restore chiral symmetry various models along the lines of the non-linear sigma model [GL 60,IZ 80] have been proposed. In these models the chiral symmetry of the Lagrangian is 'hidden' and the pion emerges as a Goldstone boson.

5.1 The MIT Bag Model

The MIT bag [Cho+ 74] was the first of the modern bag models. The MIT bag confines the quarks to a finite region of space. Now the free quark gas inside the bag produces a pressure on the bag wall which will expand the bag indefinitely unless it is opposed. So it is necessary to introduce a bag pressure, or energy per unit volume, B, which ensures that the bag remains finite in extent. Presumably B is a universal constant which mimics the non-perturbative QCD processes which lead to confinement.

To see the rôle of the bag constant B more clearly, let us consider the energy-

momentum tensor for free quarks inside the bag:

$$\Theta^{\mu\nu}_{\text{quarks}} = [\frac{i}{2}\bar{q}(x)\gamma^{\mu} \overleftrightarrow{\partial^{\nu}} q(x)]\theta_V \tag{5.1}$$

where $q(x)$ is a quark field, $\overleftrightarrow{\partial}=\overrightarrow{\partial} - \overleftarrow{\partial}$ and θ_V is unity inside the bag and zero outside. Now the condition for energy-momentum conservation is that the divergence of the energy-momentum tensor vanishes. But this is not the case; restricting the quarks to the interior of the bag leads to problems. We have

$$\partial_{\mu}\theta_V = n_{\mu}\Delta_S \tag{5.2}$$

where Δ_S is a surface delta function

$$\Delta_S = -n \cdot \partial(\theta_V). \tag{5.3}$$

If the bag was a static sphere of radius R, then we would have $\theta_V = \theta(R - r)$ and $\Delta_S = \delta(R - r)$. The divergence of the energy-momentum tensor is

$$\partial_{\mu}\Theta^{\mu\nu}_{\text{quarks}} = -\frac{i}{2}\bar{q}\gamma \cdot n \overleftrightarrow{\partial^{\nu}} q\Delta_S. \tag{5.4}$$

Now the boundary condition imposed on the bag model by the condition that there be no colour current flowing through the bag surface is

$$n_{\mu}\bar{q}\gamma^{\mu}q = 0 \tag{5.5}$$

which is guaranteed by the linear boundary condition (lbc):

$$i\gamma \cdot nq = q \tag{5.6}$$

so that we obtain

$$\partial_\mu \Theta^{\mu\nu}_{\text{quarks}} = -\frac{1}{2}\partial^\nu[\bar{q}q]\Delta_S = -P_D n^\nu \Delta_S, \tag{5.7}$$

where P_D is the pressure exerted by the Dirac gas

$$P_D = -\frac{1}{2} n \cdot \partial(\bar{q}q)|_{\text{surface}}. \tag{5.8}$$

Thus if we add a term involving the phenomenological energy density to the energy-momentum tensor

$$\Theta^{\mu\nu}_{\text{MIT}} = \Theta^{\mu\nu}_{\text{quarks}} + Bg^{\mu\nu}, \tag{5.9}$$

then the divergence of the energy-momentum tensor will be

$$\partial_\mu \Theta^{\mu\nu}_{\text{MIT}} = (-P_D + B) n^\mu \Delta_S \tag{5.10}$$

which vanishes if

$$B = P_D = -\frac{1}{2} n \cdot \partial[\bar{q}(x)q(x)]\Big|_{\text{surface}} \cdot \tag{5.11}$$

Eqn. (5.11) is referred to as the non-linear boundary condition (nlbc).

For the static spherical case we can solve the free Dirac equation

$$\vec{\alpha} \cdot \vec{p}\psi = i\frac{\partial \psi}{\partial t} \tag{5.12}$$

inside the bag, and obtain the solutions

$$\psi^\mu_\chi = N_\chi \begin{pmatrix} j_l(\omega r/R)\chi^\mu_\chi \\ \pm i j_{l\mp 1}(\omega r/R)\chi^\mu_\chi \end{pmatrix} \tag{5.13}$$

where j_l is a spherical Bessel function, χ^μ_χ a spinor, and the subscript χ specifies the l and j quantum numbers (see [Tho 84] for details), in particular $\chi = -1$ corresponds to the $s_{1/2}$ state and χ^μ_{-1} is the usual Pauli spinor. The energy of the state is given by

$$E = \omega/R, \tag{5.14}$$

the $1s_{1/2}$ level corresponding to $\omega = 2.04$. The explicit solution for the ground state $(1s_{1/2})$ is:

$$\psi_{1s_{1/2}}(\vec{r}) = \frac{N_1}{\sqrt{4\pi}} \begin{pmatrix} j_0(\omega r/R) \\ i\vec{\sigma}\cdot\vec{r}j_1(\omega r/R) \end{pmatrix} \chi^{\mu}_{1/2} \tag{5.15}$$

with $\chi^{\mu}_{1/2}$ a Pauli spinor and the normalization given by

$$N_1^2 = \frac{\omega^3}{2R^3(\omega-1)\sin^2\omega}. \tag{5.16}$$

Interestingly the density $\bar{\psi}\gamma^0\psi$ does not vanish at $r = R$, but the flow of colour current normal to the bag surface does vanish,as guaranteed by the lbc (eqn. (5.6)).

The total energy of a bag is given by

$$P^0 = \int d^3x\, \Theta^{00}(x) \tag{5.17}$$

which we label $E(R)$. For a bag containing n quarks in the ground state we find

$$E(R) = n\frac{\omega_{1s_{1/2}}}{R} + \frac{4\pi}{3}R^3B. \tag{5.18}$$

The first term is the kinetic energy of the quarks, while the second is a volume term which implies that it costs energy BV to make a bag in the vacuum. The virial theorem for the bag (equivalent to the nlbc, see [Tho 84]) implies that $\partial E/\partial R = 0$ or

$$E(R) = (n+1)\frac{4\pi}{3}R^3B, \tag{5.19}$$

so that for a baryon $(n = 3)$ the volume energy is one quarter of the total energy.

If we assume that the quarks in the bag are quanta of coloured fields, then the feature of QCD that only colour singlet states can exist in nature follows. By construction colour electric fields, like quarks, can only exist in bags. However the colour analogy of Gauss' law states that colour electric fields must emanate from bags with net colour. The only consistent solution is that bags must be colour singlets. This automatically gives us the mesons and the baryons as $q\bar{q}$ and qqq configurations in the bag. In addition exotic states such as 'glueballs' [JJ 76] and $q^2\bar{q}^2$ are allowed in the bag model, although states with more than three quarks are generally unstable [DeG+ 75].

In order to calculate hadron masses etc. in the bag model we need to extend our expression for the total energy of the bag state, eqn. (5.18). The N and Δ masses are split by the hyperfine spin-spin interaction, which in the bag model is provided solely by one gluon exchange. The philosophy of the bag model is that the bag itself provides a suitable phenomenological description of all the non-perturbative gluon interactions, including gluon self-coupling. Thus all that is left is the first order in α_c gluon exchange, which gives the energy shifts via first order perturbation theory. The energy term for the one-gluon exchange is:

$$\Delta E_g^M = \frac{\lambda \alpha_c}{R} \sum_{i<j} \bar{M}(m_i, m_j, R) \vec{\sigma}_i \cdot \vec{\sigma}_j \tag{5.20}$$

where m_i and m_j are the quark masses, $\lambda = 1$ for baryons and 2 for mesons, and $\bar{M}$ has a closed form [DeG+ 75].

Other possible contributions to the masses of hadrons are to include massive quarks, centre of mass motion effects and zero-point energies. The effect of having

massive quarks (ie. $m_s \sim 300\text{MeV}$) is to increases the magnitude of the energy eigenfrequency ω ($\omega \sim 2.5$).

Because we have quantized fields in a finite region there will be a finite contribution to the energy from zero-point terms. There are difficulties in calculating these terms, and they are usually parametrized as a constant Z_0 divided by R [DeG+ 75]. Similarly centre of mass effects are parametrized by a $1/R$ term [Tho 84].

The complete mass formula can be summarized as

$$M(R) = \sum_i \frac{\omega_i}{R} + \frac{4\pi}{3} R^3 B + \Delta E_g^M - Z/R \tag{5.21}$$

where the last term includes correction for both the zero-point energy and centre of mass effects. The radius of the bag is determined by the stability requirement

$$\frac{\partial M}{\partial R} = 0. \tag{5.22}$$

There are four adjustable parameters: m_s, B, α_c and Z. The values of these parameters are usually determined by fitting eqn. (5.21) to the low lying hadron masses. The original fit by DeGrand *et. al.* [DeG+ 75] gives an excellent description of the baryon octet and decuplet and the pseudoscalar and vector meson nonets. The only exception is the pion, which the bag model assigns a large mass. Much of the problem with the pion may be due to centre of mass effects [DJ 80], as the $1/R$ correction is really only applicable for fairly heavy states.

5.2 Chiral Symmetry and Bag Models

Let us consider the Lagrangian density describing the MIT bag model, keeping only those pieces involving the quark fields:

$$\mathcal{L}(x) = [\frac{i}{2}\bar{q}(x)\gamma^{\mu} \overleftrightarrow{\partial}_{\mu} q(x) - B]\theta_V - \frac{1}{2}\bar{q}(x)q(x)\Delta_S \tag{5.23}$$

where the final term of eqn. (5.23) is a Lagrange multiplier guaranteeing that $\bar{q}q$ is zero at the bag surface ie. the lbc, eqn. (5.6), is satisfied.

Now if chiral symmetry were conserved in the bag model, the Lagrangian eqn. (5.23) would be invariant under the arbitrary, infinitesimal change in the quark fields

$$q \rightarrow q - i(\vec{\tau} \cdot \vec{\epsilon}/2)\gamma^5 q \tag{5.24}$$

where the $\vec{\tau}$ are the 2×2 Pauli matrices and $\vec{\epsilon}$ is constant. Under this transformation we find:

$$\mathcal{L} \rightarrow \mathcal{L} + \frac{1}{2}\bar{q}(\gamma^5\gamma^{\mu} + \gamma^{\mu}\gamma^5) \overleftrightarrow{\partial}_{\mu} (\vec{\tau} \cdot \vec{\epsilon}/2)q\theta_V + \frac{i}{2}(\vec{\tau} \cdot \vec{\epsilon})\gamma^5 q\Delta_S. \tag{5.25}$$

The second term vanishes as $\{\gamma^{\mu}, \gamma^5\} = 0$, but the last term is definitely non-zero. It is intuitively simple to see what this lack of invariance means. In Fig. 5.1 we see that any quark incident on the bag wall must be reflected. But there is no spin-flip associated with the reflection, so the quark's helicity or chirality is changed.

The so-called axial current associated with the transformation eqn. (5.24) is

$$\vec{A}^{\mu} = \bar{q}\gamma^{\mu}\gamma^5(\vec{\tau}/2)q\theta_V, \tag{5.26}$$

which is not a conserved current. The divergence of the axial current is

$$\partial_{\mu}\vec{A}^{\mu} = -\frac{i}{2}\bar{q}\gamma^5\vec{\tau}q\Delta_S \neq 0. \tag{5.27}$$

This again emphasizes the fact that the confining bag wall causes the violation of chiral symmetry, despite the fact that the quarks are massless.

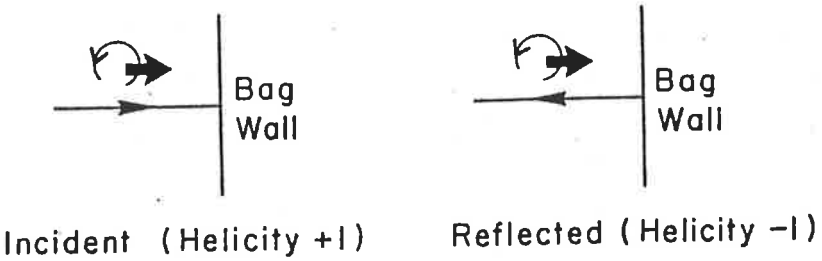

Fig 5.1 Violation of chiral symmetry at the bag surface.

The solution to the problem of violation of chiral symmetry is along similar lines to the classical sigma model of Gell-Mann and Levy [GL 60] which was outlined in Chapter 4. We introduce new fields $(\sigma, \vec{\pi})$ with the appropriate transformation properties under $SU(2)_L \times SU(2)_R$ so that the new Lagrangian is invariant. This new Lagrangian density replacing eqn. (5.23) is

$$\begin{aligned} \mathcal{L}' &= [\frac{i}{2}\bar{q}(x)\gamma^\mu \overleftrightarrow{\partial}_\mu q(x) - B]\theta_V - \frac{\lambda}{2}\bar{q}(\sigma + i\vec{\tau}\cdot\vec{\pi}\gamma^5)q\Delta_S \\ &\quad + \frac{1}{2}(\partial_\mu\sigma)^2 + \frac{1}{2}(\partial_\mu\vec{\pi})^2. \end{aligned} \tag{5.28}$$

where λ is a Lagrange multiplier which turns out to be simply $(\sigma^2 + \vec{\pi}^2)^{-1/2}$. We note that the σ and $\vec{\pi}$ fields must be massless, so the pion is a good candidate for the pseudoscalar field $\vec{\pi}$, but there is no realistic candidate for the σ. Thus the σ-field is usually eliminated. We note that $f^2 = (\sigma^2 + \vec{\pi}^2)$ is invariant under the transformations of $SU(2)_L \times SU(2)_R$, so we can eliminate σ in a chiral invariant way. The resulting theory is necessarily non-linear, and there exist a multitude of possible theories, depending on how σ is eliminated. The cloudy bag model (CBM) arises via the introduction of a new pion field, $\vec{\phi}$, through the definitions [Tho 83b]:

$$\begin{aligned} \sigma &= f\cos(\phi/f) \\ \vec{\pi} &= f\hat{\phi}\sin(\phi/f). \end{aligned} \tag{5.29}$$

To first order in the pion field, all the theories lead to a surface coupling of the pion field to the confined quarks of the form

$$H_{int} = -\frac{i}{2f}\bar{q}\vec{\tau}\cdot\vec{\phi}\gamma^5 q\Delta_S. \tag{5.30}$$

However in higher order the theories can differ markedly.

Thus, by coupling an elementary pion field to the MIT bag model we can restore chiral symmetry. While it might appear that this is one step further removed from QCD, this is not the case. One can argue on very general grounds that QCD must produce light pseudoscalar mesons in order to break the symmetry of the vacuum. These bosons are not obtained in perturbation theory in terms of the quark fields, nor can their effects be obtained using the original quark fields and perturbation theory. It is of course an idealization to treat the pion as point-like. However the pion is unique amongst hadrons in that its Compton wavelength is much greater than its spatial extent (measured by the r.m.s. charge radius). So to a first approximation we can neglect the internal structure of the pion and use what is essentially a long-wavelength approximation. This approximation remains valid so long as the pion cloud contains only one or two pions.

We shall omit a full discussion of the various chiral bag models available, and simply introduce probably the most successful of them, the cloudy bag model (CBM) [Tho 84]. The CBM keeps most of the good features of the MIT bag model. Its Lagrangian can be used to define a renormalizable theory of strong interactions, which permits systematic calculation of higher order corrections. The CBM stays well within the bounds of our long-wavelength approximation as the pion cloud contains, on average, about one pion. This means that the CBM has good convergence properties and that low order perturbation theory works well in the model.

An alternative version of the CBM may be obtained by a unitary transformation which couples the pion field to the quark fields throughout the volume of the bag ie. the quark fields are dressed by pions:

$$\begin{aligned} q &\rightarrow q_w = Sq \\ \bar{q} &\rightarrow \bar{q}_w = \bar{q}S \end{aligned} \tag{5.31}$$

with

$$S = \exp[i\vec{\tau}\cdot\vec{\phi}(\gamma^5/2f)]. \tag{5.32}$$

Then to $O(\phi^2)$ the CBM Lagrangian density becomes [Tho 84]

$$\begin{aligned} \mathcal{L}_{\rm CBM}(x) &= [\frac{i}{2}\bar{q}_w(x)\gamma^\mu \overleftrightarrow{\partial}_\mu q_w(x) - B]\theta_V - \frac{1}{2}\bar{q}_w q_w \Delta_S \\ &\quad -\frac{\theta_V}{4f^2}\bar{q}_w\gamma^\mu\vec{\tau}q_w\cdot(\vec{\phi}\times\partial_\mu\vec{\phi}) + \frac{\theta_V}{2f}\bar{q}_w\gamma^\mu\vec{\tau}q_w\cdot\partial_\mu\vec{\phi} \\ &\quad +\frac{1}{2}(\partial_\mu\vec{\phi})^2 - \frac{1}{2}m_\pi^2\vec{\phi}^2 \end{aligned} \tag{5.33}$$

where the last term explicitly breaks $SU(2)_L \times SU(2)_R$ symmetry, so that the partially conserved axial current (PCAC) condition [Col 68,AD 68]

$$\partial_\mu\vec{A}^\mu = -fm_\pi^2\vec{\phi} + O(\vec{\phi}^2) \tag{5.34}$$

is satisfied, where f is the pion decay constant ($f = 93$MeV). This Lagrangian density incorporates the major results of current algebra for low energy pion scattering, and generalizes to the whole hadron sector.

5.3 The MIT Bag in Two Spacetime Dimensions

In two spacetime dimensions we can solve the bag exactly. In this case we consider a two component Dirac field confined to a line segment. This is not a field theory

as it does not allow for the creation or annihilation of bags. Instead of the vacuum the ground state is an 'empty' bag containing no quanta, in which the bag pressure, B, is balanced by pressure generated by quantum fluctuations of the confined field.

In two-dimensional spacetime it is most convenient to work with light-cone coordinates:

$$\begin{aligned} \tau &\equiv x^+ = \frac{1}{\sqrt{2}}(x^0 + x') \\ x &\equiv x^- = \frac{1}{\sqrt{2}}(x^0 - x') \end{aligned} \tag{5.35}$$

and a light-cone basis for the two component Dirac spinors:

$$\gamma^\pm = \frac{1}{\sqrt{2}}(\gamma^0 \pm \gamma^1) \tag{5.36}$$

where

$$\gamma^0 = \begin{pmatrix} 0 & 1 \\ 1 & 0 \end{pmatrix}, \qquad \gamma^1 = \begin{pmatrix} 0 & -1 \\ 1 & 0 \end{pmatrix}. \tag{5.37}$$

The free Dirac equation is satisfied by any spinor of the form

$$q(x,\tau) = \begin{pmatrix} ig(x) \\ f(\tau) \end{pmatrix}. \tag{5.38}$$

We choose τ to be the development parameter for the system. The conjugate variables to τ and x are H ($\equiv P^-$) and P ($\equiv P^+$) respectively. At any τ the bag is a line segment with endpoints $x_1(\tau)$ and $x_2(\tau)$. The solutions are given in terms of a parameter σ defined implicitly [Cho+ 74]:

$$\frac{d\sigma}{dx} = \frac{\sqrt{2}}{P}(g^{*\prime}(x)g(x)) \tag{5.39}$$

$$\sigma(x_1(0)) = 0. \tag{5.40}$$

The virtue of the parameter σ is that although the boundaries of the bag $x_i(\tau)$ fluctuate in τ, the bag extends over a fixed interval in σ:

$$\begin{aligned} \sigma(x_1(\tau)) &= \sigma_1(\tau) = B\tau/P \\ \sigma(x_2(\tau)) &= \sigma_2(\tau) = 1 + B\tau/P \end{aligned} \tag{5.41}$$

where B is the bag constant. The Dirac field is then given by:

$$f(\tau) = \left(\frac{B}{\sqrt{2}P}\right)^{1/2} {\sum_{m=-\infty}^{\infty}}' b_m e^{-2\pi i m B\tau/P} \tag{5.42}$$

$$\begin{aligned} \tilde{g}(\sigma) &\equiv \left(\frac{dx}{d\sigma}\right)^{1/2} g(x(\sigma)) \\ &= \left(\frac{1}{2}\right)^{1/4} {\sum_{m=-\infty}^{\infty}}' b_m e^{-2\pi i m\sigma} \end{aligned} \tag{5.43}$$

where the prime on the summation indicates that m is summed over half-odd integers.Now substituting eqn. (5.43) into eqn. (5.39) gives a differential equation for $x(\sigma)$:

$$\frac{dx}{d\sigma} = \frac{\sqrt{2}}{P} Im(\tilde{g}^{*\prime}(\sigma)\tilde{g}(\sigma)). \tag{5.44}$$

Integrating this we have:

$$x(\sigma) = \bar{x}_0 + \frac{2\pi}{P} L_0(\sigma - \frac{1}{2}) + \frac{i}{P} \sum_{n\neq 0} \frac{1}{n} L_n e^{-2\pi i n\sigma} \tag{5.45}$$

where

$$L_n = {\sum_{m=-\infty}^{\infty}}' (m + \frac{1}{2}) b_m^* b_{n+m} \tag{5.46}$$

and $\bar{x}_0$ is a constant of integration. The Hamiltonian of the system is given by

$$H = \frac{2\pi B}{P} {\sum_{m=-\infty}^{\infty}}' m(b_m^* b_m - b_{-m}^* b_{-m}) \tag{5.47}$$

We may now make the transition to quantum mechanics by replacing Poisson brackets by commutators or anticommutators as appropriate:

$$\begin{aligned} \{b_m, b_n^\dagger\} &= \delta_{mn} \\ \{b_m, b_n\} &= 0 \end{aligned} \tag{5.48}$$

$$\begin{aligned} [\bar{x}_0, P] &= -i \\ [\bar{x}_0, b_m] &= [P, b_m] = 0, \end{aligned} \tag{5.49}$$

and as usual we define antiparticle creation operators:

$$d_m^\dagger \equiv b_{-m}, \qquad m > 0. \tag{5.50}$$

The empty bag is defined by

$$\begin{aligned} b_m|0\rangle_B &= d_m|0\rangle_B = 0 \qquad m > 0 \\ P|0\rangle_B &= p|0\rangle_B, \end{aligned} \tag{5.51}$$

where p is the eigenvalue of P, and

$$H|0\rangle_B = \frac{m_0^2}{2P}|0\rangle_B \tag{5.52}$$

where m_0^2 is a zero-point energy obtained in normal ordering H:

$$H = \frac{2\pi B}{P} \sum_{m=1/2}^{\infty}{}' m(b_m^\dagger b_m + d_m^\dagger d_m) + \frac{m_0^2}{2P}. \tag{5.53}$$

We note that the fundamental operators fall into two commuting classes: internal variables $\{b_m\}$, and collective variables $\bar{x}_0$ and P. We can construct a Lorentz boost operator:

$$\Lambda = -\frac{1}{2}(\bar{x}_0 P + P\bar{x}_0) \tag{5.54}$$

$$
\begin{aligned}
[\Lambda, P] &= iP \\
[\Lambda, H] &= -iH
\end{aligned}
\tag{5.55}
$$

which transforms the states

$$
e^{i\beta\Lambda}|p\{n\}\rangle = |e^{\beta}p\{n\}\rangle \tag{5.56}
$$

where $|p\{n\}\rangle$ denotes a general bag state, $\{n\}$ are the occupation numbers of the internal modes and p is the eigenvalue of P.

We now want to construct the quark field operator. The quark field defined implicitly by eqns. (5.42–5.45) describes an infinite chain of linked bags rather than a single one. To obtain the field for a single bag we multiply by appropriate θ-functions, restricting $q(x,\tau)$ to a single bag. We consider first the plus component of q:

$$
q_+ = \frac{1}{2}\gamma^-\gamma^+ q, \tag{5.57}
$$

and we define

$$
Q_+(x,\tau) \equiv \int_{x_1(\tau)}^{x_2(\tau)} dx'\, \delta(x-x')q_+(x') \tag{5.58}
$$

so $Q_+(x,\tau)$ is equal to $q_+(x)$ for $x_1(\tau) \leq x \leq x_2(\tau)$ and is zero elsewhere. As our model has a canonical Hamiltonian form, it will suffice to calculate $Q_+(x,0)$ as $Q_+(x,\tau)$ can be obtained for any τ by evolution with the Hamiltonian. If we change to the variable σ, we have

$$
Q_+(x,0) = \int_0^1 d\sigma \frac{dx'}{d\sigma}\delta(x-x'(\sigma))q_+(x'(\sigma)). \tag{5.59}
$$

We now use eqn. (5.43) to insert the field $\tilde{g}(\sigma)$. Multiplying and dividing eqn. (5.59) by P, and using the exponential representation for $\delta(xP - x'(\sigma)P)$ we find

$$Q_+(x,0) = \frac{i}{2\pi}\int_{-\infty}^{\infty} d\alpha \int_0^1 d\sigma \ \exp[i\alpha(Px + \Lambda - \Gamma(\sigma))]\tilde{g}(\sigma)\left(\frac{dx'}{d\sigma}\right)^{1/2} P. \quad (5.60)$$

We have used eqn. (5.45) to write $Px(\sigma) = -\Lambda + \Gamma(\sigma)$ where

$$\Gamma(\sigma) \equiv 2\pi L_0(\sigma - \frac{1}{2}) + i\sum_{n\neq 0}\frac{1}{n}L_n e^{-2\pi i n\sigma} \quad (5.61)$$

is independent of $\bar{x}_0$ and P. The ordering of terms in eqn. (5.60) can be shown to be unique [Jaffe 81].

Using eqn. (5.55) we can derive the identity:

$$e^{iPx}\Lambda e^{-iPx} = \Lambda + Px \quad (5.62)$$

which can be generalized to

$$e^{i\alpha(Px+\Lambda)} = e^{iPx}e^{i\alpha\Lambda}e^{-iPx}. \quad (5.63)$$

Using this identity we can establish that $Q_+(x,0)$ is translation invariant ie.

$$Q_+(x,0) = e^{iPx}Q_+(0,0)e^{-iPx}. \quad (5.64)$$

Because P commutes with all the operators except Λ in eqn. (5.60), we can move the factors $e^{\pm iPx}$ from the identity to the outside, giving the form required by translation invariance, and leaving

$$Q_+(0,0) = \frac{i}{2\pi}\int_{-\infty}^{\infty}\int_0^1 d\sigma \ \exp[i\alpha\Lambda - i\alpha\Gamma(\sigma)]\tilde{g}(\sigma)\left(\frac{d\Gamma}{d\sigma}P\right)^{1/2} \quad (5.65)$$

This form also establishes Lorentz covariance, as it is clear that $Q_+(0,0)$ transforms like $\sqrt{P}$.

We can easily find the minus component of Q by making a parity transformation on Q_+, since the parity operator Π interchanges the null planes $\tau = 0$ and $x = 0$:

$$Q_-(0,0) = \Pi Q_+(0,0)\Pi, \tag{5.66}$$

$$\begin{aligned} \Pi P \Pi &= H \\ \Pi \Lambda \Pi &= -\Lambda \\ \Pi b_n \Pi &= b_n \end{aligned} \tag{5.67}$$

Thus

$$Q_-(0,0) = \frac{i}{2\pi}\int_{-\infty}^{\infty}\int_0^1 d\sigma\, \exp[-i\alpha\Lambda - i\alpha\Gamma(\sigma)]\tilde{g}(\sigma)\left(\frac{d\Gamma}{d\sigma}H\right)^{1/2}. \tag{5.68}$$

Now the operator $e^{-i\alpha\Gamma(\sigma)}$ is very poorly understood. This is because the $\{L_n\}$ do not commute with each other so the operator is highly ambiguous. So we need now to make approximations to the full quantum theory of the bag in two spacetime dimensions.

5.3.1 The Cavity Approximation

The simplest approximation to the bag model in two dimensions is a static line-segment of length $2l$, which we centre at the origin. In this case the bag boundaries $x_i(\tau)$ are given by:

$$\begin{aligned} x_1(\tau) &= \sqrt{2}(\tau - l) \\ x_2(\tau) &= \sqrt{2}(\tau + l) \end{aligned} \tag{5.69}$$

which we may compare with the boundaries in terms of the parameter σ, given by eqn. (5.41). Now in the cavity approximation the transformation between x and σ will be linear, so by comparing the boundary equations eqns. (5.41) and (5.69) we have

$$\frac{d\sigma}{dx} = \frac{-1}{2\sqrt{2}l}. \tag{5.70}$$

Then substituting in eqn. (5.43) gives

$$ig(x) = \frac{1}{2\sqrt{l}} \sum_m{}' b_m e^{-i\sqrt{2}E_m(x+\phi)} \tag{5.71}$$

where

$$E_m = \frac{\pi m}{2l}, \tag{5.72}$$

and ϕ is an irrelevant phase factor, which we shall ignore. Now using eqns. (5.39) and (5.42) we obtain

$$\frac{B}{P} = \frac{1}{2\sqrt{2}l} \tag{5.73}$$

and

$$f(\tau) = \frac{1}{2\sqrt{l}} \sum_m{}' b_m e^{-i\sqrt{2}E_m\tau}. \tag{5.74}$$

If there are j massless quarks in the cavity with energies $E_{m_1} \ldots E_{m_j}$ then

$$B = \frac{1}{2l} \sum_{k=1}^{j} E_{m_k} \tag{5.75}$$

and

$$\begin{aligned} M &= 2Bl + \sum_{k=1}^{j} E_{m_k} \\ &= 4Bl. \end{aligned} \tag{5.76}$$

We may now write the quark field in terms of the usual time and space variables $t(\equiv x^0)$ and $\xi(\equiv x')$:

$$q(t,\xi) = \frac{1}{2\sqrt{l}} \sum_m{}' b_m \begin{pmatrix} e^{iE_m\xi} \\ (-1)^{(m-1/2)} e^{-iE_m\xi} \end{pmatrix} e^{-iE_m t}. \tag{5.77}$$

5.3.2 The L_0 Approximation

The cavity approximation is not translation invariant because the bag's position is fixed. In the L_0 approximation the bag is a cavity of fixed length, but the centre of the cavity is not fixed. The operators $\{L_n\}$ in eqn. (5.45) are set to zero for $n \neq 0$, and L_0 is replaced by its expectation value $\langle L_0 \rangle$.

Thus in the L_0 approximation $\Gamma(\sigma)$, eqn. (5.61) becomes

$$\Gamma(\sigma) = 2\pi \langle L_0 \rangle (\sigma - \frac{1}{2}). \tag{5.78}$$

We can replace σ by a new variable z, which measures the distance from the boundary σ_1 in the bag's rest frame. Using eqn. (5.45) we have:

$$z \equiv \frac{2\sqrt{2}\pi}{M} \langle L_0 \rangle (\sigma - \frac{1}{2}) \tag{5.79}$$

where $M/\sqrt{2}$ is just P in the rest frame,

$$g(z) = \left(\frac{dz}{d\sigma} \right)^{-1/2} \tilde{g}(\sigma(z)). \tag{5.80}$$

Substituting these into our expression for $Q_+(0,0)$, eqn. (5.65) we obtain

$$Q_{+,0}(0,0) = \frac{i}{2\pi} \int_{-\infty}^{\infty} d\alpha \, e^{i\alpha\Lambda} \bar{g}(\alpha) \sqrt{\frac{\sqrt{2}P}{M}} \tag{5.81}$$

$$\bar{g}(\alpha) = \frac{M}{\sqrt{2}} \int_{-\sqrt{2}l}^{\sqrt{2}l} dz \, e^{i\alpha M z/\sqrt{2}} g(z), \tag{5.82}$$

where $2l$ is the length of the bag (in x') in its rest frame:

$$2l = \frac{2\pi}{M}\langle L_0 \rangle, \tag{5.83}$$

and the subscript 0 indicates that we are using the L_0 approximation.

We can obtain $g(z)$ from eqn. (5.43):

$$g(z) = \frac{1}{2\sqrt{l}} \sum_m b_m e^{-i\sqrt{2}E_m(z+1/2)} \tag{5.84}$$

which is identical with $g(x)$, eqn. (5.71), up to irrelevant phase factors. Thus in the L_0 approximation we take the Fourier transform of a cavity field operator, modulate by the boost operator $e^{i\alpha\Lambda}$, and obtain a translation invariant operator.

Unfortunately, because we have no understanding of the operator $e^{-i\alpha\Gamma(\sigma)}$, it is difficult to demonstrate the validity of the L_0 approximation. In particular it is not clear whether the L_0 approximation is any closer to the full quantum bag theory than the cavity approximation. There does exist another method of restoring translation invariance to the cavity approximation. This is the Peierls-Yoccoz method [PY 57] which is well known in nuclear physics. We will discuss the Peierls-Yoccoz procedure in the next chapter.

5.3.3 The Cavity Approximation with Background Fields

Our ultimate aim is to calculate deep inelastic scattering (DIS) structure functions using bag model wavefunctions. Because of the great amount of interest in nuclear DIS that has been generated by the discovery of the EMC effect, we would like not only to calculate structure functions for free bag states, but also for bag states immersed in some background fields which simulate the nuclear environment. In

particular we want to solve the two dimensional cavity in the presence of a vector field and a scalar field.

Following the considerations of Guichon [Gui 88], the Dirac equation inside the cavity becomes

$$i\gamma^\mu \partial_\mu \psi + V_S \psi - V_0 \gamma^0 \psi = 0 \tag{5.85}$$

where V_S corresponds to a attractive scalar potential, arising, say, from the σ-field, and V_0 is the time component of a repulsive vector potential, which could arise from the ω-field in nuclear matter. Because of the scalar potential V_S, it is no longer convenient to use light-cone coordinates, so we revert to the usual spacetime coordinates $t = x^0$ and $x = x'$. We still have the boundary conditions:

$$\begin{aligned} i\gamma^\mu n_\mu \psi &= \psi \\ n^\mu \partial_\mu \textstyle\sum(\bar{\psi}\psi) &= -2B. \end{aligned} \tag{5.86}$$

The solution to eqn. (5.85) is:

$$\psi(x,t) = \sum_{n=-\infty}^{\infty} b_n N_n \left[\begin{pmatrix} 1 \\ \alpha_n \end{pmatrix} e^{iE_n x} + (-1)^n \begin{pmatrix} \alpha_n \\ 1 \end{pmatrix} e^{-iE_n x} \right] e^{-i\varepsilon_n t} \tag{5.87}$$

where n is an integer,

$$E_n = \sqrt{(\varepsilon_n - V_0)^2 + V_S^2} \tag{5.88}$$

$$\alpha_n = [E_n - (\varepsilon_n - V_0)]/V_S \tag{5.89}$$

$$N_n = \frac{1}{2}[(1+\alpha_n^2)l + (-1)^n \frac{\alpha_n}{E_n} \sin 2E_n l]^{-1/2} \tag{5.90}$$

and the energy eigenvalues ε_n are determined by the solutions of the transcendental equation:

$$2E_n l - \tan^{-1}\frac{\varepsilon_n - V_0}{V_S} - n\pi = 0. \tag{5.91}$$

The bag constant B is found from the nlbc, eqn. (5.86):

$$B = \sum_{k=1}^{j}(-1)^n |N_n|^2 2E_{n_k}(1+\alpha_{n_k}^2)\sin 2E_{n_k} l \tag{5.92}$$

where, as before, we have j quarks in the cavity with quantum numbers $n_1 \ldots n_j$. Using the virial theorem we obtain the mass of our cavity state:

$$M = 2Bl + \sum_{k=1}^{j}\varepsilon_{n_k}. \tag{5.93}$$

Taking the limit $V_S \to 0$, $V_0 \to 0$ we obtain the free cavity wavefunction, eqn. (5.77).

The effect of introducing the scalar potential is to lower the values of the energy eigenvalues ε_n and the bag constant B, hence lowering the mass of the cavity state. On the other hand, the vector potential increases the energy eigenvalues but does not alter the mass of the cavity state (because of Lorentz invariance). If we take a 'nucleon' cavity state with three quarks in the ground ($n = 0$) state, then with no background fields we have

$$\varepsilon_0 = \frac{\pi}{4l}, \quad B = \frac{3\pi}{8l^2}, \quad M = \frac{3\pi}{2l}. \tag{5.94}$$

Switching on a scalar potential of strength $V_S = \frac{\pi}{50l}$ reduces ε_0 by 6%, B by 10% and M by 8%. Switching on a vector potential of the same strength, we increase ε_0 by 8% and reduce B by a similar amount, so M stays constant. So we see that introducing the background fields into the cavity approximation produces changes in the energies of the cavity state which are of a similar magnitude to the fields themselves.

Chapter 6

Deep Inelastic Scattering on Bag States

Fu — Returning

Freedom and progress lie ahead ... movement in any direction will be of advantage ... All ... actions are in harmony with the will of heaven.

The calculation of the matrix elements involved in DIS is extremely difficult. This is because we do not fully understand the non-perturbative QCD processes which bind quarks and gluons into hadrons. However if we were to adopt some model of confinement then it should be possible to calculate DIS matrix elements in that model. This can serve not only to test quark confinement models, but also to enrich our understanding of the matrix elements and the structure functions that may be derived from them.

An obvious first choice of model is the MIT bag. As we have already noted in Chapter 5, the MIT bag model has two of the desired features of QCD: absolute confinement and asymptotic freedom. The property of asymptotic freedom is crucial to the calculation of DIS matrix elements, and we expect that Bjorken scaling should

follow from the asymptotic freedom in the model. The lack of chiral symmetry in the MIT bag is not too great a concern. In Chapter 4 we calculated what the pionic contribution to DIS looks like in the CBM. The effect was of the order of 5% of the total structure function $F_2(x)$ integrated over all x, and was mostly at small x. So we expect that at medium to large values of x the effects of breaking chiral symmetry will be small.

Most of this chapter will be concerned with DIS in two spacetime dimensions. As we have seen in Chapter 2, DIS is primarily a light-cone process, so in doing calculations in two rather than four dimensions we will not be discarding any of the important light-cone physics. The two dimensional model has been an important laboratory for the calculation of DIS matrix elements because of the relative ease with which ideas can be tested.

At first sight, DIS in two dimensions appears impossible as the Compton amplitude for a vector current scattering off a Dirac particle in two dimensions in fact vanishes [Jaffe 75]. However using a hypothetical scalar current of the form $J(\xi) = \bar{\psi}(\xi)\psi(\xi)$ leads to non-vanishing matrix elements which are very similar to the matrix elements in four dimensions. This similarity between the two and four dimensional cases further reassures us that we are not discarding any of the essential physics of DIS by doing calculations in two dimensions.

We will look first at the original calculations of DIS matrix elements by Jaffe in the cavity approximation [Jaffe 75], and in the translation invariant L_0 approximation [Jaffe 81]. We will then turn to a second method of restoring translation

invariance to the cavity approximation, the Peierls-Yoccoz projection [PY 57], and calculate the quark distribution functions. These distributions are an improvement on the original cavity calculations. In Section 6.3 we will examine the importance of momentum conservation to these calculations, and we will see the important rôle of the intermediate state. The final section brings together the Peierls-Yoccoz projection and the ideas concerning momentum conservation in the intermediate state, to give us a new calculation of the quark distribution functions, which appears to satisfy the physical constraints better than any previous calculation.

We note that our calculations of DIS matrix elements using bag states may well break down at small x. In Chapter 2 we derived the relation $|\xi^3| < 1/Mx$, from which it follows that we require

$$x > \frac{1}{2Ml} \simeq 0.1$$

in the static cavity approximation and $x > 0.05$ in the case of the Peierls-Yoccoz projected cavity. This is a fairly cautious lower limit [Tho 88].

6.1 DIS in the Cavity Approximation

The first calculation of bag model matrix elements in DIS was done by Jaffe [Jaffe 75]. We repeat that calculation here in order to set the stage for our later work, and to introduce the problems associated with the calculations. Jaffe computed the structure functions using the cavity approximation of Chapter 5 in both two and four dimensions. As was expected, scaling emerged quite naturally, however the structure functions extended into the non-physical region ($x > 1$). It was noted immediately

that the problem of bad support for the structure functions arose from the breaking of translation invariance in the cavity approximation. A second problem was that the calculation implied that the antiquark distributions were negative, which violates the positivity restrictions on the distribution functions which we derived in Chapter 2.

However a major success of this calculation was that it showed that an analysis similar to that we used in the QPM in Chapter 2 can be applied to the calculation of DIS matrix elements in the cavity approximation. This simplification of the problem results from the interior of the bag having essentially no binding interactions.

The general structure function for DIS is conventionally given by:

$$W_{\mu\nu} = \frac{1}{4\pi} \int d^4\xi \, e^{iq\cdot\xi} \langle p|[J_\mu(\xi), J_\nu(0)]|p\rangle_c \tag{6.1}$$

where the states have the covariant normalization

$$\langle p|p'\rangle = (2\pi)^3 2p^0 \delta^{(3)}(\vec{p} - \vec{p'}). \tag{6.2}$$

Of course in two dimensions we drop the Lorentz indices as we are considering a scalar current, and we alter the superscripts in an obvious way. Unfortunately the bag states are not covariantly normalized, but normalized to unity. Also, because the cavity approximation breaks translation invariance, Jaffe centred the cavity at the origin and had the currents act at the two spacetime points ξ_1 and ξ_2. Thus he obtained

$$W_{\mu\nu} = \frac{p^0}{(2\pi)^2 \delta(0)} \int d^4\xi_1 d^4\xi_2 \, e^{iq\cdot(\xi_1 - \xi_2)} \langle T|[J_\mu(\xi_1), J_\nu(\xi_2)]|T\rangle_c \tag{6.3}$$

where he defined

$$|T\rangle \equiv [(2\pi)^3 2p^0 \delta^{(3)}(0)]^{-1/2}|p\rangle \tag{6.4}$$

which is normalized to unity. We may integrate over the average time $(\xi_1^0 + \xi_2^0)/2$ in eqn. (6.3) which will cancel the delta function leaving

$$W_{\mu\nu} = \frac{M}{2\pi}\int dt \int d^3\vec{\xi}_1\, d^3\vec{\xi}_2\, e^{iq^0 t - i\vec{q}.(\vec{\xi}_1 - \vec{\xi}_2)} \langle T|[J_\mu(t,\vec{\xi}_1), J_\nu(0,\vec{\xi}_2)]|T\rangle_c \tag{6.5}$$

where M is the mass of the target state. For bag states the space integrals are restricted to the interior of the bag, however in a fully translation invariant theory they would have to be evaluated over all space. Thus for our cavity in two dimensions, where we drop the Lorentz indices, we have the structure function:

$$W = \frac{M}{2\pi}\int dt \int_{-l}^{l} d\xi_1 \int_{-l}^{l} d\xi_2\, e^{iq^0 t - iq'(\xi_1 - \xi_2)} \langle T|[J(t,\xi_1), J(0,\xi_2)]|T\rangle_c. \tag{6.6}$$

The commutator in eqn. (6.6) can be expanded in terms of the fields in the cavity:

$$\begin{aligned}[J(t,\xi_1), J(0,\xi_2)] \;=\; & \bar{q}(t,\xi_1) S_{\rm cav}(t,\xi_1,\xi_2) q(0,\xi_2) \\ & -\bar{q}(0,\xi_2) S_{\rm cav}(-t,\xi_2,\xi_1) q(t,\xi_1)\end{aligned} \tag{6.7}$$

where $S_{\rm cav}$ is the anticommutator function for the fields:

$$S_{\rm cav}(t,\xi_1,\xi_2) \equiv \{q(t,\xi_1), \bar{q}(0,\xi_2)\}. \tag{6.8}$$

The quark field in the two dimensional cavity was found in the previous chapter:

$$q(t,\xi) = \frac{1}{2\sqrt{l}} \sum_m{}' b_m \begin{pmatrix} e^{iE_m\xi} \\ (-1)^{(m-1/2)} e^{-iE_m\xi} \end{pmatrix} e^{-iE_m t}, \quad E_m = \frac{\pi m}{2l} \tag{6.9}$$

where the prime on the summation indicates that m is summed over half-odd integers. Using the usual anticommutation relations between the destruction and creation operators for fermions, the anticommutator function $S_{\rm cav}$ can be calculated explicitly:

$$S_{\rm cav}(t,\xi_1,\xi_2) = \frac{1}{4l}\sum_n{}' \begin{pmatrix} (-1)^{(n-\frac{1}{2})}e^{iE_n(\xi_1+\xi_2)} & e^{iE_n(\xi_1-\xi_2)} \\ e^{-iE_n(\xi_1-\xi_2)} & (-1)^{(n-\frac{1}{2})}e^{-iE_n(\xi_1+\xi_2)} \end{pmatrix} e^{-iE_nt} \quad (6.10)$$

where the sum ranges over positive and negative n. The first term in the commutator, eqn. (6.7), is given by:

$$\frac{1}{(4l)^2}\sum_{m,n}{}' e^{-i(E_m-E_n)t} \quad \Big\{(-1)^{m+n-1}\left(e^{i(E_m+E_n)(\xi_1+\xi_2)} + e^{-i(E_m+E_n)(\xi_1+\xi_2)}\right) + \left(e^{i(E_m+E_n)(\xi_1-\xi_2)} + e^{-i(E_m+E_n)(\xi_1-\xi_2)}\right)\Big\}, \quad (6.11)$$

where the first two terms are from the diagonal terms in the anticommutator function, and the final two terms are from the off-diagonal terms.

Now the integral over t in eqn. (6.6) will give an energy conserving delta function which tells us that q^0 must be the energy difference of two cavity modes. The Bjorken limit is defined:

$$q' \to q^0 + Mx, \quad q^0 \to \infty \quad (6.12)$$

and we see that the diagonal and off-diagonal terms in the anticommutator give vastly different results. Using the delta function to eliminate E_n, we have for the integrals over the off-diagonal terms:

$$2\frac{\sin(2E_m - Mx)l}{2E_m - Mx} \times 2\frac{\sin(Mx - 2E_m)l}{Mx - 2E_m},$$

but for the diagonal terms we have

$$2\frac{\sin(2E_m - Mx)l}{2E_m - Mx} \times 2\frac{\sin(2q^0 + Mx + 2E_m)l}{2q^0 + Mx + 2E_m} \to 0.$$

Thus in the Bjorken limit the structure function becomes

$$\lim_{Bj} W(q^0, x) = \frac{M}{4} \sum_{m,n}{}' \left\{ \begin{array}{l} \delta(q^0 + E_m - E_n)\frac{\sin^2(2E_m l - Mlx)}{(2E_m l - Mlx)^2} \\ -\delta(q^0 - E_m + E_n)\frac{\sin^2(2E_m l + Mlx)}{(2E_m l + Mlx)^2} \end{array} \right\} \tag{6.13}$$

where the matrix elements $\langle T|b_m^\dagger b_m|T\rangle$ are taken to be unity.

Realistically we 'smear' the delta functions by averaging the structure function W over a Gaussian distribution, where the spread of the Gaussian is much larger than the energy gap $\pi/2l$. This will take into account the finite lifetimes of the intermediate states. The final result then is:

$$\lim_{Bj} W_{\rm cav}(x) = \frac{Ml}{2\pi} \sum_m{}' \left\{ \frac{\sin^2(2E_m l - Mlx)}{(2E_m l - Mlx)^2} - \frac{\sin^2(2E_m l + Mlx)}{(2E_m l + Mlx)^2} \right\} \tag{6.14}$$

where the cavity state's mass is given by

$$M = 2 \sum_{\{m\}}{}' E_m \tag{6.15}$$

with the set $\{m\}$ labelling the quantum numbers of the state. $W_{\rm cav}$ is shown in Fig. 6.1 for n quarks in the ground state.

As we stated earlier, eqn. (6.14) displays explicit Bjorken scaling and is non-zero for $x > 1$. About 7% of the quark distribution function is in the kinematically forbidden region. The second term in eqn. (6.14) would correspond, in the QPM, to antipartons with negative distribution functions, so it is clearly a problem.

In Fig. 6.2 we show the three possible graphs for Compton scattering in the cavity. The first term in eqn. (6.14) corresponds to the usual Compton diagram Fig. 6.2a. The second term corresponds to the so-called 'z-graph', Fig. 6.2b. Usually

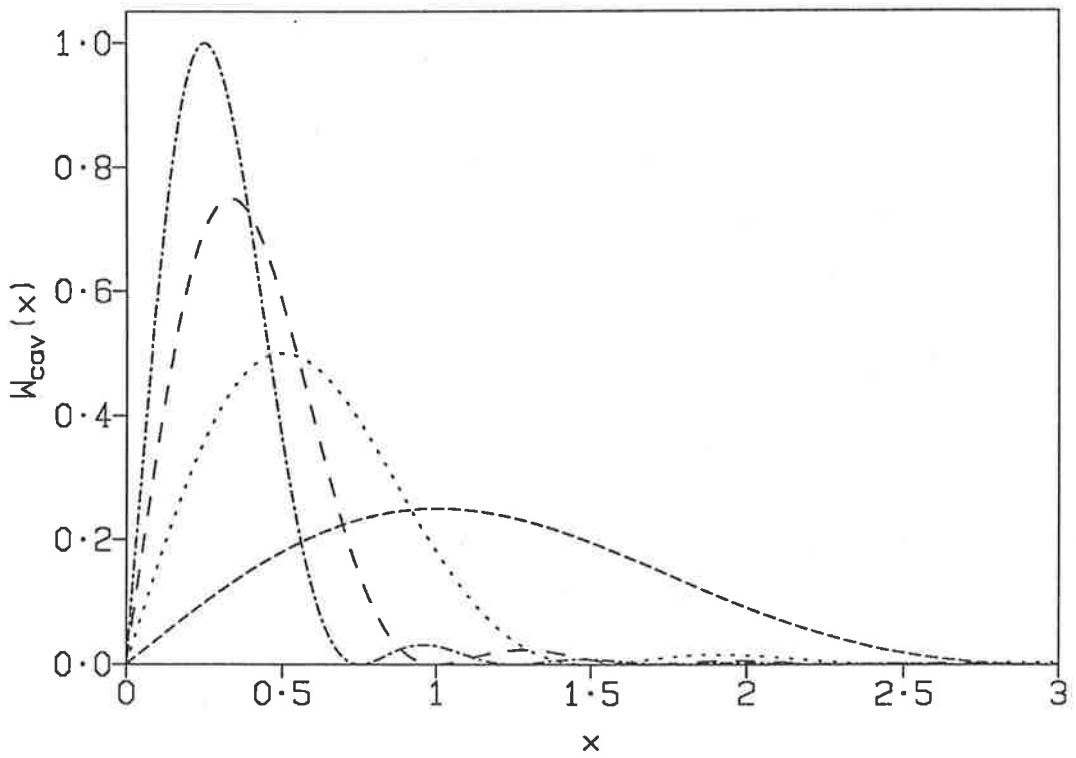

Fig. 6.1. The structure functions W_{cav} for n quarks in the ground state of the cavity. The dashed lines are for $n = 1$, 2, 3 and the dot-dash line is for $n = 4$. We can see that as n gets larger, the structure function tends to $\delta(x - 1/n)$.

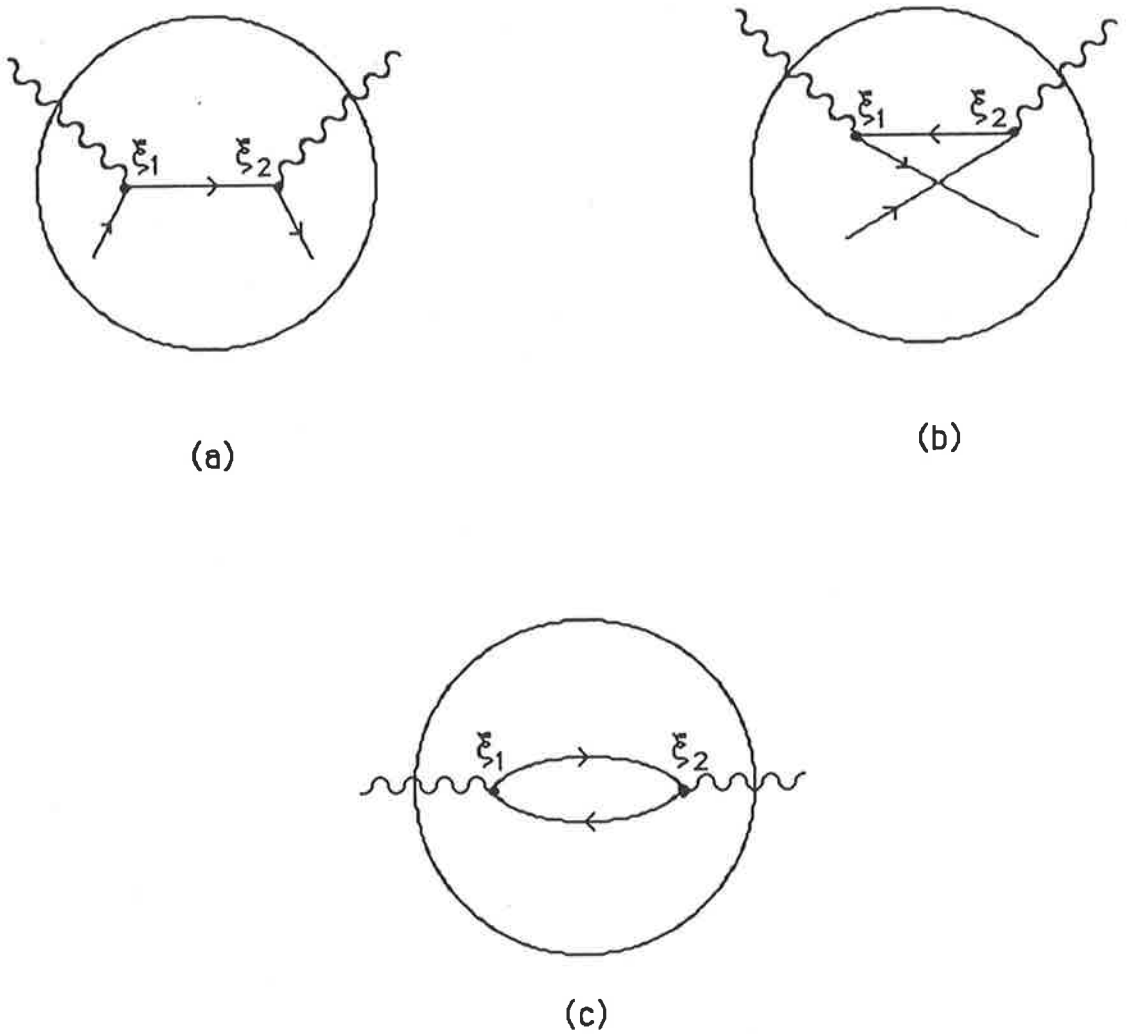

Fig 6.2 Diagrams for Compton scattering in the cavity approximation to the bag.

this graph is excluded for spacelike q^2 because of momentum conservation. However we have not guaranteed momentum conservation in the cavity so we must keep this negative term. The third graph, Fig. 6.2c, is the so-called 'bubble graph' which can only contribute to singlet operators eg. F_2 (to the extent that we ignore the exclusion principle for quarks in the cavity — see the final section of this chapter for more). Jaffe's original calculation excluded these because they are disconnected in free space, however Bell and co-workers [Bell+ 78] calculated this contribution on the basis that the interior of the cavity is different from free space as the pair must have energies equal to one of the eigenenergies of the cavity. The result for the contribution of the bubble graph is:

$$\lim_{Bj} W_{\text{bubble}}(x) = \frac{Ml}{2\pi} 2 \sum_{p=0}^{\infty}{}' \frac{\sin^2(2E_p l + Mlx)}{(2E_p l + Mlx)^2}. \tag{6.16}$$

Note that half of the first term of W_{bubble} cancels the z-graph term. The sum is finite, and is a special case of the generalized Riemann zeta function or trigamma function. In Fig. 6.3 we show the three contributions to the quark distribution function arising from Compton scattering in the cavity for three quarks in the ground state of the cavity.

Unfortunately in four dimensions the bubble graph gives a sum which is unbounded, which led Bell *et.al.* to conclude that Bjorken scaling did not apply in the cavity approximation. However again we also have a problem with momentum conservation in bubble graphs, so it may be somewhat rash to write off the cavity approximation all together, as a proper treatment of momentum conservation in the cavity may well rectify the infinite contribution of the bubble term.

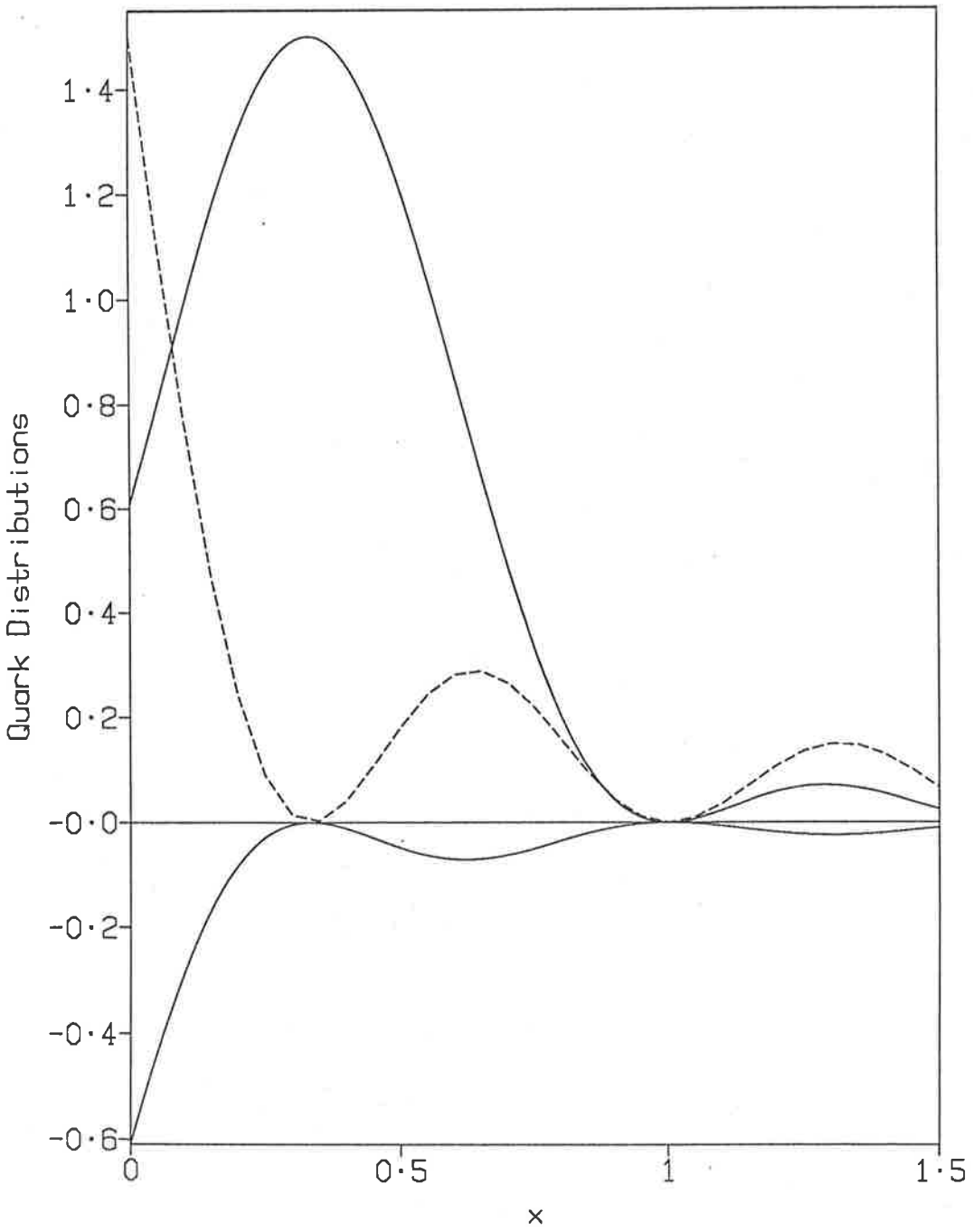

Fig. 6.3. The quark distribution functions for three quarks in the cavity approximation. The dashed curve is the 'bubble' contribution, and the curve below the x axis is the 'antiquark' distribution arising from 'z graphs'.

It is useful to check the momentum sum rule. Recalling our result from Chapter 2 we have

$$k^+_{\text{quarks}}/p^+ = \int_0^\infty dx\, 2xW_{\text{cav}}(x). \tag{6.17}$$

For three quarks in the ground state of the two dimensional cavity the contribution from eqn. (6.14) is $3 \times (0.35 - 0.02) = 1.0$, and for three colours and two flavours of light quarks, the contribution from the bubble term eqn. (6.16) is $3 \times 2 \times 0.08 = 0.48$. Thus the momentum sum rule is oversaturated when we include the bubble graphs. However even if the bubble graphs are excluded, we know that in the two dimensional cavity the valence quark fields do not carry all of p^+, some is carried by the cavity walls, which means that we have overestimated the momentum carried by the valence quarks in our calculation of the DIS matrix element. In four dimensions we have a similar problem: the momentum sum rule gives 100% of p^+ being carried by the valence quarks. We would expect our DIS calculations to put less than 100% of the momentum of the cavity on the valence quarks, and to put the remainder on 'sea' distributions, somewhat similar to the 'bubble' terms, but not oversaturating the momentum sum rule.

We can examine the anticommutator function S_{cav} more closely. As we have already seen, in the Bjorken limit only the off-diagonal terms contribute to the propagator. Thus we have

$$\lim_{Bj} S_{\text{cav}}(t, \xi_1, \xi_2) = \frac{\sqrt{2}}{8l} \sum_n{}' [\gamma^+ e^{-iE_n(t+\xi_1-\xi_2)} + \gamma^- e^{-iE_n(t-\xi_1+\xi_2)}] \tag{6.18}$$

$$= \frac{1}{2}[\gamma^+ \delta_P(\xi^+) + \gamma^- \delta_P(\xi^-)] \tag{6.19}$$

where $\xi = \xi_1 - \xi_2$ is the spacetime separation of the currents, and δ_P is the periodic (cavity) delta function

$$\delta_P(\xi) = e^{-i\pi\xi/4l} \sum_n \delta(\xi + 4nl). \tag{6.20}$$

Now for free fields the anticommutator function is [IZ 80]

$$S_{\text{free}} = \frac{1}{2\pi} \int d^2k \;\; \not{k}\varepsilon(k^0)\delta(k^2)e^{-ik.\xi} \tag{6.21}$$

$$= \frac{1}{2}[\gamma^+\delta(\xi^+) + \gamma^-\delta(\xi^-)]. \tag{6.22}$$

Using eqn. (6.19) we obtain a structure function which is the sum over discrete delta functions. 'Smearing' these delta functions gives a continuous structure function, which is the same as that which would have been obtained if we had used eqn. (6.22) directly. Thus S_{cav} and S_{free} yield the same structure function in the Bjorken limit. This means that we can apply QPM-like analysis to our calculations of matrix elements using bag states because the struck quark is essentially free, as in the QPM, and so travels along the light-cone unaffected by the bag boundaries or other quarks in the bag. In two dimensions the equivalence of S_{cav} and S_{free} in the Bjorken limit is completely general, so we can use it in our later calculations. This equivalence also holds in four dimensions, as was shown by Jaffe and Patriscioiu [JP 75] using a proof that imitated Huygen's principle for the propagation of light.

6.2 Translation Invariance

The lack of translation invariance in the cavity approximation is a very serious handicap in our calculations of DIS matrix elements using bag states. We cannot,

for instance, calculate the moments of the structure functions beyond the second or third moment, as for large n the high x contributions to the structure functions lead to infinities. We would like to be able to use translation invariant states in order to get the correct support for the structure functions. In Chapter 5 we introduced the L_0 approximation to the full quantum bag theory in two dimensions, which avoided ordering ambiguities yet retained translation invariance. We shall soon make use of the L_0 approximation and also a method commonly used in nuclear physics, the Peierls-Yoccoz (PY) approximation, to calculate DIS structure functions. Firstly we need to find an expression for the quark distribution function for translation invariant states in two dimensions.

The structure function in two dimensions will be given by

$$W = \frac{1}{4\pi} \int d^2\xi \; e^{iq\cdot\xi} \langle p|[J(\xi), J(0)]|p\rangle_c. \tag{6.23}$$

Now expanding the current commutator in terms of the quark fields, and using eqn. (6.22) for the anticommutator function in the Bjorken limit, we obtain

$$\begin{aligned} \lim_{Bj} W &= \lim_{q^-\to\infty} \frac{1}{8\pi} \int d\xi^+ d\xi^- \; e^{iq^+\xi^- + iq^-\xi^+} \langle p|\bar\psi(\xi)[\gamma^+\delta(\xi^+) + \gamma^-\delta(\xi^-)]\psi(0) \\ &\qquad -\bar\psi(0)[\gamma^+\delta(\xi^+) + \gamma^-\delta(\xi^-)]\psi(\xi)|p\rangle_c \qquad (6.24) \\ &= \lim_{q^-\to\infty} \frac{1}{8\pi} \left\{ \begin{array}{l} \int d\xi^+ \; e^{iq^-\xi^+} \langle p|\bar\psi(\xi^+)\gamma^-\psi(0) - \bar\psi(0)\gamma^-\psi(\xi^+)|p\rangle_c|_{\xi^-=0} \\ + \int d\xi^- \; e^{iq^+\xi^-} \langle p|\bar\psi(\xi^-)\gamma^+\psi(0) - \bar\psi(0)\gamma^+\psi(\xi^-)|p\rangle_c|_{\xi^+=0} \end{array} \right\}. \qquad (6.25) \end{aligned}$$

Now the integral over ξ^+ in eqn. (6.25) may be evaluated by parts, and is seen to vanish as $q^- \to \infty$. Thus we have the same expression in two dimensions as we had in four dimensions, eqn. (2.56), for the structure function, except that in two

dimensions we have dropped any reference to the transverse components $\vec{\xi}_\perp$. This is exactly what we expect from the light-cone nature of DIS and the fact that we can use the free propagator inside the bag. Thus as in four dimensions, we obtain

$$F_2(x) = x \sum_a e_a^2 (f_a(x) + f_{\bar{a}}(x)) \tag{6.26}$$

where e_a is the charge on a quark of flavour a, and

$$f_a(x) = \frac{\sqrt{2}}{4\pi} \int d\xi^- e^{-ixp^+\xi^-} \langle p|\psi^\dagger_{a+}(\xi^-)\psi_{a+}(0)|p\rangle_c \tag{6.27}$$

$$f_{\bar{a}}(x) = -\frac{\sqrt{2}}{4\pi} \int d\xi^- e^{-ixp^+\xi^-} \langle p|\psi^\dagger_{a+}(0)\psi_{a+}(\xi^-)|p\rangle_c \tag{6.28}$$

$$= -f_a(-x). \tag{6.29}$$

Translation invariance limits the support of the distribution functions to $x < 1$.

6.2.1 The L_0 Approximation

In Chapter 5 we found the full translation invariant two dimensional bag quark field operator, eqn. (5.65). In the L_0 approximation the bag becomes a cavity of fixed length, which is free to move, and the field operator becomes [Jaffe 81]

$$Q_{+,0}(0) = \frac{i}{2\pi} \int d\alpha \, e^{i\alpha\Lambda} \bar{g}(\alpha) \sqrt{\frac{\sqrt{2}p^+}{M}} \tag{6.30}$$

$$\bar{g}(\alpha) = \frac{M}{\sqrt{2}} \int_{-\sqrt{2}l}^{\sqrt{2}l} dz \, e^{-i\alpha M z/\sqrt{2}} g(z) \tag{6.31}$$

where $g(z)$ is the plus component of the cavity approximation wavefunction, $2l$ is the length of the cavity in its rest frame, and Λ is the Lorentz boost operator. Substituting eqn. (6.30) into our expression for the quark distribution function eqn. (6.27)

and dropping the flavour indices we obtain

$$f_0(x) = \frac{p^+}{2M}\int d\xi^- \int \frac{d\alpha}{2\pi}\frac{d\alpha'}{2\pi}\, e^{i(1-x)p^+\xi^-} \times \langle p|\bar{g}^\dagger(\alpha')e^{-i\alpha'\Lambda}e^{-iP.\xi}e^{i\alpha\Lambda}\bar{g}(\alpha)|p\rangle_c. \tag{6.32}$$

where the subscript 0 indicates that $f(x)$ is calculated using the L_0 approximation. Now the boost operator and the energy-momentum operator do not commute, but from the commutation relation eqn. (5.55), we can derive the identity

$$e^{-i\alpha\Lambda}Pe^{i\alpha\Lambda} = Pe^{\alpha} \tag{6.33}$$

from which it follows that

$$e^{-i\alpha\Lambda}e^{-iP.\xi}e^{i\alpha\Lambda} = \exp(-iP.\xi e^{\alpha}). \tag{6.34}$$

We now have a boost acting on our momentum eigenstate $|p\rangle$

$$e^{-i(\alpha'-\alpha)\Lambda}|p\rangle = |e^{\alpha-\alpha'}p\rangle, \tag{6.35}$$

and since the matrix element is now diagonal in momentum we may take the states to be at rest and extract a factor

$$4\pi p\delta(p - e^{\alpha-\alpha'}p) = 4\pi\delta(\alpha-\alpha'). \tag{6.36}$$

This leaves

$$f_0(x) = \frac{1}{2\sqrt{2}\pi^2}\int d\xi^- \int d\alpha\, e^{i(1-x-e^{\alpha})p^+\xi^-}\langle p'=0|\bar{g}^\dagger(\alpha)\bar{g}(\alpha)|p'=0\rangle_c. \tag{6.37}$$

Now the integral over ξ^- yields a delta function

$$\frac{2\pi}{p^+}\delta(1-x-e^{\alpha}) = \frac{2\sqrt{2}\pi}{M}\frac{1}{1-x}\delta(\alpha-\ln(1-x)) \tag{6.38}$$

which means that $f(x)$ only has support for $x < 1$,

$$f_0(x) = \frac{1}{M\pi}\frac{1}{1-x}\langle p' = 0|\bar{g}^\dagger(\alpha)\bar{g}(\alpha)|p' = 0\rangle_c|_{\alpha=\ln(1-x)}. \tag{6.39}$$

Now evaluating $\bar{g}(\alpha)$, eqn. (6.31) gives

$$\bar{g}(\alpha) = \frac{M}{\sqrt{l}}\sum_m{}' \frac{\sin(2E_M l + Ml\alpha)}{2E_m + M\alpha}, \tag{6.40}$$

and so we have

$$f_0(x) = \frac{Ml}{\pi}\frac{1}{1-x}\sum_m{}' \frac{\sin^2(2E_m l + Ml\alpha)}{(2E_m l + Ml\alpha)^2}\,|_{\alpha=\ln(1-x)}\,. \tag{6.41}$$

Comparing eqn. (6.41) with the first term of eqn. (6.14) we have the result [Jaffe 81]

$$f_0(x) = \frac{1}{1-x} f_{\rm cav}(-\ln(1-x)) \tag{6.42}$$

where $f_{\rm cav}$ is the quark distribution function calculated in the cavity approximation. The factor $(1-x)^{-1}$ can be thought of as a Jacobian factor for the transformation, eqn. (6.42), which ensures that the integral of $f_0(x)$ over all x is unity.

Now $f_0(x)$ is positive for $x < 0$. This implies that we still have z graphs persisting in the L_0 approximation which lead to negative antiquark distributions. In Fig. 6.4 we show the positive quark and negative quark distributions calculated using eqn. (6.42). We see that the L_0 approximation has not overcome the problems associated with z graphs or bubble graphs.

If we take the $x \to 1$ limit we have

$$\lim_{x\to 1} f_0(x) = \lim_{\alpha\to\infty} e^\alpha \sum_m{}' \frac{\sin^2(2E_m l - Ml\alpha)}{(2E_m l - Ml\alpha)^2} \to \infty. \tag{6.43}$$

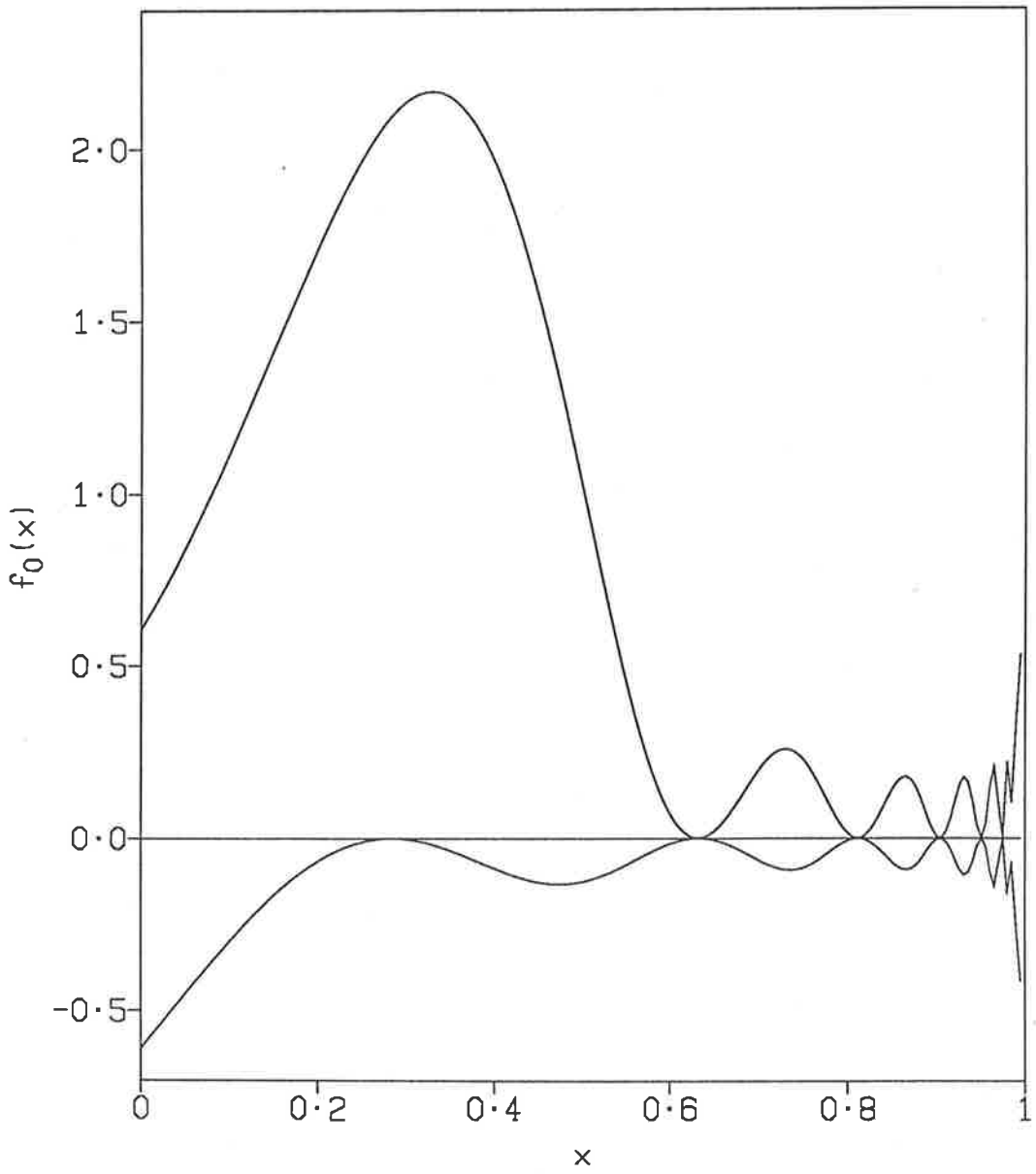

Fig. 6.4. The quark and antiquark distribution functions in the L_0 approximation for a two dimensional bag with three quarks in the ground state.

In fact the structure function oscillates wildly as $x \rightarrow 1$. This behavior would probably not be detectable experimentally because of experimental acceptances, but it is worrying to have this strange behavior in the theoretical structure function where it is certainly not expected.

We can again check the momentum sum rule. We find that for three quarks in the ground state the sum rule is nearly saturated, that is the quark fields are carrying close to 100% of the plus component of momentum of the bag state.

Unfortunately the L_0 approximation is not directly generalizable to four dimensions because there are no solutions to the four dimensional bag which respect translation invariance, and hence nothing like the L_0 approximation is available to us. However Jaffe [Jaffe 81] and Jaffe and Ross [JR 80] hypothesized that the transformation eqn. (6.42) holds in four dimensions, and they then used the quark distribution functions in four dimensions to calculate the moments of F_2 and F_3 in the bag. Using QCD moment analysis (see Chapter 2) and the experimental values of the moments at large Q^2, they extrapolated the twist two results until they agreed with their calculated moments, which happened around $Q^2 \simeq 0.7\text{GeV}^2$. We note that this calculation is of some importance to the CRRJ model of dynamical rescaling which we reviewed in Chapter 3.

6.2.2 The Peierls-Yoccoz Method

In order to remove the effects of centre of mass motion from the dynamics of a collective body of particles eg. a nucleus of nucleons or a bag of quarks, Peierls and Yoccoz (PY) proposed a superposition of the particle wavefunctions [PY 57].

That is, the lack of translation invariance in the particle wavefunctions leads to a degeneracy since $\psi(\vec{x}-\vec{r})$ has the same energy eigenvalue as $\psi(\vec{x})$. So we can remove the degeneracy by forming a new wavefunction which is some linear combination of the old wavefunctions

$$\psi'(\vec{x}) = \int d^3\vec{r}\,\chi(\vec{r})\psi(\vec{x}-\vec{r}). \tag{6.44}$$

The state ψ' is now a momentum eigenstate. The function $\chi(\vec{r})$ can be determined by variational principles to be proportional to $\exp(+i\vec{k}.\vec{r})$ where $\vec{k}$ is the momentum of the state. The constant of proportionality, ϕ^{-1}, which may be dependent on $\vec{k}$, is found from the normalization of the states

$$\begin{aligned}\bar{\psi}'(\vec{k}_1)\psi'(\vec{k}_2) &= (2\pi)^3 2k_1^0\delta^{(3)}(\vec{k}_1-\vec{k}_2) \\ &= \int d^3\vec{r}_1 d^3\vec{r}_2\, e^{-i(\vec{k}_1.\vec{r}_1-\vec{k}_2.\vec{r}_2)}[\phi^\dagger(\vec{k}_1)\phi(\vec{k}_2)]^{-1}\bar{\psi}(\vec{r}_1)\psi(\vec{r}_2). \end{aligned}\tag{6.45}$$

In our case we want to form a momentum eigenstate $|p\rangle$ from our solutions to the two dimensional cavity approximation [Wong 81]

$$|p\rangle = \frac{1}{\phi_n(p)}\int dr\; e^{ipr}|B_n(r)\rangle \tag{6.46}$$

where $|B_n(r)\rangle$ is our cavity state with the quantum numbers labelled by n. Using the normalization $\langle p|p'\rangle = 4\pi p^0\delta(p-p')$ we find

$$|\phi_n(p)|^2 = \frac{1}{2p^0}\int dr\; e^{ipr}\langle B_n(-r/2)|B_n(r/2)\rangle. \tag{6.47}$$

The matrix element in eqn. (6.47) is called the Hill-Wheeler overlap function [HW 53], denoted $I_n(r)$, and the normalization $\phi(p)$ is proportional to the square root of its Fourier transform.

We note that our momentum eigenstates $|p\rangle$ are not in fact exact eigenstates of energy. PY showed that for an harmonic oscillator potential the projected wave-function $\psi'(x)$ gives the correct centre of mass kinetic energy $\vec{k}^2/2M$, but in general the kinetic energy differs from this by a factor close to unity. Also the PY approximation is only good for small $\vec{k}$, if the velocity of the centre of mass approaches that of the internal particles, then the approximation, which is based on a stationary potential, is expected to fail.

For DIS from bag states we shall form an eigenstate at rest using the PY method. The mass of the eigenstate will be slightly lower than the mass of the cavity state. To see this we evaluate

$$\begin{aligned} M(l) &= \frac{\langle p'=0|H_{\rm cav}|p'=0\rangle}{\langle p'=0|p'=0\rangle} \\ &= \sum_{\{m\}}{}' E_m + B\frac{\langle p'=0|v|p'=0\rangle}{\langle p'=0|p'=0\rangle} \end{aligned} \tag{6.48}$$

where the energy eigenvalues E_m are the same as those of the cavity approximation (because kinetic energy is translation invariant): $E_m = \pi m/2l$, and v is the cavity's 'volume' operator. The matrix element in eqn. (6.48) just gives $2l$ in the cavity approximation where the two states must overlap completely, but with the PY projection the states do not overlap completely, which lowers the value of the matrix element to $0.87 \times 2l$. Taking $\partial M/\partial l = 0$ fixes the mass

$$Ml = 2\sum_{\{m\}}{}' E_m l \tag{6.49}$$

as before, but because the bag constant B in eqn. (6.48) is also the same, the length l must increase which means M decreases by about 6%.

We may now insert our states $|p'=0\rangle$ projected from cavity states with three quarks in the ground state into the expression for the quark distribution function in two dimensions eqn. (6.27) to obtain

$$f(x) = \frac{\sqrt{2}}{4\pi}\frac{1}{|\phi_3(0)|^2}\int d\xi^- \, e^{-ixp^+\xi^-}\int dr_1 dr_2 \times\langle B_3(r_1)|\psi_+^\dagger(\xi^-)\psi_+(0)|B_3(r_2)\rangle_c|_{\xi^+=0} \tag{6.50}$$

where $\phi_3(0)$ is the normalization appropriate to the three quark state at rest:

$$|\phi_3(0)|^2 = \frac{1}{2M}\int_{-2l}^{2l} dr \left(1-\frac{|r|}{2l}\right)^3 \cos^3 E_0 r. \tag{6.51}$$

The operator ψ removes a quark from the ground state, and changing coordinates to $R=(r_1+r_2)/2,\ r=(r_1-r_2)$ gives

$$f(x) = \frac{\sqrt{2}}{4\pi}\frac{1}{|\phi_3(0)|^2}\int d\xi^- \int dR dr \, e^{-ixp^+\xi^-} \times u_{0+}^\dagger(-\xi^- - R - \frac{r}{2})e^{iE_0\xi^0}u_{0+}(-R+\frac{r}{2})\langle B_2(\frac{r}{2})|B_2(\frac{-r}{2})\rangle|_{\xi^+=0} \tag{6.52}$$

where the matrix element has no dependence on R and $u_0(r)$ is the ground state eigenfunction in the cavity at time zero:

$$u_{0+}(r) = \frac{1}{2\sqrt{l}}e^{iE_0 r}, \quad E_0 = \frac{\pi}{4l}. \tag{6.53}$$

Now the matrix element in eqn. (6.52) is $I_2(-r)$, so it is convenient to work with its Fourier transform $|\phi_2(p)|^2$, and with the Fourier transforms of the eigenfunctions

$$\tilde{u}_{0+}(k) = \int dr \, e^{ikr}u_{0+}(r) = \sqrt{l}\,\frac{\sin(k+E_0)l}{(k+E_0)l}. \tag{6.54}$$

Then eqn. (6.52) becomes

$$f(x) = \frac{\sqrt{2}}{4\pi}\frac{1}{(2\pi)^3}\frac{1}{|\phi_3(0)|^2}\int d\xi^- \int dR dr \int dk_1 dk_2 dk_3\, e^{-ixp^+\xi^0} e^{iE_0\xi^0} \times e^{-ik_1(\xi^1+R+r/2)} e^{ik_2(R-r/2)} e^{-ik_3 r} \times \tilde{u}^\dagger_{0+}(k_1)\tilde{u}_{0+}(k_2)(2k_3^0|\phi_2(k_3)|^2). \quad (6.55)$$

Now the integrals over the space coordinates R and r yield delta functions relating k_1, k_2 and k_3. Thus we have

$$f(x) = \frac{\sqrt{2}}{4\pi}\frac{1}{|\phi_3(0)|^2}\int \frac{dk}{2\pi}\int d\xi^-\, e^{-ixp^+\xi^-} e^{i(E_0-k)\xi^0} \times \tilde{u}^\dagger_{0+}(-k)\tilde{u}_{0+}(-k)(2k^0|\phi_2(k)|^2) \quad (6.56)$$

$$= \frac{Ml}{\pi}\frac{\sin^2(2E_0 l - Mlx)}{(2E_0 l - Mlx)^2}\frac{2k^0|\phi_2(E_0 - Mx)|^2}{2M|\phi_3(0)|^2}. \quad (6.57)$$

Thus we obtain the same quark distribution as in the unprojected case, modified by the Fourier transforms of the Hill-Wheeler overlap functions for two and three quark states. Unfortunately the kinematic region $x > 1$ is still allowable in this calculation because we do not ensure that the intermediate state is on the mass-shell after the struck quark has been removed, and because our states are not eigenstates of p^+. However the contributions in the region $x > 1$ are greatly damped (see Fig. 6.5). We find [ST 88b] that over 99.5% of $f(x)$ is in the region $0 < x < 1$, so this is a good improvement on the unprojected cavity approximation calculation of Section 6.1. We note that this method has been used by Bickerstaff and Thomas [BT 87b] in four dimensions using Gaussian wavefunctions, and independently by Benesh and Miller [BM 87] in two and four dimensions using cavity wavefunctions.

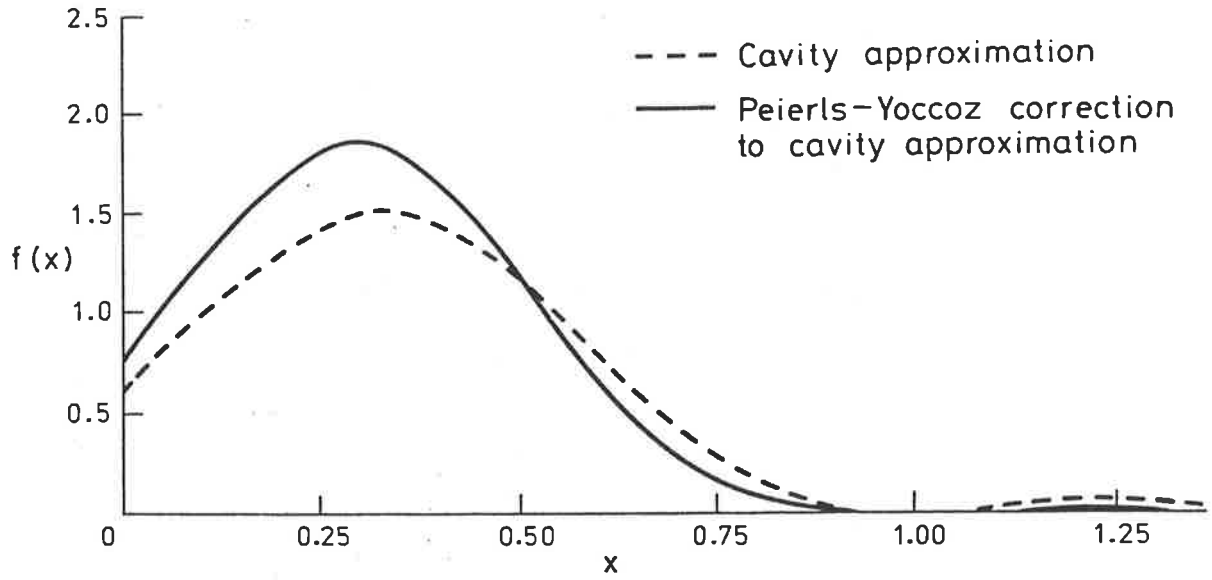

Fig 6.5 The quark distribution function f(x) of a bag containing three valence quarks for the cavity approximation and the cavity with the Peierls-Yoccoz correction.

To improve this calculation, we could use the Peierls-Thouless projection [PT 62], which would project our momentum eigenstates on to an energy eigenstate, and so ensure that we stay in the kinematically allowed region. Unfortunately it is very difficult to determine the function $\chi(\vec{k},\vec{r})$ which would multiply our wavefunctions under the integral.

Checking the sum rules on our two dimensional calculation we find

$$\int_0^\infty dx\, f(x) = 0.92 \tag{6.58}$$

$$3\int_0^\infty dx\, x f(x) = 0.92, \tag{6.59}$$

which again indicates that the valence quarks are carrying all of the p^+ of the target. We also note that the negative z graph term still persists in this calculation, being given, as in the unprojected case, by changing the minus signs in eqn. (6.57) to plus, and with an overall minus sign.

6.3 Momentum Conservation

We noted in the previous section that unphysical contributions to the structure functions can arise if the spectator quarks do not form an on mass-shell state. This is true both in the cavity approximation and in the PY projected version of the cavity. We would like to see if imposing momentum conservation constraints on the intermediate state can improve the support and other properties of the structure functions.

The quark distribution function in two dimensions is given by eqn. (6.27). As in the QPM in Chapter 2 we may insert a complete set of states $\sum_n |n\rangle\langle n| = 1$ between

the quark field operators. Then assuming translation invariance of the operators we can translate the ξ^- dependence out of $\psi_+^\dagger$, and integrate over ξ^- to obtain

$$f_a(x) = \frac{1}{\sqrt{2}} \sum_n \delta(p^+ - xp^+ - p_n^+) |\langle n|\psi_{a+}(0)|p\rangle|^2, \tag{6.60}$$

where p_n is the momentum of the intermediate state $|n\rangle$, which is the same as we obtained in the QPM, eqn. (2.61). The delta function fixes $p_n^+ = (1-x)p^+$, and if the state $|n\rangle$ is on-shell then $p_n^+ > 0$, which implies that $x < 1$.

Taking the double Fourier transform of the cavity quark field in light-cone coordinates, we obtain the momentum space representation

$$\begin{aligned} \varphi(k^-, k^+) &= 2\pi\sqrt{\frac{l}{2}} \sum_m{}' b_m(k) \delta(k^- + k^+ - \sqrt{2}E_m) \\ &\qquad \times \begin{pmatrix} j_0(\sqrt{2}k^+ l - 2E_m l) \\ j_0(\sqrt{2}k^+ l) \end{pmatrix} \qquad (6.61) \\ &= 2\pi \sum_m{}' b_m \delta(k^- + k^+ - \sqrt{2}E_m) \varphi(k^+) \qquad (6.62) \end{aligned}$$

where j_0 is the circular Bessel function $j_0(x) = \sin(x)/x$.

Now to a first approximation we treat the intermediate state as two quarks both on the mass-shell ie. with $k^+ > 0$. This ignores the binding of the quarks in the intermediate state as bound quarks can have $k^+ < 0$ in a state with $p_n^+ > 0$. Thus this is a 'quasi-free' approximation. The matrix element in eqn. (6.60) can then be written

$$\begin{aligned} |\langle n|\psi_{a+}|p\rangle|^2 &= \int dk_1^+ dk_2^+ dk_3^+ \, |\varphi(k_1^+)|^2 |\varphi(k_2^+)|^2 |\varphi(k_3^+)|^2 \\ &\qquad \times \delta(k_3^+ - xp^+) \delta(p^+ - k_1^+ - k_2^+ - k_3^+) \qquad (6.63) \end{aligned}$$

where the delta functions remind us that the struck quark carries momentum fraction x, and that we have put all of the momentum of the target onto the valence quarks.

Before we can insert the matrix element in to eqn. (6.60) we need to multiply by p^+ to account for the fact that the normalization of the states φ is 2π not $4\pi M$. The quark distribution function thus becomes

$$f_a(x) = \frac{p^+}{\sqrt{2}}|\varphi_{a,0+}(xp^+)|^2 \int_0^{(1-x)p^+} dk_1^+ \int_0^{(1-x)p^+-k_1^+} dk_2^+ |\varphi(k_1^+)|^2|\varphi(k_2^+)|^2 \times\delta((1-x)p^+ - k_1^+ - k_2^+) \quad (6.64)$$

$$= \frac{Ml}{\pi}\frac{\sin^2(2E_0l - Mlx)}{(2E_0l - Mlx)^2} \times \int_0^{(1-x)p^+} dk^+ |\varphi(k^+)|^2|\varphi((1-x)p^+ - k^+)|^2. \quad (6.65)$$

We recognize the cavity quark distribution function which, as in the case of the PY projection, is multiplied by a damping function, the integral over the momenta of the spectators. This integral cuts off the distribution function at $x = 1$ and so enforces momentum conservation.

We see in Fig. 6.6 that this structure function is similar in shape to that of the L_0 approximation, and also the PY projected cavity approximation. We again note that the momentum sum rule is saturated [ST 88b] as in our previous calculations. However this time we expected this to be the case as we ignored binding and put all of the plus component of momentum of the target on to the valence quarks. This now suggests that in our previous calculations we have unconsciously done the same: ignored the rôle of binding in the target and intermediate states. It is possible that this has come about through an attitude to the QPM which is too slavish, however given the success of the QPM and the encouraging fact that our bag model calculations all show scaling behavior indicative of asymptotic freedom, we will perservere within the current framework. However we need to examine more

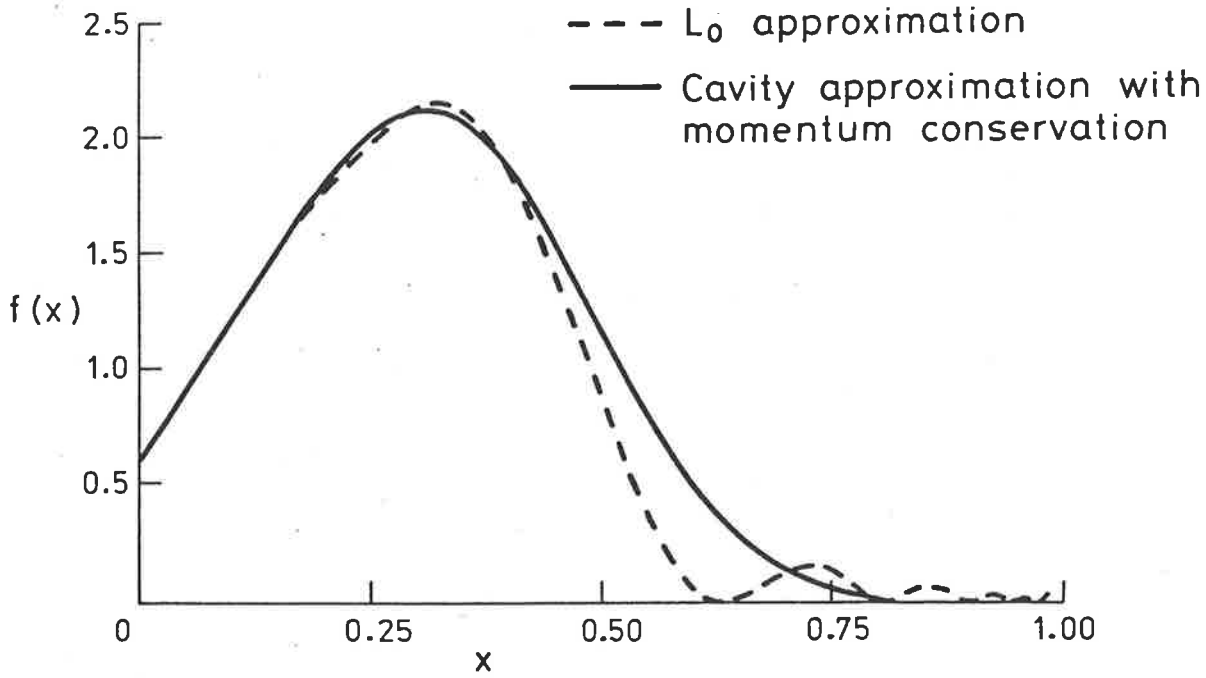

Fig 6.6 The quark distribution function f(x) of a bag containing three valence quarks for the L_0 approximation and the cavity approximation with the correction for momentum conservation.

closely our assumptions about the QPM and the bag model.

6.4 DIS From a Bound System of Quarks

We want to find a prescription to calculate, using bag model states, the quark distribution function:

$$f(x) = \frac{\sqrt{2}}{4\pi} \int d\xi^- \, e^{-ixp^+\xi^-} \langle p|\psi_+^\dagger(\xi^-)\psi_+(0)|p\rangle_c|_{\xi^+=0} \tag{6.66}$$

and other similar distribution functions. We have seen that if we use a bag field operator at this stage we break translation invariance. We need to retain translation invariance and hence guarantee momentum conservation at the quark- target vertex. Where we have translation invariance we may write

$$\psi_+^\dagger(\xi) = e^{i\hat{p}.\xi} \, \psi_+^\dagger(0) \, e^{-i\hat{p}.\xi} \tag{6.67}$$

where $\hat{p}$ is the full energy-momentum operator for the strongly interacting system.

Now, as in the QPM in Chapter 2, we may introduce a complete set of states, $\sum_n |n\rangle\langle n| = 1$ with momentum p_n and rest mass M_n, into eqn. (6.66). Because both the states $|p\rangle$ and $|n\rangle$ are eigenstates of $\hat{p}$, we have

$$f(x) = \frac{\sqrt{2}}{4\pi} \sum_n \int \frac{dp_n'}{4\pi p_n^0} \int d\xi^- \, e^{i(p^+ - xp^+ - p_n^+)\xi^-} \, |\langle n|\psi_+(0)|p\rangle_c|^2 \, |_{\xi^+=0} \tag{6.68}$$

$$= \frac{1}{\sqrt{2}} \sum_n \int \frac{dp_n'}{4\pi p_n^0} \delta(p_n^+ - (1-x)p^+) |\langle n|\psi_+(0)|p\rangle|^2. \tag{6.69}$$

At this stage we can now use bag states, provided that the state is translation invariant. Thus we use the Peierls-Yoccoz (PY) procedure to construct our initial state, at rest, from bag states containing three quarks in the ground state:

$$|p\rangle = [\phi_3(0)]^{-1} \int dr\, |B_3(r)\rangle \tag{6.70}$$

where $|B_3(r)\rangle$ is a MIT bag state centred at r containing three ground state quarks. The choice of the intermediate states $|n\rangle$ is crucial. Obviously $|n\rangle$ must be the result of acting on the initial state $|p\rangle$ with the operator ψ_+. We choose the intermediate states to be MIT bag states with the same radius as the initial state, but with a different number of quarks. That is, the result of the operator ψ_+ acting on $|p\rangle$ is to add or subtract quanta from the bag. The bag radius is taken to be constant because, on the typical time scales of DIS, the change in bag radius caused by the addition or subtraction of quanta takes a long time. Again we apply the PY procedure to construct an approximate momentum eigenstate:

$$|n\rangle = [\phi_j(p'_n)]^{-1} \int dr\, e^{ip'_n r} |B_j(r)\rangle \tag{6.71}$$

where j labels the quanta in the intermediate state.

We need now to consider the delta function in eqn. (6.69). This delta function fixes p_n^+ to be $(1-x)p^+$, but we need to convert this to a delta function which fixes p'_n the momentum of the intermediate state. We have

$$p_n^+ = \frac{1}{\sqrt{2}}(p'_n + \sqrt{M_n^2 + (p'_n)^2}) \tag{6.72}$$

where M_n is the rest mass of the intermediate state. Manipulating the delta function we obtain

$$\delta(p_n^+ - (1-x)p^+) = \frac{1}{\sqrt{2}}\left[1 + \frac{M_n^2/M^2}{(1-x)^2}\right] \times \delta\left(p'_n - \frac{M^2(1-x)^2 - M_n^2}{2(1-x)M}\right). \tag{6.73}$$

It may seem surprising that as $x \to 1$, $p_n^+ \to 0$ but $p'_n \to -\infty$. However in this limit we are removing a very fast quark from the initial state, which is at rest. Thus the

intermediate state will have a large recoil in order to conserve momentum. We note that we must expect the PY projection to break down in the $x \to 1$ limit, as it is based on a static approximation, as was discussed in Section 6.2.2.

The first term in our sum over the states $|n\rangle$ will use the most obvious intermediate state, which contains two quarks in the ground state. Using our PY projections, eqns. (6.70) and (6.71), the matrix element in eqn. (6.69) becomes

$$\begin{aligned} \langle n|\psi_+(0)|p\rangle &= [\phi_2^\dagger(p'_n)\phi_3(0)]^{-1} \int dr_1 dr_2\, e^{-ip'_n r_1} \langle B_2(r_1)|\psi_+(0)|B_3(r_2)\rangle \quad (6.74) \\ &= [\phi_2^\dagger(p'_n)\phi_3(0)]^{-1} \int dR dr\, e^{-ip'_n r} u_{0+}(-r) e^{-ip'_n R} \langle B_2(R)|B_2(0)\rangle \\ &= [2p_n^0 \phi_2^\dagger(p'_n)/\phi_3(0)]\, \tilde{u}_{0+}(p'_n) \quad (6.75) \end{aligned}$$

where $\tilde{u}_0(p)$ is the Fourier transform of the ground state eigenfunction.

Thus the first term in the quark distribution function, denoted $f_1(x)$, is given by

$$f_1(x) = \frac{M}{2\pi}\left[1 + \frac{M_n^2/M^2}{(1-x)^2}\right] \frac{2p_n^0|\phi_2(p'_n)|^2}{2M|\phi_3(0)|^2} |\tilde{u}_{0+}(p'_n)|^2 \Big|_{p'_n=[M^2(1-x)^2-M_n^2]/2(1-x)M} \quad (6.76)$$

We can see by inspection that $f_1(x)$ is only defined for $x < 1$, hence we have the correct support for the structure functions. We also see that for negative x, the quark distribution function is again positive, implying a negative antiquark distribution.

It is now time to address the problem of the negative antiquark distribution functions. In Section 2.5.2 we saw that the QPM emerged when we made a choice of the kinematic region ie. range of x, and of the diagrams we wished to consider. For quark distribution functions the QPM is only applicable in the region $x > 0$, so the formalism we have thus far been using only applies for positive x. For negative x the quark distribution function is a sum of the connected diagram *plus* the partially

connected diagrams, as were shown in Fig. 2.7, and we have not yet attempted to take these partially connected graphs into account. However when x is negative it is possible to define a quark distribution function in the QPM in terms of the antiquark distribution function at *positive* x. using the results of Section 2.5.1 we have

$$f_a(-x) \equiv -f_{\bar{a}}(x) \tag{6.77}$$

$$= -\frac{\sqrt{2}}{4\pi}\int d\xi^- e^{-ixp^+\xi^-}\langle p|\psi_{a+}(\xi^-)\psi^\dagger_{a+}(0)|p\rangle_c|_{\xi^+=0} \tag{6.78}$$

$$= -\frac{1}{\sqrt{2}}\sum_n \int \frac{dp'_n}{4\pi p^0_n}\delta(p^+ - xp^+ - p^+_n)|\langle n|\psi^\dagger_{a+}(0)|p\rangle|^2, \quad x>0. \tag{6.79}$$

Thus all the structure functions in the QPM are defined in terms of distribution functions at positive x and using the QPM analysis in the bag model will not lead to negative antiquark distributions. Instead we must calculate different matrix elements to those we have thus far calculated. On inspection we see that only 'bubble-like' contributions to the antiquark distributions can occur, at least when we only include valence quarks in our model.

Now the operator ψ_+ ($\psi^\dagger_+$) involves two types of terms: those in b (d) which destroy a quark (antiquark), and those in $d^\dagger$ ($b^\dagger$) which create an antiquark (quark). Thus we also expect a term in the quark distribution function in which the intermediate state $|n\rangle$ contains three ground state quarks plus an antiquark. Since the mass of this intermediate state M'_n is greater than that of the target state, this term will peak near $x = (M - M'_n)/M$, which is less than zero. Thus in the physical region ($x > 0$) this new term will contribute mainly at small x. We note that this behavior is similar to that expected from the $q\bar{q}$ 'sea'.

We need to have this new term contributing to the *connected* matrix element in eqn. (6.66). Now the operator product $\psi_+^\dagger(\xi^-)\psi_+(0)$ involves four types of terms: $b^\dagger b$, $dd^\dagger$, $b^\dagger d^\dagger$ and db. The $b^\dagger b$ term simply corresponds to the first term in the quark distribution function where a quark is removed from the target and later inserted back. The terms in $b^\dagger d^\dagger$ and db vanish as we cannot form any physical intermediate states. The term in $dd^\dagger$ is usually assumed to vanish, as in a free field theory it can only contribute to a disconnected matrix element. However the bag model is certainly not a free theory, and it is possible for an antiquark to be inserted into the target bag, interact inside the bag, and then be removed. That is, similar to the bubble contributions and the z graphs, a pair is created and one of the pair interacts with the bag while the other travels along the light-cone where it eventually annihilates with its partner. We must consider the intermediate state carefully.

We are inserting an antiquark into the cavity, where it will be in an eigenstate. Now it can occupy any of the antiquark levels in the bag, and to find the total contribution to the quark distribution function we need to sum over all these levels ie. sum over all the possible intermediate states. However by far the largest contribution comes when the antiquark is inserted into the ground state of the cavity. The reason for this is simply that this intermediate state will have the smallest mass M'_n of any of the intermediate states, which will mean that the peak of this contribution is the closest to $x = 0$, and so is the largest contribution for *positive* x. The next contribution (from inserting the antiquark in the first excited state) gives less than 10% of the first, and if we insert the antiquark in the mth level, then its contribution

goes asymptotically like $1/m^3$, so the series is dominated by the first term.

For the new term, the matrix element in eqn. (6.69) becomes

$$\langle n|\psi_+(0)|p\rangle \propto [\phi_4(p'_n)/\phi_3(0)]\tilde{u}^\dagger_{0+}(p'_n) \tag{6.80}$$

and the new term in the quark distribution function is

$$f_2(x) = \frac{M}{2\pi}\left[1+\frac{M'^2_n/M^2}{(1-x)^2}\right]\frac{2p^0_n|\phi_4(p'_n)|^2}{2M|\phi_3(0)|^2}|\tilde{u}^\dagger_{0+}(p'_n)|^2\Big|_{p'_n=[M^2(1-x)^2-M'^2_n]/2(1-x)M} \tag{6.81}$$

We note that this term is positive.

Now the $b^\dagger b$ contributions to $f(x)$ have three components, one for each quark in the initial bag state. However the new $dd^\dagger$ contributions of eqn. (6.81)will have six components in two dimensions, two flavours and three colours, and in four dimensions the addition of spin will allow twelve components

In a similar fashion we may use eqn. (6.79) to calculate the antiquark distribution. As we mentioned earlier, our target contains no valence antiquarks, so the only contribution to the antiquark distribution comes from terms in $b^\dagger b$ in $\psi_+(\xi^-)\psi^\dagger_+(0)$. This will correspond to a quark being inserted into the target, interacting inside the bag, and then being removed. It will have the same shape and sign as $f_2(x)$, eqn. (6.81). However there are only three components instead of the six above, as three of the available levels for a ground state quark are already occupied in the intermediate state.

Thus we identify half of the six $dd^\dagger$ terms in $f_2(x)$ with valence quark contributions, and the remaining half is identified with the flavour symmetric sea. In four dimensions the sea contribution is larger because there are more energy levels

available to the sea quarks because of spin. The sea distribution is intrinsic to the bag, and it is positive. This sea arises from the fact that matrix elements which may be disconnected in a free field theory are connected in bag theory. This points to a fundamental difference between the vacuum inside the bag, which has discrete energy levels, and free space, where energy levels are continuous.

Obviously the value of the mass of the recoiling intermediate state is crucial to our determination of $f_1(x)$ and $f_2(x)$. As we mentioned earlier, we have taken for our intermediate states cavity states with one less, or one more, quark than the initial state, and the same binding energy as the initial state. We now appear to have a problem in that the intermediate state will have a net colour charge, and so should have infinite mass. However we must remember though that the 'free' struck quark travelling along the light-cone (which also has a net colour charge) and the intermediate state do not travel 'far' from one another. That is to say that if we were able to separate the struck quark and the intermediate state, there would be an infinite energy associated with an infinite string between them, but asymptotic freedom tells us that this is not the case and that the colour flux line between the struck quark and the intermediate state only has a finite (and small) energy associated with it. A possible reason for this is that on the short time scales of DIS a large flux string (with infinite energy) does not have time to grow.

Using the mass formula for the cavity, we can calculate the masses of the intermediate states M_n and M'_n in terms of the mass of the initial state M, where the initial state contains as usual three quarks in the ground state

$$M_n = \frac{5}{6}M, \quad M_n' = \frac{7}{6}M. \tag{6.82}$$

Using these masses we are able to calculate the distribution functions $f_{1,2}(x)$, see Fig. 6.7. We find

$$\int_0^1 dx\, f_1(x) = 91\% \quad \int_0^1 dx\, f_2(x) = 5.2\% \tag{6.83}$$

$$3\int_0^1 dx\, x f_1(x) = 81\% \quad \int_0^1 dx\, f_2(x) = 0.6\% \tag{6.84}$$

so now the valence quarks are clearly not carrying all of the four momentum of the target but around 80% of it. We note that decreasing M_n to $\frac{2}{3}M$ leads to the valence quarks saturating the momentum sum rule, as we saw in our earlier calculations. So the choice of intermediate mass is indeed crucial. This again highlights the importance of the binding of the quarks and the nature of the interior of the bag. The total area under $f_1(x)$ and $f_2(x)$ is about 96%. We presume that the missing 4% of the valence quark distribution is lost because the Peierls-Yoccoz projection for the intermediate states breaks down at large x.

We also note the presence of unphysical zeroes in the distribution functions $f_1(x)$ and $f_2(x)$. These zeroes occur because in the two dimensional bag there are no transverse components in the momenta of the bag or its constituent quarks. We do not expect to see these zeroes in four dimensional calculations. In practice we can avoid any bad side effects of the zeroes by averaging the distributions around the zeroes.

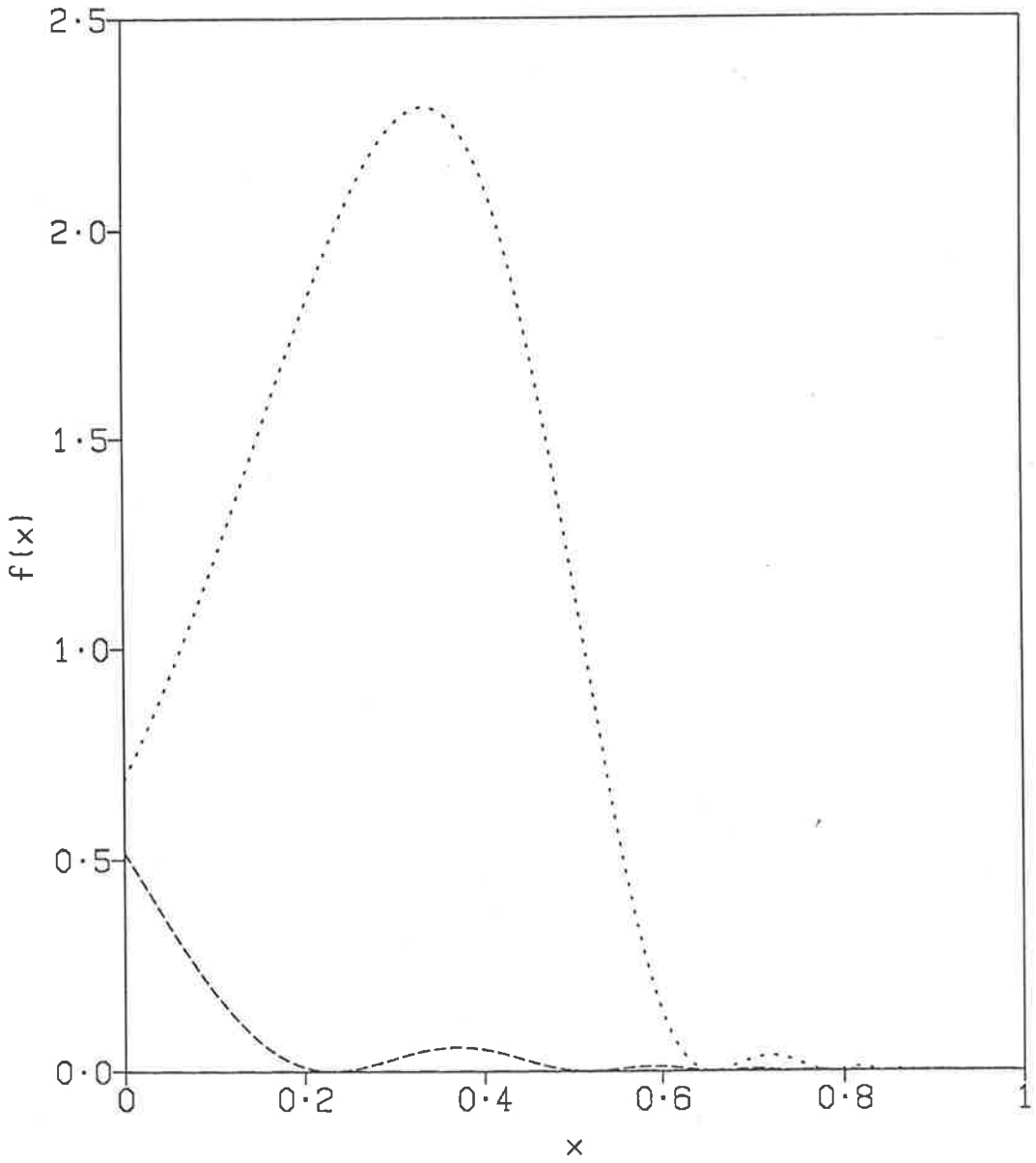

Fig. 6.7. The quark distribution functions $f_1(x)$ (dotted line) and $f_2(x)$ (dashed line) for a cavity containing three quarks in the ground state.

Chapter 7

Properties of the Quark Distribution Functions

Kên — Stillness

When all movement and resting take place at the appropriate times, one's progress is brilliant.

7.1 Structure Functions

In the final section of the previous chapter we presented a novel method of calculating quark distribution functions using the wave functions of a two dimensional bag model. We now wish to use these distributions to calculate the structure functions measured by experiments, and to compare with experimental determinations.

We have calculated two different distribution functions:

$$\begin{aligned} f_1(x) &= \text{contributions to } q(x) \text{ from } b^\dagger b \text{ terms,} \\ f_2(x) &= \text{contributions to } q(x) \text{ from } dd^\dagger \text{ terms} \\ &= \text{contributions to } \bar{q}(x) \text{ from } bb^\dagger \text{ terms.} \end{aligned}$$

We saw that in addition to the valence quark distribution $q_V(x) = f_1(x) + f_2(x)$

there is an unavoidable sea quark distribution $q_S(x) = 3f_2(x)$ (the factor of three arises from colour). Now we can calculate the experimentally observed neutrino structure functions $F_2(x) = F_2^{\nu N}(x) + F_2^{\bar{\nu} N}(x)$ and $xF_3(x) = xF_3^{\nu N}(x) + xF_3^{\bar{\nu} N}(x)$

$$\begin{aligned} F_2(x) &= \sum_a x(q_a(x) + q_{\bar{a}}(x)) \\ &= 3x(f_1(x) + 3f_2(x)) \quad \text{as there is no flavour dependence} \qquad (7.1) \\ xF_3(x) &= \sum_a x(q_a(x) - q_{\bar{a}}(x)) \\ &= 3x(f_1(x) + f_2(x)). \qquad (7.2) \end{aligned}$$

These are shown in Fig. 7.1 along with the antiquark distribution $x\bar{q}^{\bar{\nu}}$. We can compare this directly with the experimental measurements plotted in Fig. 2.11.

We note that the shapes of the structure function $xF_3(x)$ agree qualitatively, which tells us that our calculations of the valence quark distribution compare well with the experimental determinations. However our calculated $F_2(x)$ is not at all like the experimental structure function in the range $0 < x < 0.3$. The reason for this is that the sea distributions differ greatly, as is seen by comparing the curves denoted $\bar{q}^{\bar{\nu}}$ in Fig. 2.11 and $x\bar{q}^{\bar{\nu}}$ in Fig. 7.1, both of which show the momentum distribution of the sea. Experimentally we see that at low x the sea carries a significant proportion of the momentum of the nucleon, whereas our calculations put very little momentum on the sea quarks. Recalling the results of Section 2.6, as the momentum transfer of the lepton probe Q^2 increases, we observe more sea quarks. This implies that our calculations must correspond to a low value of Q^2 as we only calculate a small sea. This agrees qualitatively with the conclusions of Jaffe and Ross [JR 80], who calculated that the Q^2 appropriate for twist two matrix elements

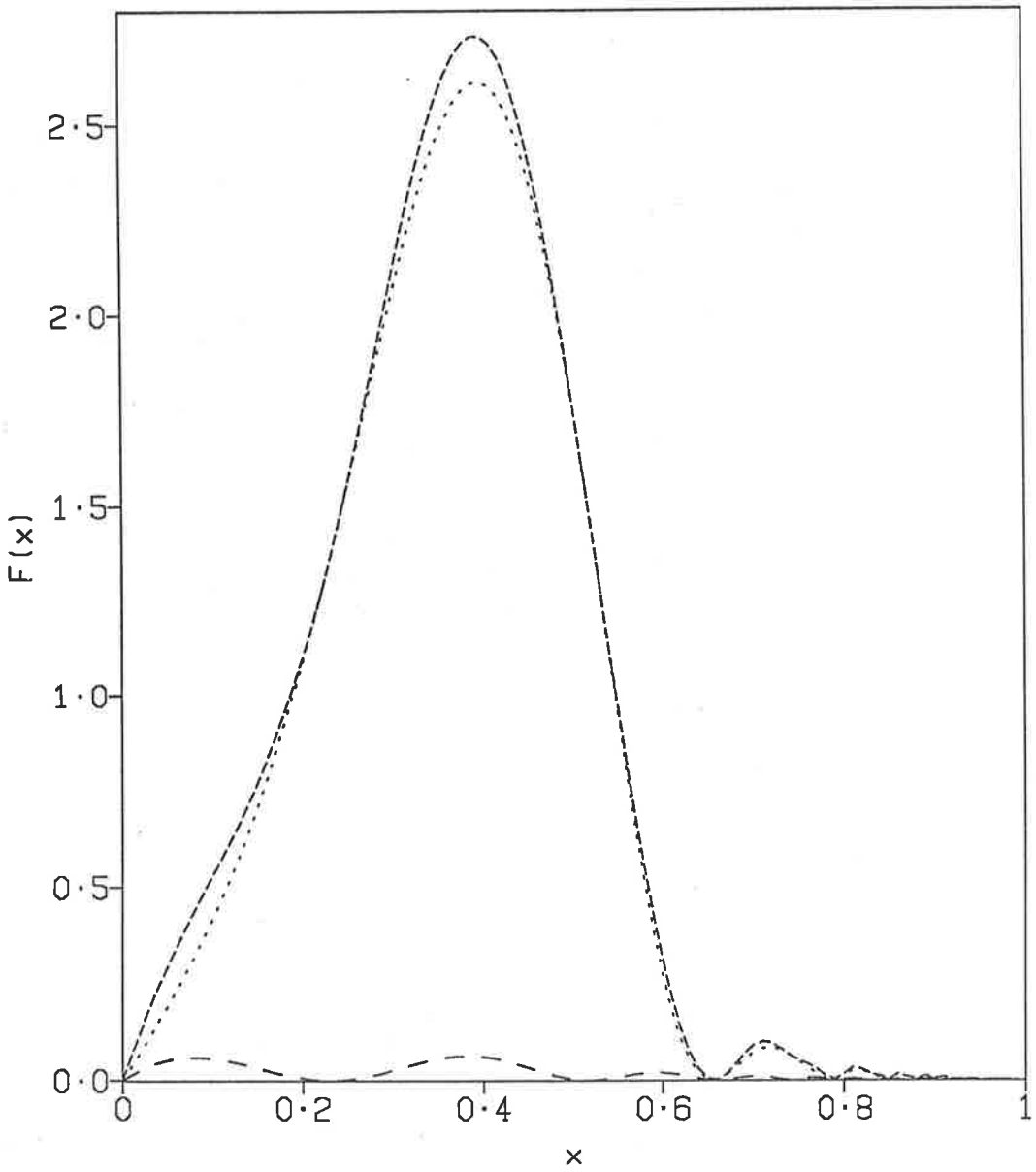

Fig. 7.1. The structure functions $F_2(x)$ (dotted line), $xF_3(x)$ (dashed line) and $x\bar{q}(x)$ (long dashed line) for a cavity containing three quarks in the ground state (cf Fig. 2.11).

in the L_0 approximation was around 0.7 GeV^2.

We also note that in the limit $x \rightarrow 0$ our calculated sea distribution gives a finite number of sea quarks, whereas the experimental sea distribution shows an infinite number of sea quarks. This behavior of the experimental sea distribution agrees with the predictions of Regge theory [LP 82,AGT 69] where an $SU(2)$ singlet 'Pomeron' is exchanged between the nucleon and the lepton probe. In our bag model calculations we have not included any Regge effects, so we do not expect to calculate an infinite number of sea quarks at low x. Finally we should remind ourselves of the argument at the beginning of Chapter Six that our calculations of DIS structure functions in the bag model are probably only applicable for x greater than ~ 0.05, so we do not expect to be able to accurately predict the low x behavior of the sea (or valence) distributions.

Having calculated the structure functions $F_2(x)$ and $xF_3(x)$, we should check that they satisfy the sum rules given in Section 2.7. For the Adler sum rule we obtain

$$\int_0^1 dx \, \frac{1}{x}[F_2^{\bar{\nu}p}(x) - F_2^{\nu p}(x)] = 0.96 \tag{7.3}$$

which is in good agreement with the QPM expected value of 1. For the Gross - Llewellyn-Smith sum rule we have

$$\int_0^1 dx \, [F_3^{\nu p}(x) + F_3^{\nu n}] = 2.89 \tag{7.4}$$

which also agrees reasonably well with the results of the QPM. In fact next-to-leading order QCD gives the value of this integral as $3(1 - g^2(Q^2)/4\pi^2)$, where g^2 is

given by eqn. (2.88), and Q^2 is the scale at which the measurements (or calculations) are taken.

We also have the results that

$$\int_0^1 dx\ F_2^N(x) = 0.85 \tag{7.5}$$

and

$$\int_0^1 dx\ xF_3^N(x) = 0.83 \tag{7.6}$$

which show that about 85% of the plus component of momentum of the bag is carried by quarks and antiquarks, and that only a small part of this is carried by the sea, 83% is on the valence quarks. Presumably the remaining 15% or so is carried by the binding field of the bag. Experimentally (in the four dimensional world) the integral over $F_2(x)$ is around 50%, indicating that the binding glue carries about half of the momentum of the nucleon. Again the difference between the experimental results and our calculation implies that our calculations are appropriate for a low value of Q^2.

7.2 One Gluon Exchange

In our calculations of the quark distribution functions and other structure functions, we have so far neglected the effect of one gluon exchange (OGE) in the bag model. As we saw in Chapter Five, one gluon exchange leads to a hyperfine splitting between the nucleon and the delta. Thus the mass of the 'proton' bag state is lowered by about 150 MeV, this lowering being shared equally between the two

quark flavours u and d (we ignore the strange component of the sea as this is small). More importantly for our calculations, the recoiling states will have different flavour content and hence different masses. As the two dimensional bag model neglects spin (which is important in the OGE, see eqn. (5.20)), our philosophy in this section is to avoid the actual mechanics of the OGE, and to treat our model as a two dimensional analogue of the four dimensional model.

We consider first the contribution of di-quark intermediate states. In the case of the u distribution the appropriate recoil state has flavour content ud, whereas for the the d distribution the recoil state will be uu. The OGE lowers the mass of the uu state relative to the ud state. This will have the effect of shifting the d distribution to lower x, and the u distribution to higher x, as was discussed in the final section of Chapter Six. In the case of four quark intermediate states, the differences between the masses of the differently flavoured recoil states will be small (from the form of eqn. (5.20)), and we shall ignore it for the time being. If we think of adding a quark or an antiquark to a colourless three quark state, the OGE will have little effect on the inserted quark or antiquark.

The effects of introducing the OGE can be seen in Fig. 7.2. The valence u distribution is moved to higher x, while the valence d distribution moves to lower x, thus proportionally more of the momentum of the proton is being carried by the u quarks.

There will also be a difference between the sea distributions $u_S(x) = \bar{u}_S(x)$ and $d_S(x) = \bar{d}_S(x)$. It is easiest to see how the difference in sea distributions in the

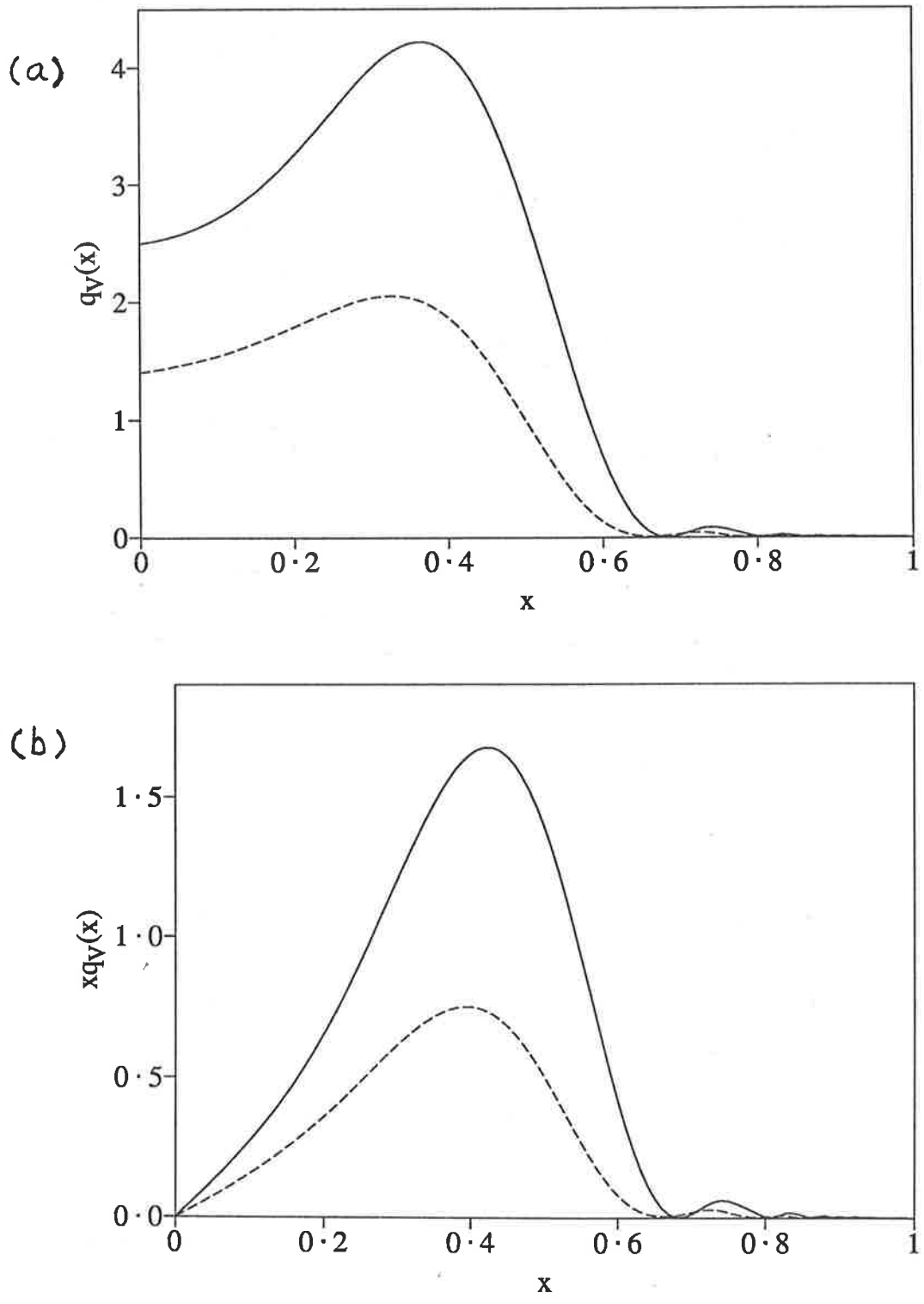

Fig. 7.2. The valence quark distributions for a 'proton'. (a) $u_V(x)$ (solid line) and $d_V(x)$ (dashed line), (b) $xu_V(x)$ (solid line) and $xd_V(x)$ (dashed line).

proton arises in the case of the antiquark distributions $\bar{u}(x)$ and $\bar{d}(x)$. In each case the appropriate intermediate state is formed by inserting a quark into the ground state of the three quark cavity. But only one u quark can be inserted into the ground state of the proton (two of the three states are occupied by the valence quarks), whereas two d quarks can be inserted into the ground state. Thus we have $\bar{d}_S(x) = 2\bar{u}_S(x)$. In the four dimensional model, where we have spin, the ratio $\bar{d}(x)/\bar{u}(x) = 5/4$, a value close to that obtained by Feynmann and Field [FF 77]. So we conclude that $SU(2)$ symmetry is broken by the sea, and quite badly in the case of our two dimensional model. In Fig. 7.3 we show our calculated sea distributions $u_S(x)$ and $d_S(x)$.

We also note that the OGE affects slightly our normalizations of the quark distributions. We obtain the integrals:

$$\int_0^1 dx\, u_V(x) = 1.86, \quad \int_0^1 dx\, x u_V(x) = 0.56 \tag{7.7}$$

$$\int_0^1 dx\, d_V(x) = 0.88, \quad \int_0^1 dx\, x d_V(x) = 0.23 \tag{7.8}$$

$$\int_0^1 dx\, u_S(x) = 0.054, \quad \int_0^1 dx\, x u_S(x) = 0.008. \tag{7.9}$$

So for the Adler and Gross - Llewellyn-Smith sum rules we obtain 0.98 and 2.74 respectively.

In Section 2.7 we saw that use of the Nachtmann relation $1/4 < F_2^{en}/F_2^{ep} < 4$ led to the conclusion that at high x, $d(x) \ll u(x)$ in the proton. However our calculations do not reproduce this. In Fig. 7.4 we have plotted the ratio $F_2^{en}(x)/F_2^{ep}(x)$. Unfortunately the oscillatory behavior of the quark distribution functions at large x makes it difficult to calculate the Nachtmann ratio in this region. We note that

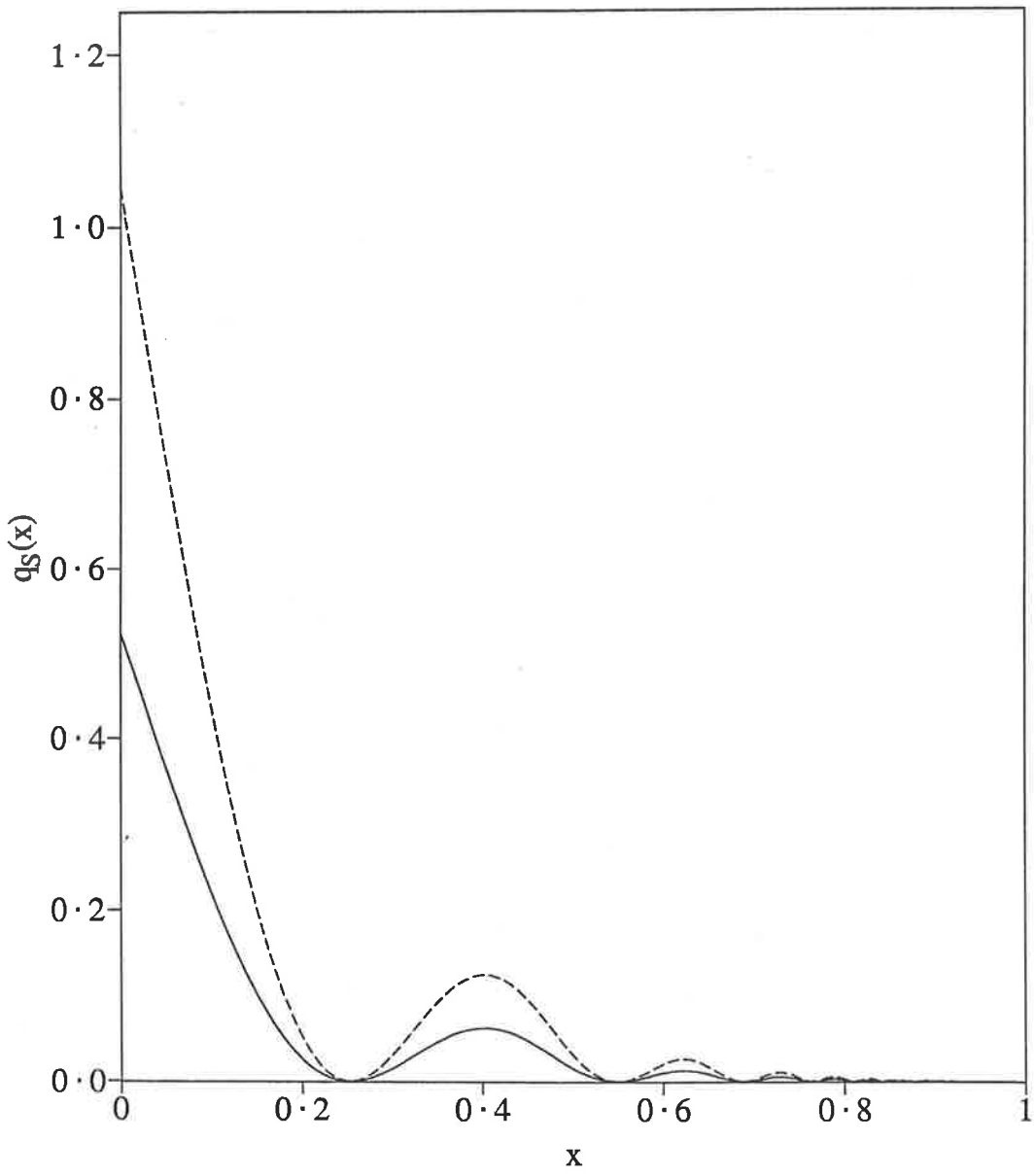

Fig. 7.3. The sea quark distributions for a 'proton', $u_S(x)$ (solid line), and $d_S(x) = 2u_S(x)$ (dashed line).

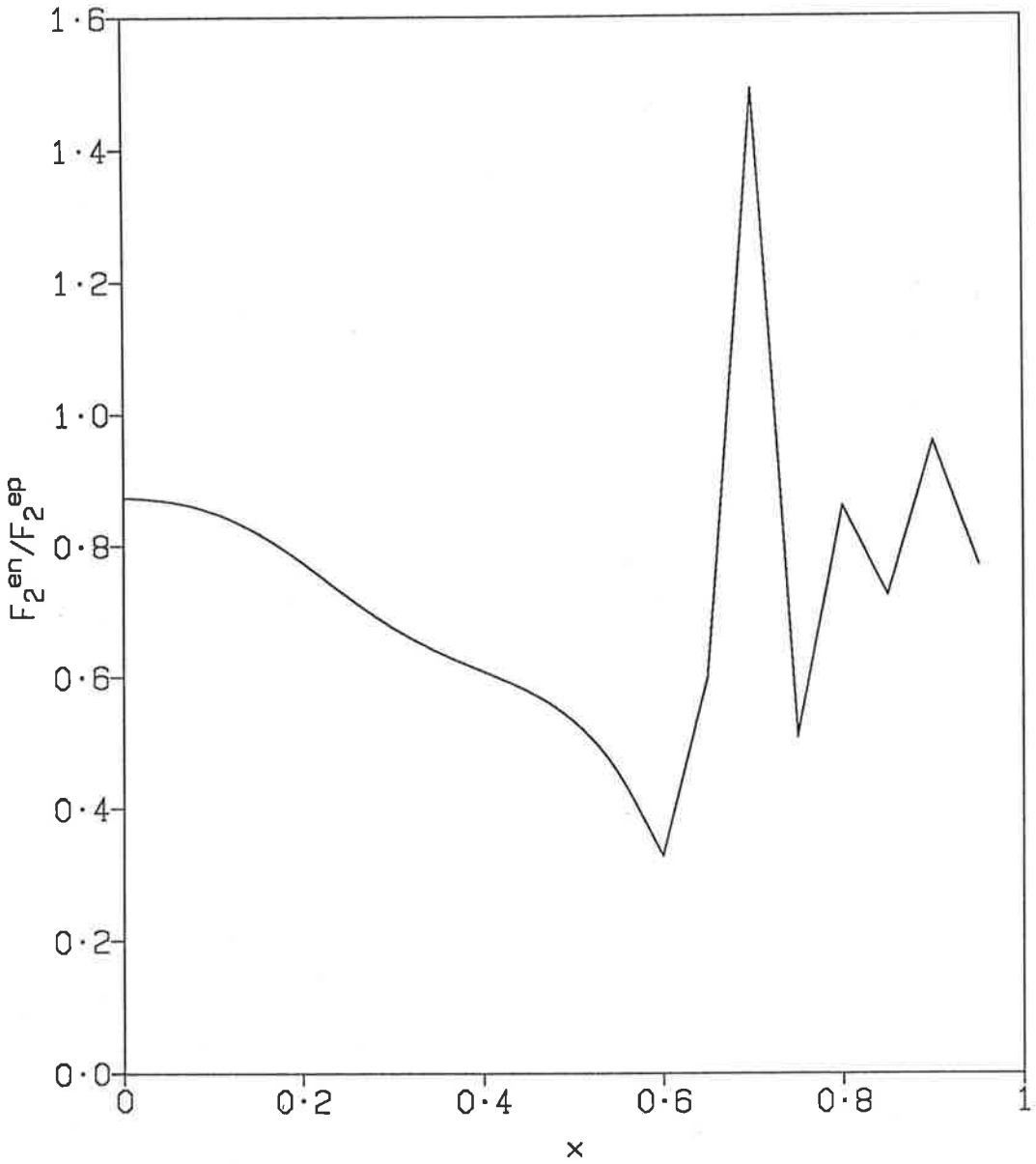

Fig. 7.4. The Nachtmann ratio $F_{1,2}^{en}(x)/F_{1,2}^{ep}(x)$. The spike near $x = 0.7$ occurs because of the zero in $u_p(x)$.

at medium x the ratio falls well below unity in agreement with experimental data [LP 82]. However in the $x \rightarrow 1$ limit the two distributions $u(x)$ and $d(x)$ that we have calculated have similar behavior, leading to a ratio close to one. This may well be due to the breakdown of our approximation for the recoil state in the high x region.

7.3 Effects of Background Fields

A nucleon in a nucleus is affected by the nuclear scalar and vector fields (σ and ω meson fields). It would seem reasonable then that a first step in modeling the EMC effect would be to take a successful nucleon model, namely the MIT bag, then introduce background scalar and vector potentials into the model, as we did in the final section of Chapter Five, and then attempt to calculate the quark distribution functions in this augmented nucleon model. This approach will consider the effects of fields on a static nucleon, and so neglect Fermi motion which is important for $x > 0.7$. An extension of this approach to modelling the EMC effect would be to do a convolution of the structure function of a nucleon in a nucleus and to add in Fermi motion in a similar manner to the 'off shell' model [DT 86,Dunne 86].

There is an immediate problem as, except at very low x where the distance travelled by the struck quark can be larger than typical nuclear diameters, the struck quark has to travel in the nucleus, and can be affected by the background fields. In particular the struck quark will not necessarily travel along the light-cone. In the case of the scalar potential V_S there will be corrections of order V_S^2/Q^2 which

arise in the same manner as quark mass corrections to DIS discussed in Chapter Two. This effect can be quite large at the low values of Q^2 appropriate to our DIS calculations using the bag model. In the case of a vector potential with time component V_0, effects of the order V_0/ε_0 may be present, where ε_0 is the ground state energy eigenvalue. However we should also keep in mind that we are trying to model QCD, which means that we should keep using the idea of asymptotic freedom. Thus, in the first instance, these calculations are made using the free quark propagator (as earlier) without any corrections introduced by the background fields. However we should keep in mind the approximation made, and in the future attempt to look at the corrections to the propagator.

In this work we take small values of V_S and V_0, typically less than one tenth of the quark eigenenergy. Using the cavity eigenfunctions eqns. (5.87–93) in the distribution calculations eqns. (6.76, 6.81) we can then obtain the quark distribution functions for a cavity in the presence of background fields. Now in nuclear physics the mean scalar and vector fields have strengths that are typically of the order of hundreds of MeV. However the potential felt by the quarks is given in terms of the quark-meson couplings as well as the mean field strengths [Gui 88]

$$V_S = g_{q\sigma}\bar{\sigma}, \quad V_0 = g_{q\omega}\bar{\omega}, \tag{7.10}$$

so V_S and V_0 will be small as long as the quark-meson coupling constants $g_{q\sigma}$ and $g_{q\omega}$ are also small.

In Figs. 7.5–7.7 we compare the valence and sea quark distribution functions of the 'free' cavity, without any background fields, with those of a cavity in some

background field(s) (weak potential). The potentials are given in units of $1/l$, where $2l$ is the length of the static cavity, so $V = \pi/50$ corresponds to a potential of $\sim$ 15 MeV. We see that at low x the difference brought about by the presence of the background field can be quite large, on the order of 10%. The scalar field enhances both the valence and sea distribution functions at low x, and also slightly (few %) at medium x (see Fig. 7.5). Around $x = 0.3$ the scalar field slightly depletes the distribution functions. The vector potential appears to have the opposite effect to the scalar potential, depleting both the distribution functions at low and medium x (see Fig. 7.6). In both cases the potentials have little effect at high x, and we would be most surprised to see any EMC-type effects there. Fig. 7.7 shows the effect on the distribution functions of having both scalar and vector potentials, giving an overall binding of the nucleon of a few MeV. The results qualitatively mimic the effect of a scalar potential on its own. We note that the magnitude of the changes in the structure functions apppears to increase with the size of the potentials (for small potentials).

In Fig. 7.8 we plot the ratio of $F_2(x)$ calculated for the cavity in the presence of background scalar and vector potentials divided by $F_2(x)$ calculated for the free cavity. The ratio is only plotted over the range $0 \leq x \leq 0.6$ as the zeroes in the distribution functions beyond $x = 0.6$ make the comparison of the structure functions meaningless. We do see some structure in this ratio up to $x = 0.6$. At low x the structure function is enhanced by the background fields — similar to the first EMC results. In the region $0.2 < x < 0.3$ the ratio dips slightly below unity, but

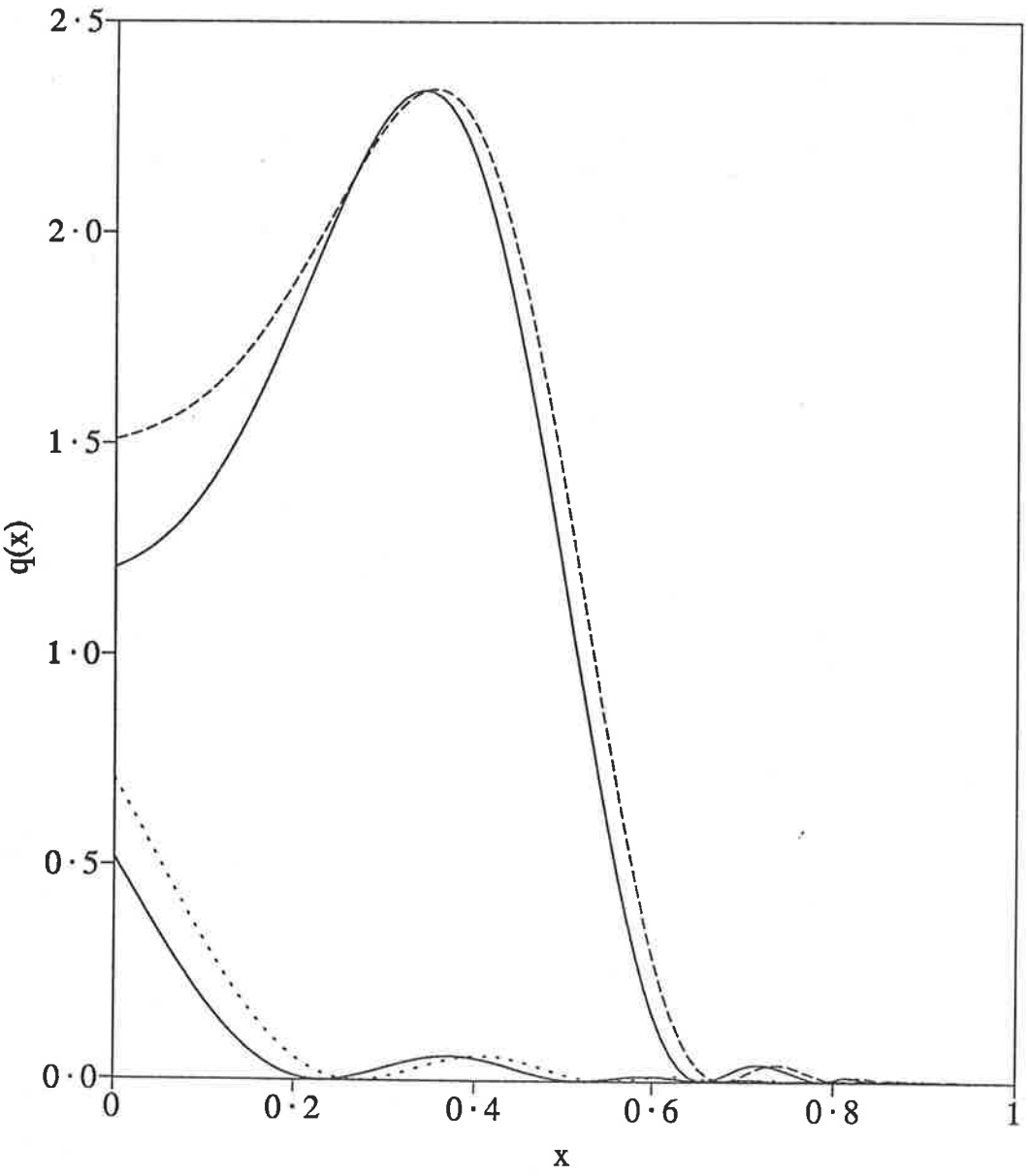

Fig. 7.5. The valence and sea quark distributions for the free cavity (solid lines) and the cavity in a scalar potential $V_S = \pi/50$ (dashed lines).

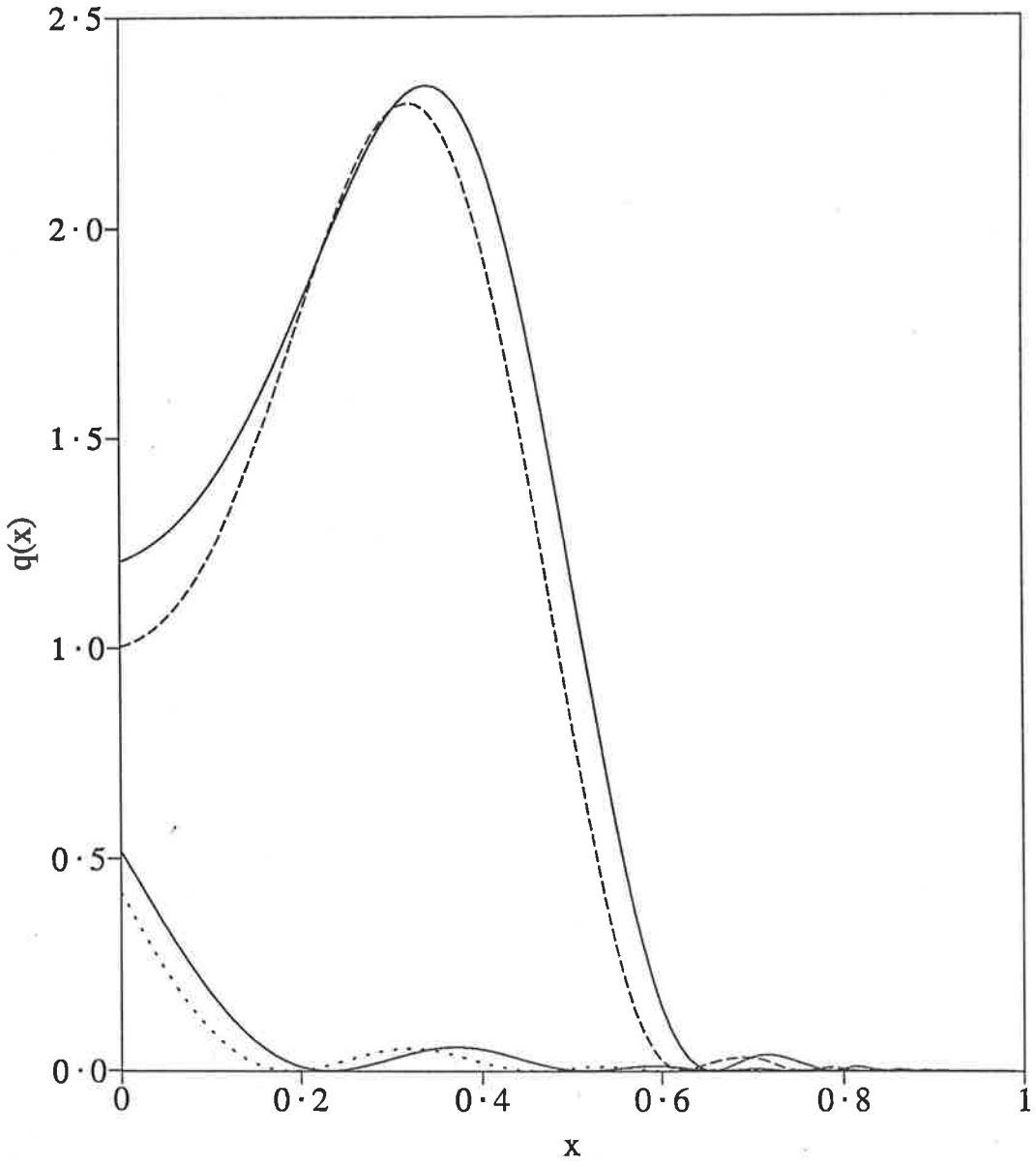

Fig. 7.6. The valence and sea quark distributions for the free cavity (solid lines) and the cavity in a vector potential $V_0 = \pi/50$ (dashed lines).

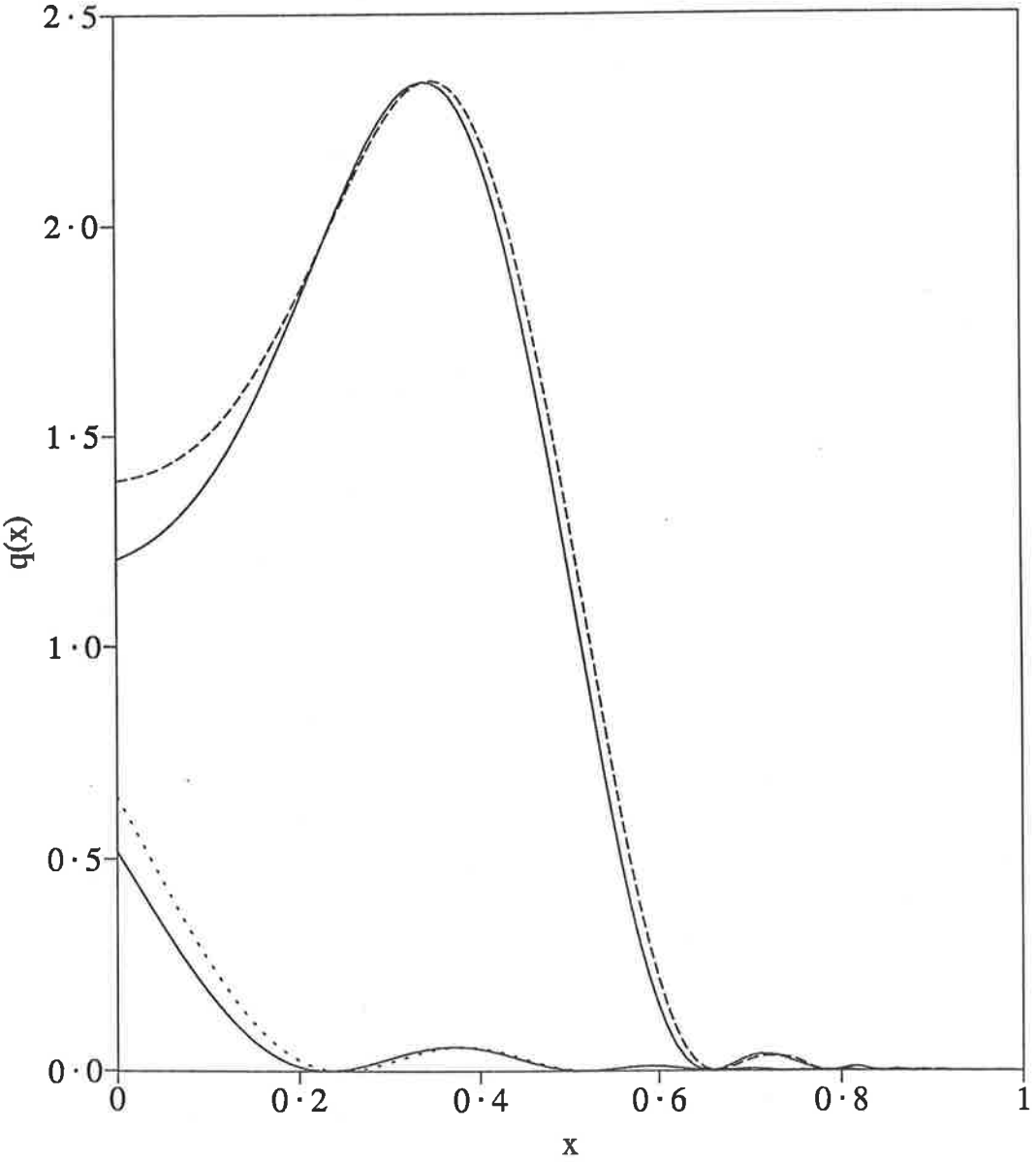

Fig. 7.7. The valence and sea quark distributions for the free cavity (solid lines) and the cavity in scalar and vector potentials $V_S = \pi/50$, $V_0 = \pi/100$ (dashed lines).

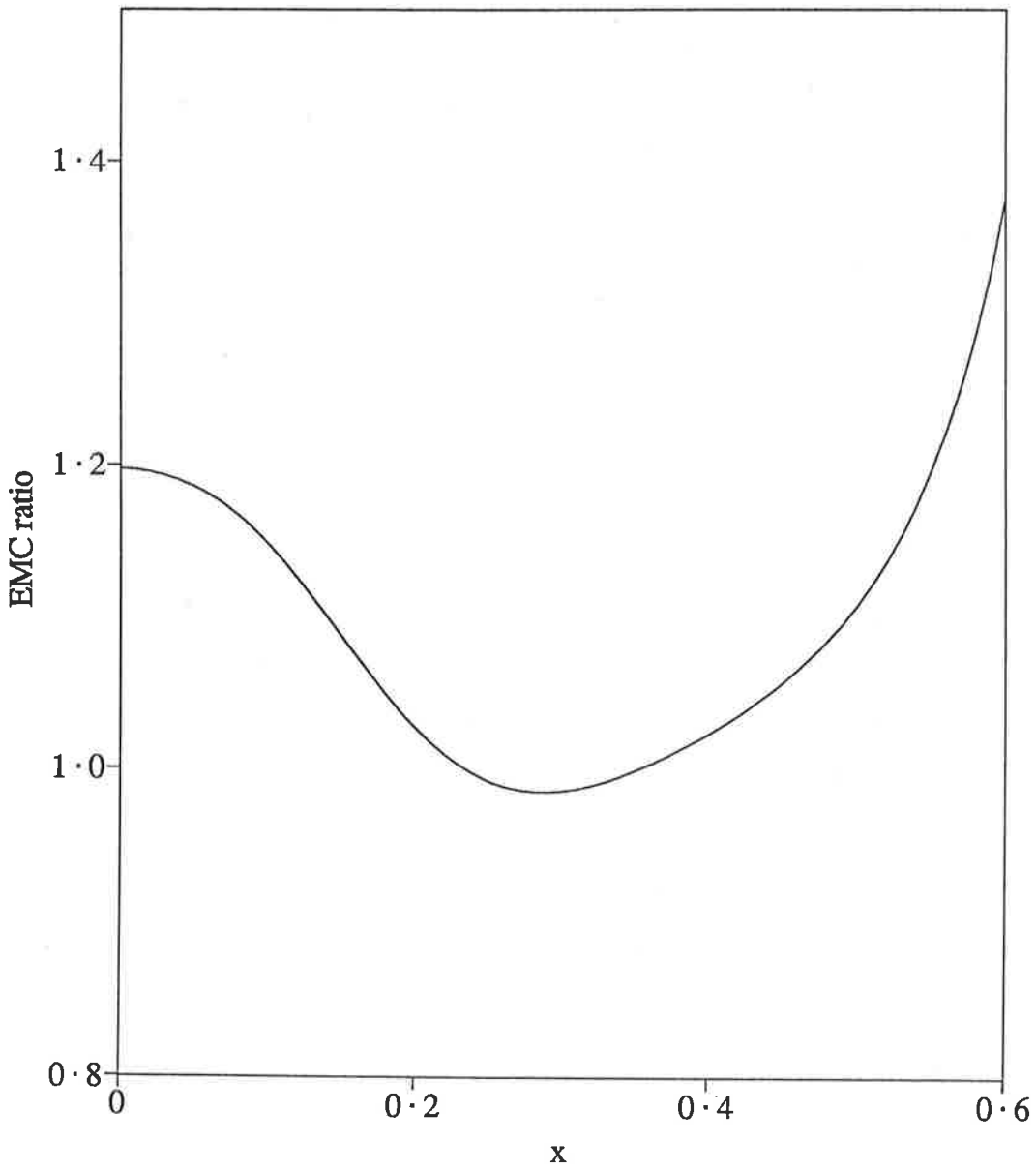

Fig. 7.8. The 'EMC' ratio $F_2^{s,v}(x)/F_2^f(x)$ where $F_2^f(x)$ is the structure function for the free cavity, and $F_2^{s,v}(x)$ is the structure function for the cavity in background scalar and vector potentials $V_S = \pi/50$, $V_0 = \pi/100$.

then it rises again, contrary to the experimental data. This is not a Fermi motion effect as there is no Fermi motion of the nucleon in this model. Even though we do not reproduce the experimental data on the EMC effect very well, it is encouraging to see that small background potentials can produce an effect on the cavity structure functions that is of the same order as the EMC effect. It is also encouraging to see some structure in our 'EMC' ratio, which gives us hope of further improvement in our results.

7.4 Lengthening the Cavity

In Chapter Three we examined the CRRJ hypothesis that an increase in the characteristic length scale of nucleons in nuclei could lead to a QCD rescaling that would explain the EMC effect. In this section we will examine the effect that stretching or lengthening the cavity has on the quark distribution function we have calculated.

We can lengthen the cavity by relaxing the non-linear boundary condition that constrains the bag constant B. The mass of the cavity state is determined by

$$Ml = 2Bl^2 + \sum_i E_i l \tag{7.11}$$

where E_i are the energies of the quarks in the cavity. Now we require that M be constant, and we know that the energy eigenvalues multiplied by l are constant, so we can see that a change in B brings about an inverse change in l, that is Bl is constant also.

In Fig. 7.9 we compare the quark distribution functions for a cavity stretched by 10% with those of the unmodified cavity. The distributions from the stretched cavity

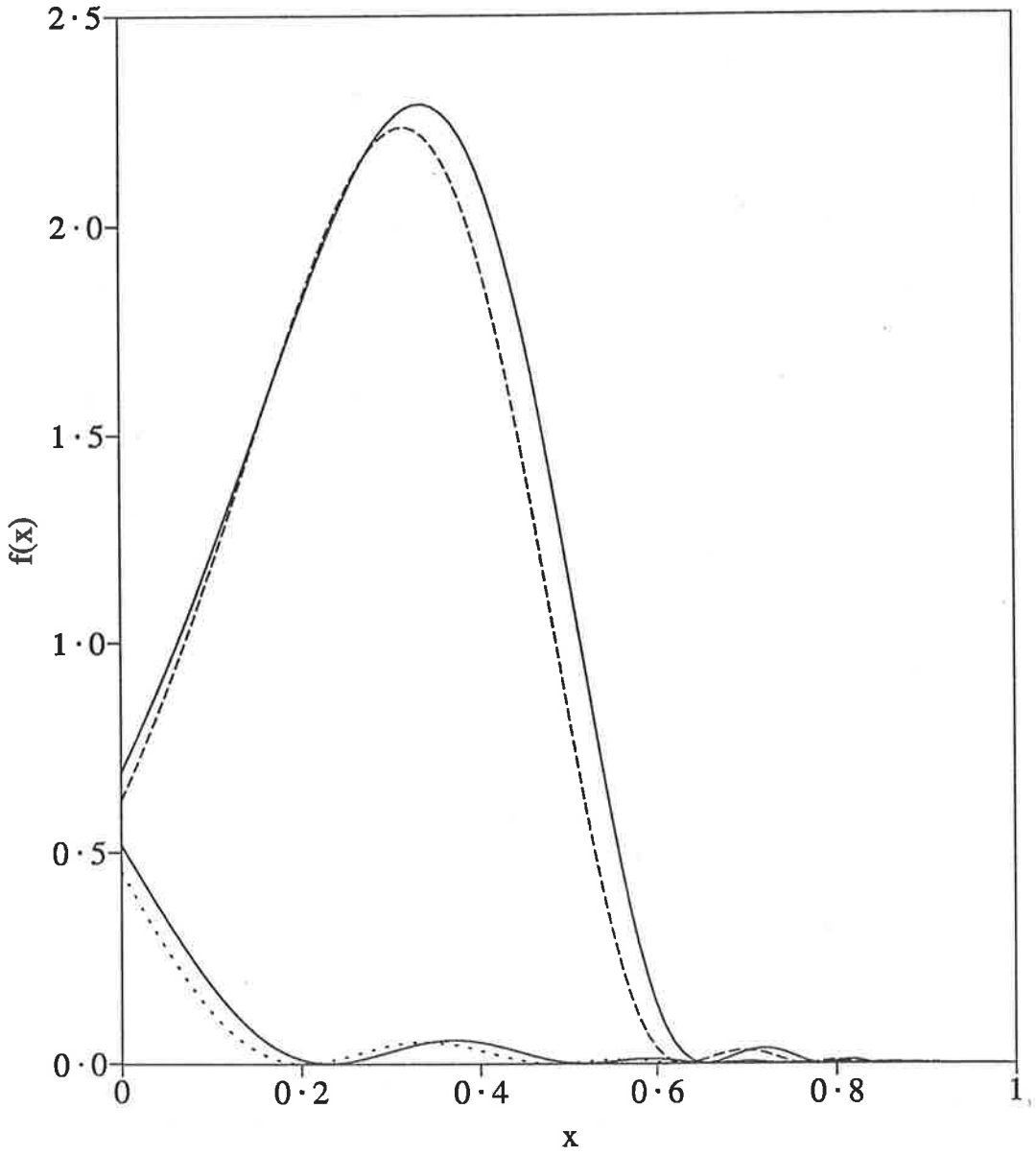

Fig. 7.9. The valence and sea quark distributions for the unstretched cavity (solid lines) and the cavity stretched by 10% (dashed lines).

are slightly sharper than those of the unmodified cavity. This is to be expected on general grounds [BT 87b]. The Heisenberg uncertainty principle tells us that in the larger cavity the spread in momentum of the quarks is less than in the usual size cavity. As x is the proportion of the plus component of the momentum of the cavity that is carried by the struck quark we should expect the distributions in x of the larger cavity to be sharper than those of the unstretched cavity.

In Fig. 7.10 we calculate the 'EMC' ratio of the structure functions in the stretched and unstretched cavities. We see that at low x the ratio is below unity, but then rises above unity for $0.2 < x < 0.3$, and then falls again, getting below one half as x nears 0.6. This behavior is qualitatively not unlike the experimental data on the EMC effect, and again the presence of some structure in our results is most encouraging.

We note the similarity between Fig. 7.9 and Fig. 7.6 which compared the usual quark distribution functions with those of a cavity in a background vector potential. We may also note that in the presence of the vector potential the bag constant B decreases while the mass M of the cavity remains constant. This implies that the length scale B^{-1} of the cavity vacuum has increased. So a background vector potential may have similar effects on the cavity as a deliberate lengthening. This means it would be very difficult to separate the effects of a change in length scale of a nucleon in a nucleus from the effects of the nuclear vector field on the nucleon. On the other hand we could argue that the nuclear vector field produces a change in the length scale of a nucleon in a nucleus, which leads to the changes in nucleon structure

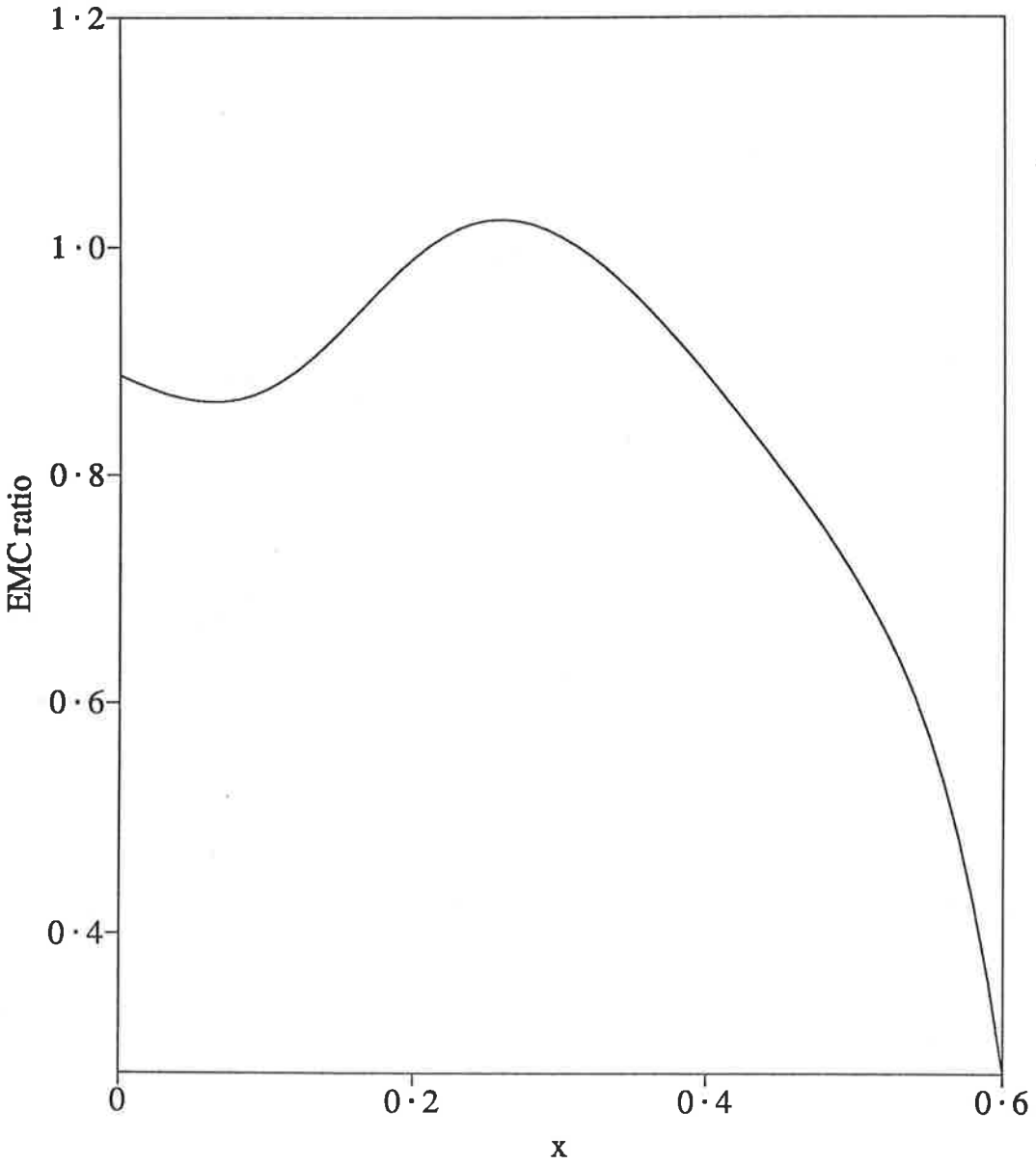

Fig. 7.10. The 'EMC' ratio $F_2^*(x)/F_2(x)$ where $F_2(x)$ is the structure function of the unstretched cavity, and $F_2^*(x)$ is the structure function for the cavity stretched by 10%.

functions that we have calculated at some low value of Q^2. Then via the QCD evolution equations we obtain the EMC effect at high values of Q^2 in accordance with rescaling. We can also note that the presence of the nuclear scalar field has the opposite effect on the cavity, that is B/M increases, leading to a shortening of the cavity, and a widening of the distribution functions as seen in Figs. 7.5 and 7.7. However it is not beyond belief that the right combination of V_0 and V_S along with rescaling could reproduce well the experimental data on the EMC effect.

7.5 Analysis of the Moments of the Distribution Functions

We have repeatedly stated throughout the last two chapters of this thesis that the quark distribution functions we have been calculating are the twist two matrix elements for deep inelastic scattering calculated at some low value of the momentum transfer Q^2. We would not expect to see these distributions experimentally, because as Q^2 becomes smaller, higher twist effects become more predominant in the experimentally measured structure functions. However we would hope that if we were to evolve our calculated distributions to some high value of Q^2 using the QCD evolution equations of Chapter Two, we would obtain distributions somewhat like those seen experimentally. The major proviso in this is that leading order QCD remains valid for low Q^2, which has not yet been established (although we are on less shaky ground in examining non-singlet rather than singlet moments [PR 81]).

The necessary first step is to determine the value of Q^2 at which our twist two calculations are valid. Following Jaffe and Ross [JR 80] we shall call this value of

n	$M_{3_{NS}}^{(n)}(\mu_0^2)$	$M_{3_{NS}}^{(n)*}(\mu_0^2)$	$M_{3_{NS}}^{(n)}(Q^2)$
1	3.0	3.0	—
2	0.86	0.85	0.38 ± 0.07
3	0.31	0.31	0.097 ± 0.004
4	0.13	0.13	0.0386 ± 0.0014
5	0.056	0.059	0.0184 ± 0.0004
6	0.026	0.028	0.0097 ± 0.0002
7	0.013	0.014	0.0055 ± 0.0002
8	0.0068	0.0078	0.0035 ± 0.0001

Table 7.1: The moments of xF_3 determined using the bag distribution functions and experimentally.

the momentum transfer μ_0^2. In order to find μ_0^2 using QCD perturbation theory, we need to calculate the moments of the non-singlet structure function $xF_3^{\nu N}(x)$ using our quark distributions and compare these moments with those determined experimentally. In Table 7.1 we list the bag model predictions for the moments of xF_3, $M_{3_{NS}}^{(n)}(\mu_0^2)$ with (denoted by an asterisk) and without magnetic (one gluon exchange) effects, and the experimentally determined moments at $Q^2 = 13$ GeV^2, $M_{3_{NS}}^{(n)}(Q^2)$ [PR 81]. The bag moments are normalized so that $M_{3_{NS}}^{(1)}(\mu_0^2) = 3$, in accordance with the Gross - Llewellyn-Smith sum rule (the difference between using normalized and non-normalized moments is slight).

Now the moment evolution equation of QCD (eqn. (2.94)) gives us the relationship (to leading order) between non-singlet moments evaluated at μ_0^2 and Q^2:

$$M_{3_{NS}}^{(n)}(Q^2) = M_{3_{NS}}^{(n)}(\mu_0^2) \left[\frac{\ln(Q^2/\Lambda^2)}{\ln(Q^2/\Lambda^2)}\right]^{-d_{NS}^{(n)}}. \tag{7.12}$$

Now the ratios Q^2/Λ^2 and μ_0^2/Λ^2 are independent of n, so rearranging eqn. (7.12) and taking logarithms leads to the relation

$$\frac{1}{d_{NS}^{(n)}} \ln \left[\frac{M_{3_{NS}}^{(n)}(\mu_0^2)}{M_{3_{NS}}^{(n)}(Q^2)} \right] = \frac{1}{d_{NS}^{(m)}} \ln \left[\frac{M_{3_{NS}}^{(m)}(\mu_0^2)}{M_{3_{NS}}^{(m)}(Q^2)} \right]. \tag{7.13}$$

We can test eqn. (7.13) by plotting the logarithm of the nth non-singlet moment of xF_3 versus the logarithm of the mth non-singlet moment. According to eqn. (7.13) the data should be on a straight line of slope $d_{NS}^{(n)}/d_{NS}^{(m)}$. In Fig. 7.11 we have reproduced the experimental results from the BEBC collaboration [LP 82,Bos+ 78], with our bag model predictions and lines with the slopes predicted by leading order QCD (with four flavours). We see that our bag model predictions lie slightly to the right of the data and the theoretical QCD line, and appear to be consistent with μ_0^2 having a fairly low value.

From eqn. (7.13) we also have that the ratio

$$D^{(n)} = \frac{1}{d_{NS}^{(n)}} \ln \left[\frac{M_{3_{NS}}^{(n)}(\mu_0^2)}{M_{3_{NS}}^{(n)}(Q^2)} \right] \tag{7.14}$$

should be independent of n, that is a plot of $D^{(n)}$ versus n should be a straight line of slope zero (higher order QCD predicts a line with a small positive slope). In Fig. 7.12 the ratios $D^{(n)}$ are plotted, and they are certainly not constant with n, in fact they decrease with n.

It would appear then that analysis of the moments of our calculated distribution functions is inappropriate. The reason for this is that moment analysis depends very critically upon the large x behavior of our distributions, but this is the regime where our approximation for the recoil state breaks down, as was pointed out in the previous chapter. Hence we do not expect that the results of analyzing the moments of the calculated distributions in two dimensions should be taken too

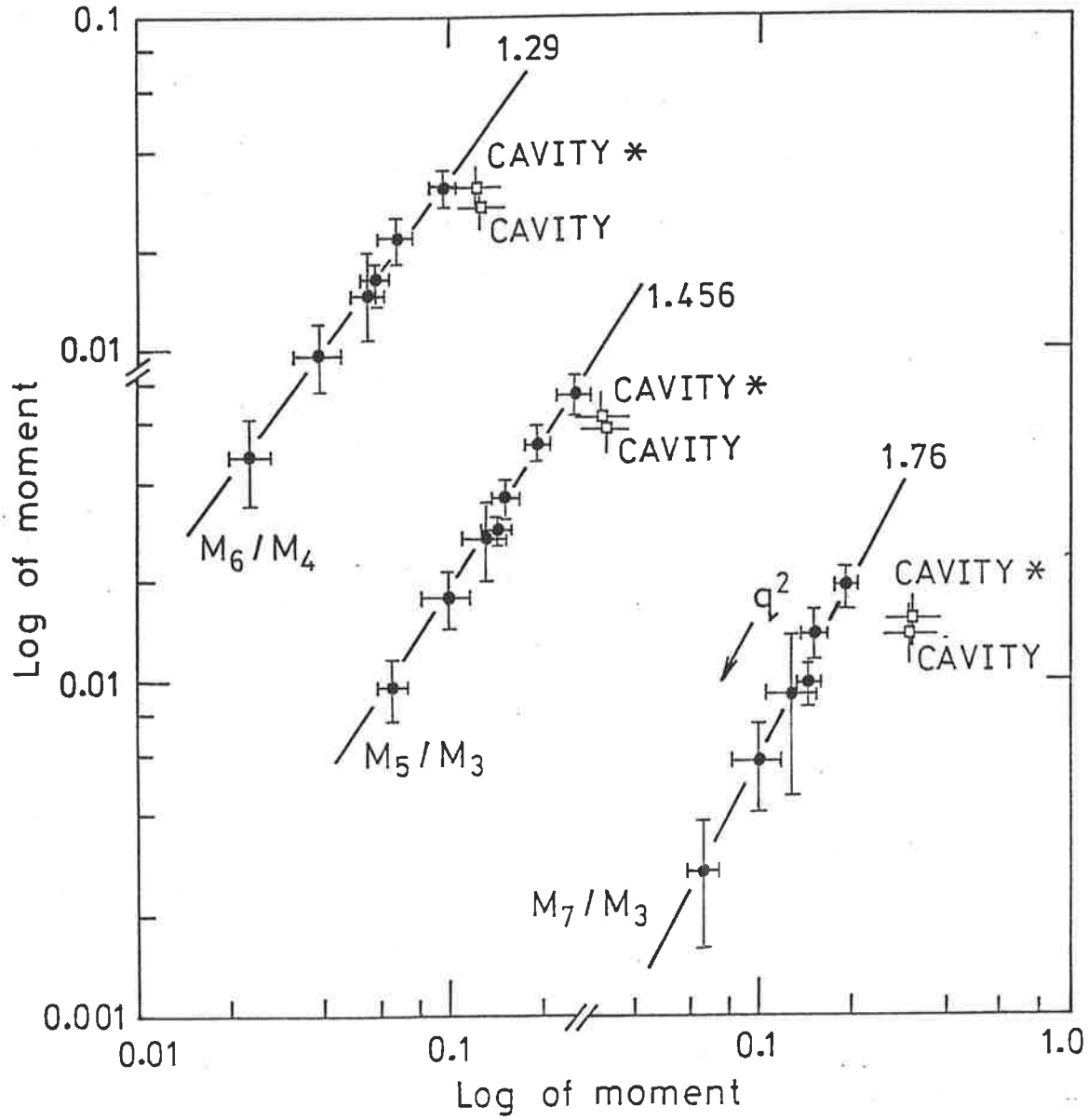

Fig. 7.11. Non-singlet moments of xF_3 plotted versus one another. The points labelled 'Cavity' and 'Cavity *' refer to the moments calculated in the 2-d cavity without and with magnetic corrections to the nucleon mass respectively.

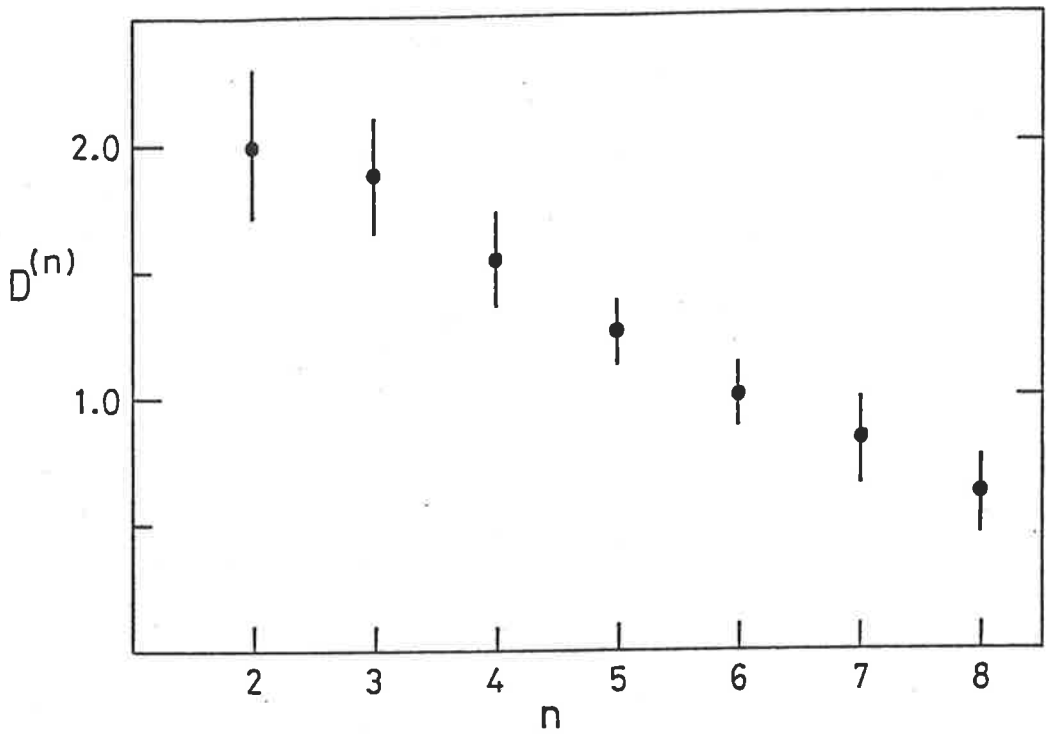

Fig. 7.12. Plot of $D^{(n)} = [d_{NS}^{(n)}]^{-1} \ln[M_{3_{NS}}^{(n)}(\mu_0^2)/M_{3_{NS}}^{(n)}(Q^2)]$ where $M_{3_{NS}}^{(n)}(\mu_0^2)$ are the moments of xF_3 calculated in the 2-d cavity (with an arbitrary uncertainty of 10%), and $M_{3_{NS}}^{(n)}(Q^2)$ are the experimentally determined moments at $Q^2 = 13$ GeV^2.

seriously. It would certainly not make s ense for us to take the moments, evolve them to large Q^2, then perform an inverse Mellin transform to obtain distribution functions 'appropriate' to this large value of Q^2.

To point this out, we may attempt to estimate the scale μ_0^2 in a manner similar to that of Jaffe and Ross [JR 80]. Leading order QCD gives the relation [PR 81]:

$$\exp[-D^{(n)}] = 1 + B^{(n)} \ln(\mu_0^2/Q^2) \tag{7.15}$$

where the $B^{(n)}$ are determined by a fit to the high Q^2 data. Using the third moment of xF_3 we obtain $\mu_0^2 = 0.8 \pm 0.1$ GeV^2, but for $n = 4, 5, 6$ we obtain $\mu_0^2 = 1.1, 1.8, 2.5$ GeV^2 respectively, indicating that the unreliability of our distributions at large x leads to large unreliability in their moments. Looking again at Table 7.1 and Fig. 7.11 we see that our cavity approximation predictions for the moments of xF_3 fall too quickly with n, which leads us to the expectation that our predicted moments might be good for small n, and that a value of $\mu_0^2 \approx 0.8$ Gev^2, is a good estimate of the scale appropriate for our bag and cavity calculations, in accordance with our earlier expectations and the calculation of Jaffe and Ross.

7.6 Summary

In Chapters Six and Seven of this thesis we have presented a new method of calculating the twist two matrix elements of DIS using the two-dimensional MIT bag model. We have then used this method to examine the flavour symmetry-breaking effects introduced by the hyperfine one gluon interaction in the proton. We also examined the EMC effect, looking at the changes in quark distribution functions that the

background nuclear fields can induce, and also changes induced by changing the nucleon length scale (*à la* CRRJ [CJRR 85]). In both cases we found effects similar in magnitude to the EMC effect, though not necessarily reproducing the x-dependence of the EMC effect. We also noted that in the bag model changes in length scale and changes in the background scalar and vector potentials were intimately related.

It was unfortunate that we could not determine the momentum transfer scale appropriate to our calculations, though this failure probably comes from uncertainties in the distribution functions at high x, which become magnified when moments of the distributions are taken, and also from the breakdown of our model for the intermediate state at high x. However we persist in our belief that the calculated distribution functions are appropriate to a low value of Q^2, probably in the region of 0.8 GeV^2, as was determined by Jaffe and Ross for the L_0 Approximation.

Our method of calculation is generalizable to four dimensions [BST 88], though the calculations of the quark overlap functions are somewhat tedious. However the slightly different wave functions, plus (more importantly) the presence of transverse components of quark momenta in the four dimensional model should do away with the unphysical zeroes at high x that appear in the calculations in two dimensions. The use of the four dimensional model may well enable us to estimate better the appropriate momentum scale for the calculations, and hopefully fine tune our calculations with regard to possible causes of the EMC effect. Also we would be able to introduce spin into our calculations and examine the important spin structure functions and asymmetries [ST 88a]. However the basis for this future work will be

the methods developed and presented in this thesis.

Bibliography

[Abr+ 82,83] H. Abramowicz *et. al.*, Z. Phys. **C15**, 19 (1982); Z. Phys. **C17**, 283 (1983).

[Adler 69] S. Adler, Phys. Rev. **177**, 2426 (1969).

[AD 68] S. Adler and R. Dashen, *Current Algebra*, Benjamin, New York (1968).

[AGT 69] H. D. I. Abarbanel, M. L. Goldberger and S. B. Treimain. Phys. Rev. Lett. **22**, 50 (1969).

[Aku+ 85a,85b] S. V. Akulinichev, S. A. Kulagin and G. M. Vagradov, Phys. Lett. **158B**, 485 (1985); S. V. Akulinichev, S. Shlomo, S. A. Kulagin and G. M. Vagradov, Phys. Rev. Lett. **55**, 2238 (1985).

[AL 73] E. S. Abers and B. W. Lee, Phys. Rep. **9C**, 1 (1973).

[All+ 81] D. Allesia *et. al.*, Phys. Lett. **107B**, 148 (1981).

[AP 77] G. Altarelli and G. Parisi, Nucl. Phys. **B126**, 298 (1977).

[Arn+ 84] R. G. Arnold *et. al.*, Phys. Rev. Lett. **52**, 1431 (1984).

[Asr+ 85,86] A. E. Asratyan *et. al.*, Sov. J. Nucl. Phys. **41**, 1193 (1985); Sov. J. Nucl. Phys. **43**, 598 (1986).

[Aub+ 83] J. J. Aubert *et. al.*, Phys. Lett. **123B**, 275 (1983).

[Aub+ 85] J. J. Aubert *et. al.*, Phys. Lett. **152B**, 433 (1985).

[Aub+ 87] J. J. Aubert *et. al.*, Nucl. Phys. **B293**, 740 (1987).

[Bad+ 80] J. Badier *et. al.*, Phys. Lett. **93B**, 354 (1980).

[Bad+ 83] J. Badier *et. al.*, Z. Phys. **C18**, 281 (1983).

[Bari+ 85] G. Bari *et. al.*, Phys. Lett. **163B**, 282 (1985).

[BBM 86] R. P. Bickerstaff, M. C. Birse and G. A. Miller, Phys. Rev. **D33**, 3228 (1986).

[BCW 84] E. L. Berger, F. Coester and R. B. Wiringa, Phys. Rev. **D29**, 398 (1984).

[BD 64 65] J. D. Bjorken and S. D. Drell, *Relativistic Quantum Mechanics*, McGraw-Hill, New York (1964); *Relativistic Quantum Fields*, McGraw-Hill, New York (1965).

[Bell+ 78] J. S. Bell and A. J. G. Hey, Phys. Lett. **74B**, 77 (1978); J. S. Bell, A. C. Davis and J. Rafelski, Phys. Lett. **78B**, 67 (1978).

[BG 78] A. J. Buras and K. J. F. Gaemers, Nucl. Phys. **B132**, 249 (1978).

[Bjor 66 69] J. D. Bjorken, Phys. Rev. **148**, 1467 (1966); Phys. Rev. **179**, 1547 (1969).

[BJ 77] R. C. Barrett and D. F. Jackson, *Nuclear Sizes and Structure*, Clarendon, Oxford (1977).

[BK 79] L. Baulieu and C. Kounnas, Nucl.Phys. **B155**, 429 (1979).

[BjP 71] J. D. Bjorken and E. A. Paschos, Phys. Rev. **66**, 578 (1971).

[BM 86] R. P. Bickerstaff and G. A. Miller, Phys. Lett. **168B**, 409 (1986).

[BM 87] C. J. Benesh and G. A. Miller, Phys. Rev. **D36**, 1344 (1987).

[Bos+ 78] P. C. Bosetti *et. al*, Nucl. Phys. **B142**, 1 (1978).

[BP 71] R. Brandt and G. Preparata, Nucl. Phys. **B27**, 373 (1971).

[BR 81] A. Bodek and J. Ritchie, Phys. Rev. **D23**, 1070 (1981).

[BST 88] R. P. Bickerstaff, A. I. Signal and A. W. Thomas, in preparation.

[BT 87a] R. P. Bickerstaff and A. W. Thomas, Phys. Rev. **D35**, 108 (1987).

[BT 87b] R. P. Bickerstaff and A. W. Thomas, University of Adelaide preprint *The Structure Function of a Swollen Nucleon*, ADP-87-1/T29 (1987).

[Buras 80] A. J. Buras, Rev. Mod. Phys. **52**, 199 (1980).

[Close 79] F. E. Close, *An Introduction to Quarks and Partons*, Academic, London (1979).

[Cho+ 74] A. Chodos, R. L. Jaffe, K. Johnson, C.B. Thorn and V. Weisskopf, Phys. Rev. **D9**, 3471 (1974); A. Chodos, R. L. Jaffe, K. Johnson and C.B. Thorn, Phys. Rev. **D10**, 2599 (1974).

[CJRR 85] F. E. Close, R. L. Jaffe, R. G. Roberts and G. G. Ross, Phys. Rev. **D31**, 1004 (1985).

[Col 68] S. Coleman, 'Soft Pions' in *Hadrons and Their Interactions*, Academic, New York (1968).

[CRR 83] F. E. Close, R. G. Roberts and G. G. Ross, Phys. Lett. **129B**, 346 (1983).

[DeG+ 75] T. DeGrand, R. L. Jaffe, K. Johnson and J. Kiskis, Phys. Rev. **D12**, 2060 (1975).

[DGG 75] A. De Rujula, H. Georgi and S. L. Glashow, Phys. Rev. **D12**, 147 (1975).

[DJ 80] J. F. Donoghue and K. Johnson, Phys. Rev. **D21**, 1975 (1980).

[DT 85] G. V. Dunne and A. W. Thomas, Nucl. Phys. **A446**, 437 (1985).

[DT 86] G. V. Dunne and A. W. Thomas, Nucl. Phys. **A455**, 701 (1986); Phys. Rev. **D33**, 2061 (1986).

[Dunne 86] G. V. Dunne, M.Sc. Thesis, University of Adelaide (1986).

[EFP 82 83] R. K. Ellis, V. Furmanski and R. Petronzio, Nucl. Phys. **B207**, 1 (1982); Nucl. Phys. **B212**, 29 (1983).

[Eis 82] F. Eisele, J. de Phys. Suppl. **C3**, 337 (1982).

[ET 83] M. Ericson and A. W.Thomas, Phys. Lett. **128B**, 112 (1983).

[Fey 69] R. P. Feynmann, Phys. Rev. Lett. **23**, 1415 (1969).

[FF 77] R. D. Field and R. P. Feynmann, Phys. Rev. **D15**, 2590 (1977).

[Fri 71] Y. Frishman, Ann. Phys. **66**, 373 (1971).

[GL 60] M. Gell-Mann and M. Levy, Nuovo Cimento **16**, 53 (1960).

[GN 64] M. Gell-Mann and Y. Ne'eman, *The Eightfold Way*, Benjamin, New York (1964).

[Gui 88] P. A. M. Guichon, Phys. Lett. **200B**, 235 (1988).

[GW 73] D. Gross and F. Wilczek, Phys. Rev. Lett. **30**, 1346 (1973).

[HW 53] D. L. Hill and J. A. Wheeler, Phys. Rev. **89**, 1102 (1953).

[Isgur 80] N. Isgur, Proc. BARYON 80 Conf., University of Toronto Press, Toronto (1980).

[IZ 80] C. Itzykson and J-B. Zuber, *Quantum Field Theory*, McGraw-Hill, New York (1980).

[Jaffe 75] R. L. Jaffe, Phys. Rev. **D11**, 1953 (1975).

[Jaffe 81] R. L. Jaffe, Ann. Phys. **132**, 32 (1981).

[Jaffe 83] R. L. Jaffe, Nucl. Phys. **B229**, 205 (1983).

[Jaffe 86] R. L. Jaffe, in *Relativistic Dynamics and Quark Nuclear Physics*, proc. Los Alamos School, 1985, eds. M. B. Johnson and A. Picklesimer, Wiley, New York (1986).

[JCRR 85] R. L. Jaffe, F. E. Close, R. G. Roberts and G.G. Ross, Phys. Lett. **134B**, 449 (1985).

[JJ 76] R. L. Jaffe and K. Johnson, Phys. Rev. **D13**, 1355 (1976).

[JM 73] G. Jacob and Th. Maris, Rev. Mod. Phys. **45**, 6 (1973).

[JP 75] R. L. Jaffe and A. Patriscioiu, Phys. Rev. **D12**, 1314 (1975).

[JR 80] R. L. Jaffe and G. G. Ross, Phys. Lett. **93B**, 313 (1980).

[JS 82] R. L. Jaffe and M. Soldate, Phys. Lett. **105B**, 467 (1982).

[LlS 83] C. H. Llewellyn-Smith, Phys. Lett. **128B**, 107 (1983).

[LP 82] E. Leader and E. Predazzi, *An Introduction to Gauge Fields and the 'New Physics'*, Cambridge University Press, Cambridge (1982).

[Light 58] M. J. Lighthill, *Fourier Analysis and Generalised Functions*, Cambridge University Press, Cambridge (1958).

[Neg 70] J. Negele, Phys. Rev. **C1**, 1260 (1970).

[Pan 68] W. Panofsky, Proc. Int. Conf. High Energy Phys. **14**, Vienna 1968.

[Pet 79] A. Peterman, Phys. Rep. **53**, 159 (1979).

[Pol 73] H. D. Politzer, Phys. Rev. Lett. **30**, 1346 (1973).

[PR 81] M. R. Pennington and G. G. Ross, Nucl. Phys. **B179**, 324 (1981).

[PT 62] R. E. Peierls and D. J. Thouless, Nucl. Phys. **38**, 154 (1962).

[PY 57] R. E. Peierls and J. Yoccoz, Proc. Phys. Soc. **A70**, 381 (1957).

[Rith 86] K. Rith, Proc. Int. Nucl. Phys. Conf.,Harrogate (1986).

[Sull 72] J. D. Sullivan, Phys. Rev. **D5**, 1732 (1972).

[ST 87a] A. I. Signal and A. W. Thomas, Phys. Lett. **191B**, 205 (1987).

[ST 87b] A. I. Signal and A. W. Thomas, Aust. J. Phys. **40**, 161 (1987).

[ST 88a] A. W. Schreiber and A. W. Thomas, University of Adelaide preprint *Spin Dependent Structure Functions in the Cloudy Bag Model*, ADP-88-83/T54 (1988).

[ST 88b] A. I. Signal and A. W. Thomas in *Progress in Nuclear and Particle Physics Vol. 20*, ed. A. Faessler, Pergamon Press, Oxford (1988).

[SV 81] E. V. Shuryak and A. Vainshteyn, Phys. Lett. **105B**, 65 (1981).

[tHo 71] G. t'Hooft, Nucl. Phys. **B33**, 1973 (1971).

[Tho 83a] A. W. Thomas, Phys. Lett. **126B**, 97 (1983).

[Tho 83b] A. W. Thomas, Lectures presented at Int. School of Nucl. Phys., 7th Course, Erice (1983).

[Tho 84] A. W. Thomas, Adv. Nucl. Phys. **13**, 1 (1984).

[Tho 88] A. W. Thomas, private communication, (1988).

[Wil 69] K. Wilson, Phys. Rev. **179**, 1499 (1969).

[Wong 81] C. W. Wong, Phys. Rev. **D24**, 1416 (1981).

[WZ 72] K. Wilson and W. Zimmerman, Comm. Math. Phys. **24**, 87 (1972); W. Zimmerman, *Brandeis Lectures 1970 Vol. 1*, Cambridge MIT Press, Cambridge (1970).

[Ynd 83] F. Yndurain, *Quantum Chromodynamics*, Springer-Verlag, Berlin (1983).

POSSIBLE STRENGTH OF THE NON-PERTURBATIVE STRANGE SEA OF THE NUCLEON

A.I. SIGNAL and A.W. THOMAS
Department of Physics, University of Adelaide, G.P.O. Box 498, Adelaide, SA 5001, Australia

Received 4 March 1987

We examine the experimental constraints on the size of a possible non-perturbative component of the strange-quark sea in the nucleon. It is found to be consistent with theoretical expectations within errors which are quite large and should be reduced.

One of the most comforting confirmations of the predictions of QCD is the observation of logarithmic scaling violations in the structure functions measured by deep inelastic scattering (DIS) [1]. In particular, there can be no doubt that an increasing fraction of the sea-quark distribution is generated perturbatively as Q^2 rises [1,2]. Nevertheless, it has long been recognised that some fraction of the sea may be associated with non-perturbative processes – like the pion cloud of the nucleon (itself necessary to ensure chiral symmetry). This component was first calculated by Sullivan as long ago as 1972 [3]. More recently, with the advent of modern data (particularly from neutrino experiments) [4], it has proven possible to put limits on the size of this pionic contribution – and indirectly on the quark confinement radius [5]. This question has become even more topical since the discovery of the EMC effect [6,7]. Amongst the multitude of explanations put forward, one of the least exotic involves possible enhancement of the virtual pion field of the nucleus (beyond that of a collection of free nucleons) [8–10].

It is our purpose to describe the extensions of this work to the strange sea of the nucleon [$s(x)$ and $\bar{s}(x)$], and to investigate the limits which recent data place on it. We shall see that a dramatic difference in shape is predicted for the non-perturbative components of $s(x)$ and $\bar{s}(x)$. For reasonable ΛNK (and ΣNK) form-factors (i.e., of similar range to the nucleon axial form-factor), the predictions are consistent with data: within its very large errors. With a not unreasonable improvement in precision the theory could be severely tested.

The mechanism which we have calculated is shown in fig. 1. For the final hyperon we include only the Λ and Σ. As already pointed out in the pionic case, the contribution from excited baryon resonances would be restricted to small x, where the assumption of incoherence eventually breaks down. By analogy with Sullivan the amplitude for fig. 1a is written as

$$A^{\mu} = g_{\mathrm{HNK}} \frac{\bar{u}_{\mathrm{H}} \mathrm{i}\gamma_5 u_{\mathrm{N}}}{k^2 - m_{\mathrm{K}}^2} (\mathrm{X}|^{\mu}j|\mathrm{K}(k)) , \qquad (1)$$

where k is the four-momentum of the exchanged meson, u and $\bar{u}$ the appropriate Dirac spinors, X the debris of the struck kaon, and g_{HNK} (H = Λ or Σ) the appropriate coupling constant. If we now square the amplitude, sum over all final states and average over initial spins we find

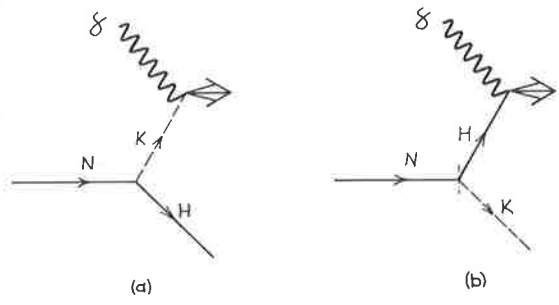

Fig. 1. Non-perturbative contributions to the strange sea of the nucleon. (a) The incoming photon is abosrbed by a virtual kaon. (b) The incoming photon is absorbed by a virtual hyperon.

0370-2693/87/$ 03.50 © Elsevier Science Publishers B.V.
(North-Holland Physics Publishing Division)

$$\frac{2m_N \, dW_N^{\mu\nu} f}{dk^2 \, dx'}$$

$$= \frac{x}{x'^2} \frac{g_{HNK}^2}{4\pi} \frac{\mathrm{Tr}[(\not{p}_N + m_N)\gamma_5(\not{p} + m_H)\gamma_5]}{(k^2 - m_K^2)^2}$$

$$\times (\pi^{-1} \, \mathrm{Im} \, C_K^{\mu\nu}) \, , \qquad (2)$$

where

$$\pi^{-1} \, \mathrm{Im} \, C_K^{\mu\nu}$$

$$= \sum_X \langle K(k)|j^\mu(0)|X\rangle\langle X|j^\nu(0)|K(k)\rangle$$

$$\times \delta^{(4)}(q + k + p_X) \, . \qquad (3)$$

In eqs. (2) and (3) x (x') is the Bjorken variable appropriate to the lepton–nucleon (lepton–kaon collision) – $x = 1/\omega$ in the notation of ref. [3].

The spin trace is easily shown to be $k^2 - (m_H - m_N)^2$. We also recognise the expression in eq. (3) as the structure function of the (off-shell) kaon. Given the experimental observation that the pion and kaon structure functions are equal within experimental errors [11] we shall use the (better determined) pion structure function for $\mathrm{Im} \, C_K^{\mu\nu}$ [12]. Finally, we neglect the possible dependence of $\mathrm{Im} \, C^{\mu\nu}$ on the invariant mass of the kaon – an approximation that deserves further work in another context too [13]. With this approximation we find the following result for $\delta F_{2N}(x, Q^2)$, which is the contribution to the structure function of the nucleon from the process shown in fig. 1a:

$$\delta F_{2N}(x, Q^2) = \int_x^1 dy \, f(y) F_{2K}(x/y, Q^2) \, , \qquad (4)$$

where

$$f(y) = y \sum_{H=\Lambda,\Sigma} f_H^1 \frac{g_{HKN}^2}{16\pi^2}$$

$$\times \int_{t_{min}}^{\infty} dt \frac{t + (m_H - m_N)^2}{(t + m_K^2)^2} F^2(t) \, . \qquad (5)$$

In eq. (5) we have as usual set $t = -k^2$ (> 0), $F(t)$ is the high-momentum cut-off (or form-factor) at the HNK vertex, and t_{min} is the minimum value of $-k^2$ for the process shown in fig. 1a at this value of y ($y \equiv x/x'$):

$$t_{min} = y[m_H^2 - (1-y) \, m_N^2]/(1-y) \, . \qquad (6)$$

For the coupling constants we use $g_{\Sigma NK}^2/4\pi = 3.7$ and $g_{\Lambda NK}^2/4\pi = 13.7$ [6]. As in earlier work we take the form-factor to have a simple analytic form motivated by the cloudy bag model [14] (in which R has the interpretation of a bag radius):

$$F(t) = \exp[-0.106 m_K^2 R^2 (t + m_K)^2/m_K^2] \, . \qquad (7)$$

The factor f_H^1 is an isospin factor, which is 3 for $H = \Sigma$ and 1 for $H = \Lambda$.

Actually the kaon case is different from the pion, because the electromagnetic structure functions of K^+ and K^0 are different, whereas those of the π^0 and π^+ should be the same. This would lead to different values of f_H^1. However, our interest is not so much in the contribution of fig. 1a to the electromagnetic structure function of the proton (which would be very small), but rather in the non-perturbative, anti-strange sea, $\bar{s}_p^{NP}(x)$, which it generates.

In terms of the $f(y)$ already defined, and given that both K^0 and K^+ contain one valence anti-strange quark (so that the values of f_H^1 given are appropriate) we find

$$x\bar{s}_p^{NP}(x, Q^2) = \int_x^1 dy \, f(y)(x/y) s_K(x/y, Q^2) \, . \qquad (8)$$

It is less obvious how to calculate the non-perturbative, strange sea, s_p^{NP}. The simplest idea, suggested by Berger, Coester and collaborators in the pionic case [10] is simply to evaluate fig. 1b using the *same* $f(y)$. In our case the source of the strange sea of the proton is therefore primarily the valence strange quarks in the recoiling Λ or Σ. Since we know no better, we take the valence distribution of the Λ and Σ to be of the form $s_H(x) = N_s x^{-1/2}(1-x)^3$ – as for valence u-quarks in the proton. Small variations in the exponents would change none of our conclusions. Our final expression for $s_p^{NP}(x, Q^2)$ is then:

$$xs_p^{NP}(x, Q^2) = \int_0^{1-x} dy \, f(y)[x/(1-y)]$$

$$\times s_H(x/(1-y), Q^2) \, . \qquad (9)$$

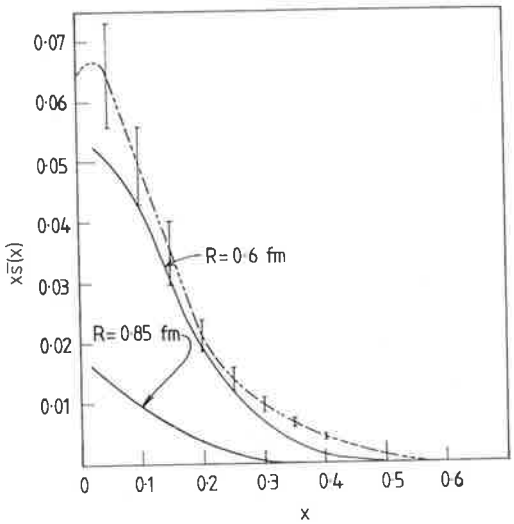

ig. 2. The non-perturbative contribution to $x\bar{s}(x)$ for two bag adii compared with the experimental determination of $x\bar{s}(x)$ dot-dash line).

The first, dramatic result of this calculation is that $\bar{s}_p^{NP}(x)$ and $s_p^{NP}(x)$ have quite different shapes. Whereas $\bar{s}^{NP}$ has a very similar shape to the usual parameterisations of sea-quark distributions, which die out beyond $x\sim 0.3$, s^{NP} is quite different. Because of its origins in the valence distribution of the Λ or Σ hyperon s^{NP} extends to quite large values of x and also carries more momentum. For example, with $R=0.8$ fm in eq. (7), the fraction of the nucleon's momentum carried by non-perturbative strange quarks is $S=0.52\%$, while $\bar{S}=0.28\%$. With $R=0.6$ and 1.0 fm the results are (1.4%, 1.0%) and (0.18%, 0.08%), respectively. This may be compared with the data of CDHS group (at $Q^2\approx 5$ GeV^2), which found $(\bar{U}+\bar{D}+2\bar{S})=7\pm 0.5\%$ and $2S/(\bar{U}+\bar{D})=52\pm 9\%$. If, as assumed in almost all phenomenology, one sets $S=\bar{S}$ this implies $\bar{S}=1.2\pm 0.2\%$, which clearly restricts the allowed values of R.

A more thorough analysis of the data requires more

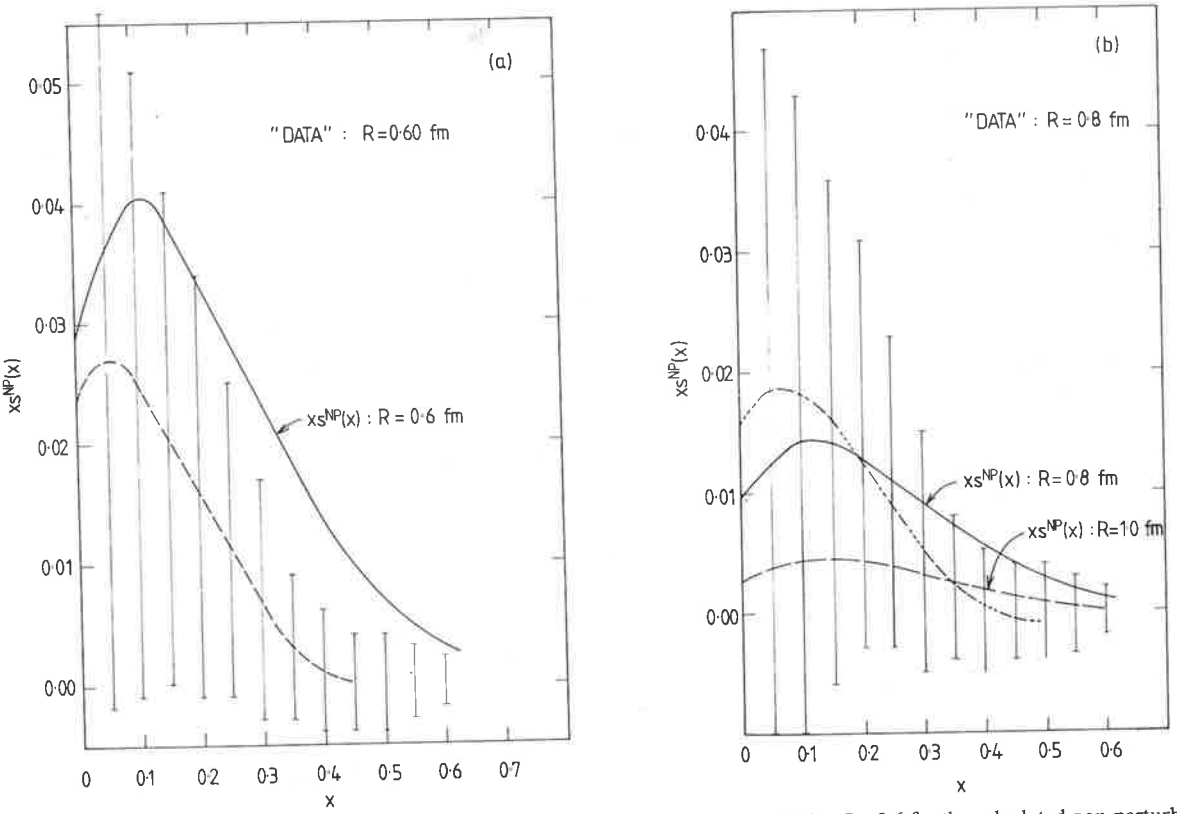

Fig. 3. Comparison of $xs^{NP}(x)$ between this calculation and experiment. (a) For bag radius $R=0.6$ fm the calculated non-perturbative contribution is larger than experiment allows. (b) For bag radii $R\lesssim 0.8$ fm there is reasonable agreement between this calculation and experiment.

effort – including a proper consideration of the errors involved. Most of the relevant data has come from di-muon ($\mu^+\mu^-$) coincidence measurements taken by CDHS. According to the usual quark–proton model and Cabibbo theory, the (ν, $\bar{\nu}$) dimuon cross sections for an isoscalar target are [1,4]

$$\frac{d\sigma^{\nu}}{dx} \propto \sin^2\theta_c\,[xu(x)+xd(x)] + \cos^2\theta_c\,[2xs(x)]\,, \tag{10a}$$

$$\frac{d\sigma^{\bar{\nu}}}{dx} \propto \sin^2\theta_c\,[x\bar{u}(x)+x\bar{d}(x)] + \cos^2\theta_c\,[2x\bar{s}(x)]\,. \tag{10b}$$

Since $\cos^2\theta_c \gg \sin^2\theta_c$ the $\bar{\nu}$ data gives a good determination of $x\bar{s}(x)$. This is compared with our calculated, non-perturbative contribution in fig. 2. Clearly the shapes agree and the magnitude of the non-perturbative contribution is less than the total observed for reasonable values of R.

Unfortunately the situation for $s(x)$ is not so simple. The size of the valence contribution to $u(x)$ and $d(x)$ in eq. (10a) counteracts the small value of $\sin^2\theta_c$ so that $s(x)$ extracted from the ν-data has large errors. We have used the parameterisations of Buras and Gaemers between 5 and 10 GeV^2 to extract $xs(x)$ from the CDHS data. If we assume the perturbative components of $s(x)$ and $\bar{s}(x)$ are identical we can then extract the experimental non-perturbative piece of $xs(x)$ by subtracting $[x\bar{s}(x) - x\bar{s}^{\mathrm{NP}}(x)]$ from the data for $xs(x)$. This is compared with our calculations for $xs^{\mathrm{NP}}(x)$ in fig. 3.

The first conclusion for fig. 3 is that theory and experiment are in reasonable agreement in shape and magnitude for $R \sim 0.80$ fm – the same region found in earlier work on the pion [5]. However, any strength of conviction is lost in the face of the typical error bars, which are also shown in fig. 3. The lack of support at large values of x ($\gtrsim 0.5$) rules out R less than about 0.8 fm, but little else can be said. Clearly we would be delighted to have better data. In order to obtain it the worst errors to be overcome are the error of 7% on $\bar{Q}^{\bar{\nu}}$ ($\equiv \bar{U}+\bar{D}+2\bar{S}$), and of 17% on $2\bar{S}/(\bar{U}+\bar{D})$.

This work was supported by the ARGS.

References

[1] E. Leader and E. Predazzi, An introduction to gauge theories and the new physics (Cambridge U.P., London, 1982); F.J. Yndurain, Quantum chromodynamics (Springer, Berlin, 1983).
[2] F. Eisele, J. Phys. (Paris) 12 (Suppl.) (1982) C3.
[3] J.D. Sullivan, Phys. Rev. D 5 (1972) 1732.
[4] H. Abramowicz et al., Z. Phys. C 15 (1982) 19; C 17 (1983) 283.
[5] A.W. Thomas, Phys. Lett. B 126 (1983) 97.
[6] J.J. Aubert et al., Phys. Lett. B 123 (1983) 275.
[7] R.G. Arnold et al., Phys. Rev. Lett. 51 (1984) 727.
[8] C.H. Llewellyn Smith, Phys. Lett. B 128 (1983) 107.
[9] M. Ericson and A.W. Thomas, Phys. Lett. B 128 (1983) 112.
[10] E.L. Berger et al., Phys. Rev. D 24 (1984) 398.
[11] J. Badier et al., Phys. Lett. B 93 (1980) 354.
[12] J. Badier et al., Z. Phys. C 18 (1983) 281.
[13] G.V. Dunne and A.W. Thomas, Nucl. Phys. A 455 (1986) 701.
[14] A.W. Thomas, Adv. Nucl. Phys. 13 (1984) 1; G.A. Miller, in: Intern. Rev. Nucl. Phys., Vol. 2 (1984).

Signal, A., & Thomas, A. (1987). Anti-neutrino cross sections for neon and deuterium. *Australian Journal of Physics, 40*(5), 601-610.

ADP-87-54/T47

Contributed paper at the
school on "Quarks and Mesons
in Nuclei"

(Erice, July 1987)

DEEP INELASTIC SCATTERING FROM A MOMENTUM CONSERVING TWO-DIMENSIONAL CAVITY

A. Signal and A.W. Thomas

Department of Physics, University of Adelaide,

P.O. Box 498, G.P.O. ADELAIDE, S.A 5001, AUSTRALIA

1. INTRODUCTION

Historically the bag model in two spacetime dimensions has been important in discussion of the deep inelastic nucleon structure functions. (Jaffe 1975, Bell and Hey 1978, Jaffe 1981). In two dimensions the light core nature of deep inelastic processes is apparent, and the existence of simple wave functions in the bag enables one to explicitly calculate structure functions. This program is not without its problems. In particular the cavity approximation to the bag model, which is frequently used, badly violates translation invariance. This leads to support for the structure functions in the non-physical region $x > 1$, where x is the Bjorken scaling variable. To overcome this problem one might attempt to restore translation invariance using the Peierls-Yoccoz projection (Peierls and Yoccoz 1957). Alternatively one might explicitly ensure momentum conservation throughout the scattering process. In this paper we apply both of these methods and compare the resulting structure functions and their support.

2. BASIC THEORY

To leading order in Q^2, the structure function of a quark, flavour a, in a target at rest is given by (Jaffe 1985):

$$f_a(x) = \frac{\sqrt{2}}{4\pi} M \int d\xi^- e^{iq^+\xi^-} < p \mid \psi^+_{a+}(\xi^-)\, \psi_{a+}(0) \mid p >_c \Big|_{\xi^+ = 0} \qquad (2.1)$$

where we have ignored the quark's charge and where we have used light cone co-ordinates

$$a^{\pm} = (a^0 \pm a^1)/2^{\frac{1}{2}} \text{ and}$$

$$\psi_+ = \tfrac{1}{2}(I + \alpha)\,\psi \quad , \quad \alpha = \begin{bmatrix} 1 & 0 \\ 0 & -1 \end{bmatrix} \qquad (2.2)$$

$$x = Q^2/_{2\, p\cdot q} \qquad (2.3)$$

with $q^+ = -xp^+$ in the Bjorken Limit ($Q^2 \to \infty$, $q^- \to \infty$), and M the mass of the target. We use the normalization $< p' \mid p > = 2\pi\delta(p-p')$. The subscript c denotes that only connected diagrams are included. Note that this structure function does not include any anti-quark contributions as we will be considering only target states consisting of valence quarks. We now insert a complete set of states between the quark field operators in eq. (2.1), and translate ξ^- dependence out of ψ^+_{a+}. Integrating over ξ^- now gives

$$f_a(x) = \frac{p^+}{\sqrt{2}} \sum_n \delta(p^+ - xp^+ - n^+) \mid < n \mid \psi_{a+} \mid p > \mid^2 \qquad (2.4)$$

which is familiar from the parton model.

Now we turn to the description of the target state. The quark field operator in a cavity of length 2ℓ centered in light-core co-co-ordinates at the origin is

$$\psi_a(\zeta^+, \zeta^-) = \frac{1}{2\sqrt{\ell}} \sum_{m>0} b_{m,a} \begin{bmatrix} e^{-i\epsilon_m \zeta^-} \\ (-1)^m e^{-i\epsilon_m \zeta^+} \end{bmatrix} \qquad (2.5)$$

with $\epsilon = \pi(m_m + \tfrac{1}{2})/\ell$ (2.6)

and colour is suppressed. The mass of the cavity plus quarks is given by the relation

$$M\ell = \sqrt{2}\,\pi \sum_m N_m (m + \tfrac{1}{2}) \qquad (2.7)$$

where N_m is the number of quarks in the mth mode.

Taking the double Fourier transform of $\psi(x^+, x^-)$ gives the momentum space representation of the operator.

$$\phi_a(p^-, p^+) = 2\pi\sqrt{\frac{\ell}{2}} \sum_{m \geq 0} b_{m,a}\, \delta(p^- + p^+ - E_m) \begin{bmatrix} \sin((p^+ - \epsilon_m)\ell)/((p^+ - \epsilon_m)\ell) \\ \sin(p^+\ell)/(p^+\ell) \end{bmatrix} \qquad (2.8)$$

$$= 2\pi \sum_{m \geq 0} b_{m,a}\, \delta(p^+ + p_m - E_m)\, \phi^+_m(p_m) \qquad (2.9)$$

In the following sections we will consider scattering from a cavity at rest populated by three valence quarks in the ground ($m = 0$) state with separable wave functions.

3. PEIERLS-YOCCOZ PROJECTION

The Peierls-Yoccoz projection approximates a translation invariant momentum eigenstate by a weighted integral over cavity states in all positions (Wong 1981)

$$| p > = [\phi(o)]^{-1} \int d\xi\, e^{-ip\xi} \mid B(\xi) > \qquad (3.0)$$

in one space dimension where $\mid B(\xi) >$ is a cavity centered at ξ and $\phi(p)$ is the Fourier transform of the Hill-Wheeler overlap function (Hill and Wheeler 1953) denoted by $I_m(\xi)$ for m independent quarks.

We now put this state into equ. (2.1) for the quark structure function and for a quark in the ground state we obtain

$$f_a(x) = \frac{\sqrt{2}}{4\pi} M \int d\xi^- e^{-i(xp^+ - \epsilon_o)\xi^-} E(\xi^-) \qquad (3.1)$$

where $E(\xi^-)$ is a light-cone correlation function given in terms of Hill-Wheeler overlap functions

$$E(\xi) = \mid \phi_3(p=0) \mid^{-2} \int d\zeta^-\, I_2(\zeta^-)\, I_1(\zeta^- - \xi) \qquad (3.2)$$

The two factors in the integral of equ. (3.3) come from the requirement that the two spectator quarks and the struck quark are all found in both the initial and final state of the virtual Compton process.

After doing the integrations in equs. (3.3) and (3.2) we arrive at the result

$$f_a(x) \propto p\ell^+ \quad \frac{\sin^2(x\,p^+\ell - \pi/2)}{(x\,p^+\ell - \pi/2)^2} \left\{ 2(2\,x\,p^+\ell - \pi/2)^{-2} \left[1 + \frac{\cos(2\,x\,p^+\ell)}{2\,x\,p^+\ell - \pi/2} \right] \right.$$

$$\left. + (2\,x\,p^+\ell + \pi/2)^{-2} \left[1 - \frac{\cos(2x p^+\ell)}{2\,x\,p^+\ell + \pi/2} \right] \quad (2\,x\,p^+\ell - 3\pi/2)^{-2} \left[1 - \frac{\cos(2\,x\,p^+\ell)}{2\,x\,p^+\ell + \pi/2} \right] \right\} \tag{3.3}$$

which is shown in fig. 1. The term outside the braces is the same as obtained by Jaffe (Jaffe 1975) and by Bell and Hey (Bell and Hey 1978). The term in the braces damps the structure function for X > 1 and arises from the Peierls-Yoccoz projection and oru requirements that the two spectators be found in both the initial and final states. We find that the ratio

$$\int_0^1 dx\, f_a(x) \Big/ \int_0^\infty dx\, f_a(x) \;\geq\; 99.5\% \tag{3.4}$$

which is an improvement on the value of ≈ 92% obtained by Jaffe (Jaffe 1975). The fact that $f_a(x) \neq 0$ for $x > 1$ arises because we do not ensure that the spectators form an on-mass-shell state after the struck quark is removed. We can examine the number and momentum sum rules. We find

$$\int_0^\infty dx\, f_a(x) = 0.92 \tag{3.5}$$

and

$$3\int_0^\infty dx\, x\, f_a(x) = 0.92 \tag{3.6}$$

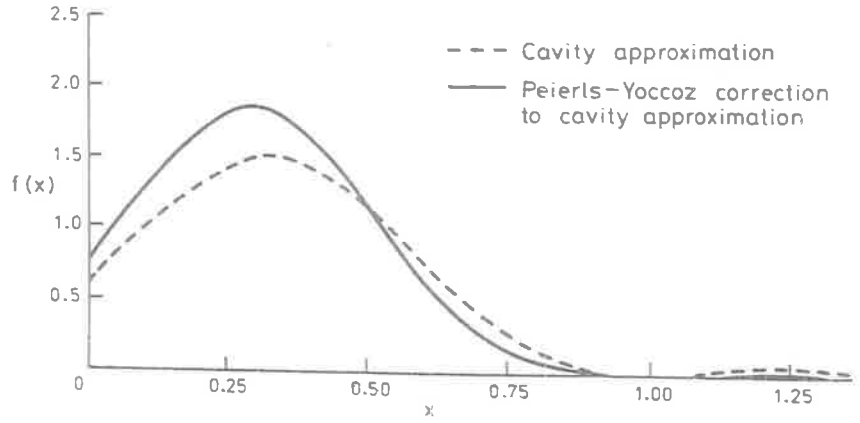

Figure 1

The quark structure function f(x) of a bag containing three valence quarks for the cavity approximation and for the cavity with the Peierls-Yoccoz correction eq. (3.4).

which shows that all the momentum is carried by the quark fields, as expected from the cavity approximation. The first sum rule should give unity, but is less than one because we have ignored any contributions from negative x. The contributions from the region $x < 0$ arise because the struck quark is in a bound system and has a small probability of having $p^+ < 0$.

4. STRUCTURE FUNCTION WITH MOMENTUM CONSERVATION ENFORCED

We noted above that unphysical contributions to the structure function $f_a(x)$ (notably beyond $x = 1$) arise if the spectator quarks do not form an on-mass-shell state. We can address this problem by examining the intermediate states $|\, n >$ in eq. (2.5) and applying appropriate constraints.

As $|\, n >$ is formed by the removal of a quark with plus component of momentum xp^+ from the state $|\, p >$, conservation of two-momentum implies that the plus component of momentum of the state $|\, n >$, n^+ is equal to $(1-x)p^+$. Also for the state $|\, n >$ to be on-mass-shell $n+$ must be greater than or equal to zero. These two constraints on $|\, n >$ imply that the only possible values that x can take are the physical values $0 \leq x \leq 1$. To a first approximation we may treat $|\, n >$ as a state made of two quarks both on the mass shell with wavefunctions which are the projections of eq. (2.9) onto free spinors:

$$\bar{\phi}_a(p^-, p^+) = 2\pi \sum b_{m,a}\, \delta(p^- + p^+ - E_m) \sqrt{\frac{\ell}{2}}\, \frac{\sin((p^+ - E_m)\ell)}{(p^+ - E_m)\ell}\, U_m \tag{4.1}$$

$$= 2\pi \sum_{m \geq 0} b_{m,a}\, \delta(p^- + p^+ - E_m)\; \bar{\phi}_m(p^+) \tag{4.2}$$

Where the U_m are two-component spinors. This approximation neglects on-shell intermediate states where one spectator quark has $p^+ < 0$ i.e. we have neglected binding in the intermediate state and treated the spectator quarks as "quasi-free"
The structure function eq. (2.5) may now be written

$$f_a(x) = \frac{p^+}{\sqrt{2}}\, |\, \phi_{0,a+}(xp^+)\, |^2 \int_0^{(1-x)p^+} dq_1^+ \int_0^{(1-x)p^+ - q_1^+} dq_2^+ \left(|\, \bar{\phi}_o(q_1^+)\, |^2\, |\, \bar{\phi}_o(q_2^+)\, |^2 \right.$$

$$\left. \times\; \delta((1-x)p^+ - q_1^+ - q_2^+) \right) \tag{4.3}$$

where q_1 and q_2 are the momenta of the two spectator quarks and the delta function ensures that the two spectators conserve momentum. Substituting in the wave functions (2.10) and (4.2) and using the delta function to evaluate one integral gives:

$$f_a(x) = \frac{p^+}{\sqrt{2}} \left(\frac{\ell}{2}\right)^3 \left(\frac{1}{2\pi}\right)^2 \quad \frac{\sin(x\,p^+\ell - \pi/2)}{(xp^+\ell - \pi/2)^2} \times$$

$$\int_0^{(1-x)p^+} dq_1^+ \frac{\sin^2(q_1^+\ell - \pi/2)}{(q_1^+\ell - \pi/2)^2} \quad \frac{\sin^2((1-x)p^+\ell - q_1^+\ell \pi/2)}{((1-x)p^+\ell - q_1^+\ell - \pi/2)^2} \tag{4.4}$$

which is shown in fig. 2.

As with the Peierls-Yoccoz projection, we obtain the same structure function as Jaffe, modified by a term which damps the contributions at large x and sifts shifts the structure function to lower x. In this case the contributions for $x > 1$ disappear as a consequence of momentum conservation. If we examine the sum rules again we find:

$$\int_0^1 dx\, f_a(x) = 0.87 \tag{4.5}$$

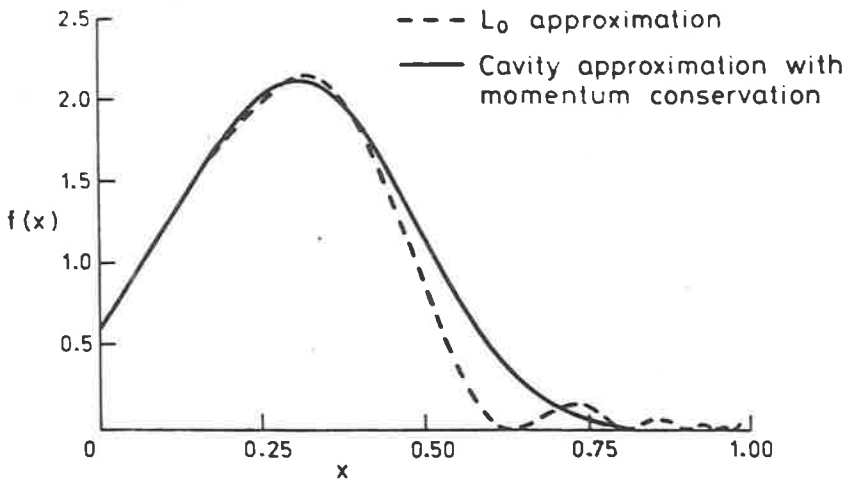

Figure 2

The quark structure function f(x) of a bag containing three valence quarks for the L_0 approximation and for the cavity aproximation with the correction for momentum conservation eq. (4.4).

$$3\int_0^1 dx\ x\ f_a(x) = 0.87 \qquad (4.6)$$

which again indicates that all the momentum of the cavity appears to be carried by the quark fields. The first integral should be unity if our normalization is correct. The difference gives an indication that, by dropping intermediate states with one spectator quark having $p^+ < 0$, we have substracted out about 10% of the possible intermediate states.

5. DISCUSSION

We have presented two procedures for restoring translation invariance to the cavity approximation in the context of deep inelastic scattering. Both procedures yield reasonable structure functions which improve on earlier cavity approximation calculations (Jaffe 1975). We may also compare our results with those of the translation invariant "L_0 approximation" (Jaffe and Ross 1980, Jaffe 1981), see fig. 2. The L_0 approximation gives structure functions with the correct support, however at large x the structure function has zeroes which are not seen, nor expected, physically and the structure function diverges as $x \to 1$ rather than going to zero.

In both of the procedures we have used, the spectator quarks have an important role, in limiting the momentum of the struck quark. In contrast the spectators are of no importance in the naive cavity or L_0 approximations. The importance of the spectators comes from the physical constraints or the forward virtual Compton process, that the intermediate state be on shell and that the final state is formed, and from translation invariance (or momentum conservation) imposed on the cavity.

It has been pointed out earlier (Thomas 1987, Jaffe and Ross 1980) that quark models such as the bag do not really apply in the Bjorken limit ($Q^2 \to \infty$, $\nu \to \infty$). However it is postulated that quark model matrix elements are those of a full field theory renormalized at a low momentum scale. That is, we have calculated the leading twist two part of the structure function at a value of Q^2 somewhat less than 1 GeV^2, which is well out of the range of experimental data. However we could connect our calculations with experiments, which also measure the leading twist two part of the structure at large Q^2, by taking moments of our distributions and evolving to higher Q^2 using the Alteralli-Parisi equations (see Bickerstaff and Thomas 1987, and Jaffe and Ross 1980 for details).
In conclusions, restoring translation invariance to the cavity or enforcing momentum conservation in deep inelastic scattering leads to structure functions with good qualitative properties including the damping, and even complete suppression, of the unphysical contributions for $x > 1$.

This work was supported by the Commonwealth Department of Education and Youth Affairs and the ARGS.

REFERENCES

J.S. Bell and A.J. Hey Phys. (1978), Phys. Lett. 74B, 77.

R.P. Bickerstaff and A.W. Thomas (1987), University of Adelaide preprint "The structure function of a swollen nucleon", ADP-87-1/T29.

D.L. Hill and J.A. Wheeler (1953), Phys. Rev. 89, 1102

R.L. Jaffe and G.G. Ross (1980), Phys. Lett. 93B, 313.

R.L. Jaffe (1981), Ann. Phys 132, 32.

R.L. Jaffe (1985). Lectures presented at 1985 Los Alamos School on Quark nuclear Physics.

R.E. Peierls and J. Yoccoz (1957), Proc. Phys. Soc. London, A70, 381.

A.W. Thomas (1987), Lectures presented at this school.

C.W. Wong (1981), Phys. Rev. D24, 1416.